การศึกษาบทบาทของ ITCH และ NUMB ที่ทำหน้าที่ควบคุมเชิงลบ

ของวิถีสัญญาณ NOTCH ในการกระตุ้นมาโครฟาจ

นายปฏิภาค เขื่อนจินดา

วิทยานิพนธ์นี้เป็นส่วนหนึ่งของการศึกษาตามหลักสูตรปริญญาวิทยาศาสตรดุษฎีบัณฑิต

สาขาวิชาจุลชีววิทยาทางการแพทย์ (สหสาขาวิชา)

บัณฑิตวิทยาลัย จุฬาลงกรณ์มหาวิทยาลัย

ปีการศึกษา 2557

THE ROLES OF NEGATIVE REGULATORS OF NOTCH SIGNALING,
ITCH AND NUMB, IN ACTIVATION OF MACROPHAGES

Mr. Patipark Kueanjinda

A Dissertation Submitted in Partial Fulfillment of the Requirements
for the Degree of Doctor of Philosophy Program in Medical Microbiology
(Interdisciplinary Program)
Graduate School
Chulalongkorn University
Academic Year 2014
Copyright of Chulalongkorn University

Thesis Title	THE ROLES OF NEGATIVE REGULATORS OF NOTCH SIGNALING, ITCH AND NUMB, IN ACTIVATION OF MACROPHAGES
By	Mr. Patipark Kueanjinda
Field of Study	Medical Microbiology
Thesis Advisor	Associate Professor Tanapat Palaga, Ph.D.

Accepted by the Graduate School, Chulalongkorn University in Partial Fulfillment of the Requirements for the Doctoral Degree

                         Dean of the Graduate School

(Associate Professor Sunait Chutintaranond, Ph.D.)

THESIS COMMITTEE

                         Chairman

(Associate Professor Ariya Chindamporn, Ph.D.)

                         Thesis Advisor

(Associate Professor Tanapat Palaga, Ph.D.)

                         Examiner

(Professor Sanipa Suradhat, D.V.M., Ph.D.)

                         Examiner

(Professor Nattiya Hirankarn, M.D., Ph.D.)

                         External Examiner

(Assistant Professor Marisa Ponpuak, Ph.D.)

ปฏิภาค เขื่อนจินดา : การศึกษาบทบาทของ ITCH และ NUMB ที่ทำหน้าที่ควบคุมเชิง
ลบของวิถีสัญญาณ NOTCH ในการกระตุ้นมาโครฟาจ (THE ROLES OF
NEGATIVE REGULATORS OF NOTCH SIGNALING, ITCH AND
NUMB, IN ACTIVATION OF MACROPHAGES) อ.ที่ปรึกษาวิทยานิพนธ์หลัก:
รศ. ดร. ธนาภัทร ปาลกะ, 96 หน้า.

การกระตุ้นมาโครฟาจทำให้เกิดการปลดปล่อยสารกระตุ้นการอักเสบที่นำไปสู่การ
อักเสบ Numb และ Itch เป็นตัวควบคุมเชิงลบของวิถีสัญญาณ Notch อย่างไรก็ตามบทบาท
ของ Itch ได้ถูกบรรยายไว้เป็นอย่างดีแล้วแต่บทบาทของ Numb ในมาโครฟาจยังไม่เป็นที่เข้าใจ
มากนัก ในการศึกษานี้ได้ทำการสำรวจบทบาทของ Numb ที่เป็นตัวควบคุมการตอบสนองต่อการ
อักเสบในมาโครฟาจ มาโครฟาจที่กลายมาจากเซลล์ไขกระดูกของหนูที่ถูกยับยั้งการแสดงออก
ของ Numb มีการหลั่ง TNFα IL-6 และ IL-12p70 ลดลงอย่างมีนัยสำคัญเมื่อถูกกระตุ้นโดยผ่าน
ตัวรับสัญญาณ TLR4 ถึงแม้ว่าจะมีวิถีสัญญาณ Notch ที่ถูกกระตุ้นเพิ่มมากขึ้น นอกจากนี้
สัญญาณทางปลายน้ำของ TLR4 ซึ่งรวมถึง p65 NF-κB และ p38 MAPK ได้รับผลกระทบจาก
การยับยั้ง Numb Numb ยังควบคุม *Il6* และ *Il12p40* ที่ระดับการถอดรหัสพันธุกรรมโดยผ่าน
p65 NF-κB ในทางตรงข้าม Numb ควบคุมความเสถียรของ *Tnfa* ที่ระดับหลังการถอดรหัส
พันธุกรรมโดยมีความเป็นไปได้ว่าจะควบคุมผ่าน p38 MAPK การยับยั้งวิถีสัญญาณ Notch
ไม่ทำให้ระดับของ TNFα ลดลงมากไปกว่านี้ซึ่งชี้แนะว่าบทบาทของ Numb ในการควบคุม
TNFα นั้นเป็นอิสระจาก Notch ยิ่งไปกว่านั้น Numb ยังถูกค้นพบว่ามีปฏิสัมพันธ์กับ Itch ใน
มาโครฟาจที่ไม่ได้ถูกกระตุ้น การเปลี่ยนแปลงระดับการแสดงออกของ Numb ส่งผลกระทบ
ต่อระดับการแสดงออกของ Itch และ p38 MAPK และ TNFα ข้อมูลโปรติโอมิกส์เปิดเผยให้
เห็นบทบาทใหม่ของ Numb ที่ปรับเปลี่ยนกระแสวิถีสัญญาณที่เกี่ยวข้องกับการอักเสบที่อยู่ทาง
ปลายน้ำของ TLR4 ในมาโครฟาจซึ่งเป็นไปได้ว่าจะผ่านวิถีสัญญาณ Akt/p65 NF-κB/p38
MAPK มากไปกว่านั้นการยับยั้ง Itch ลดการผลิตสารกระตุ้นการอักเสบในมาโครฟาจซึ่ง
เป็นไปได้ว่าจะผ่าน p38 และ JNK MAPK การควบคุมสารกระตุ้นการอักเสบโดย Itch นี้
ขึ้นอยู่กับวิถีสัญญาณ Notch เมื่อนำผลการศึกษามาเชื่อมโยงกันแล้วจึงได้รายงานบทบาทใหม่
ของ Numb ว่าเป็นตัวควบคุมเชิงบวกของการตอบสนองต่อการอักเสบในมาโครฟาจและรายงาน
การเกี่ยวข้องของวิถีสัญญาณ Notch ในการควบคุมสารกระตุ้นการอักเสบโดย Itch

สาขาวิชา จุลชีววิทยาทางการแพทย์   ลายมือชื่อนิสิต ....

ปีการศึกษา 2557   ลายมือชื่อ อ.ที่ปรึกษาหลัก ....

5187336820 : MAJOR MEDICAL MICROBIOLOGY

KEYWORDS: NUMB, ITCH, NOTCH SIGNALING, MACROPHAGE, PRO-INFLAMMATORY CYTOKINE

PATIPARK KUEANJINDA: THE ROLES OF NEGATIVE REGULATORS OF NOTCH SIGNALING, ITCH AND NUMB, IN ACTIVATION OF MACROPHAGES. ADVISOR: ASSOC. PROF. TANAPAT PALAGA, Ph.D., 96 pp.

Activation of macrophages triggers the release of pro-inflammatory cytokines leading to inflammation. Numb and Itch are negative regulators of Notch signaling. Although the role of Itch has been well characterized, the role of Numb in macrophages is not fully understood. In this study, murine macrophages wherein *Numb* was silenced, secreted significantly less TNFα, IL-6 and IL-12p70 upon activation via Toll-like receptor 4 (TLR4), despite activation of Notch signaling. Furthermore, downstream signaling pathways of TLR4, including p65 NF-κB and p38 MAPK, were affected by *Numb* silencing. Numb regulated *Il6* and *Il12p40* at transcriptional level through p65 NF-κB. In contrast, it regulated *Tnfα* mRNA stability at post-transcriptional level possibly through p38 MAPK. Inhibition of the Notch signaling pathway did not further reduce level of TNFα, suggesting a Notch-independent role of Numb in regulation of TNFα. In addition, Numb directly interacted with Itch in resting macrophages. Manipulation of Numb expression level influenced the level of Itch and TNFα. Proteomics data revealed a novel role of Numb that modulated inflammation-related signaling cascades downstream of TLR4 activation in macrophages possibly through Akt/p65 NF-κB/p38 MAPK axis. Moreover, *Itch* silencing reduced production of pro-inflammatory cytokines in macrophages possibly through p38 and JNK MAPKs. This regulation of pro-inflammatory cytokines by Itch was partially dependent on Notch signaling. Taken together, this study reported a novel role of Numb as a positive regulator of inflammatory response in macrophages and an involvement of Notch signaling in regulation of the pro-inflammatory cytokines by Itch.

Field of Study: Medical Microbiology   Student's Signature ....

Academic Year: 2014   Advisor's Signature ....

ACKNOWLEDGEMENTS

CONTENTS

LIST OF FIGURES

LIST OF TABLES

LIST OF ABBREVIATIONS

Ab	antibody
ActD	actinomycin D
ADAM	a disintegrin and metalloproteinase domain-containing protein
ATP	adenosine triphosphate
BMM	bone marrow macrophage
bps	base-pairs
ACN	acetonitrile
CD	cluster of differentiation
cm	centimeter
CSL	CBF1/Suppressor of Hairless/LAG-1
CTC	5-cyano-2,3-ditolyl tetrazolium chloride
Cyld	cylindromatosis
DAPT	N-[N-(3,5-difluorophenacetyl)-L-alanyl]-S-phenylglycine t-butyl ester
DEPC	diethylpyrorcarbonate
DMEM	Dulbecco's Modified Eagle Medium
DMSO	dimethyl sulfoxide
DPF	aspartic acid-proline-phenylalanine
DTT	dithiothreitol
ECD	electron coupled dye
ECL	enhanced chemiluminescence
EDTA	ethylenediaminetetraacetic acid

ELISA	enzyme-like immunosorbance assay
ERK1/2	extracellular signal-regulated kinase 1/2
ESI	electrospray ionization
FBS	fetal bovine serum
g	gram
g	centrifugal acceleration
GAPDH	glyceraldehyde 3-phosphate dehydrogenase
GFP	green fluorescence protein
GO	gene ontology
GSI	gamma secretase inhibitor
HA	hemaglutinin
HECT	homologous to the E6-AP C-terminus
HEPES	4-(2-hydroxyethyl)-1-piperazineethanesulfonic acid
HES	hairy and enhancer of split
HPLC	high-performance liquid chromatography
hr	hour
HRP	horse-radish peroxidase
IB	immunoblot
IgG	immunoglobulin G
IL	interleukine
JNK	c-Jun N-terminal kinase
k	kilo
Da	Dalton

LC	liquid chromatography
LPS	lipopolysaccharide
M	molar
mA	milliampere
MAML	Mastermind-like protein
MAPK	mitogen activated protein kinase
MFI	mean fluorescence intensity
MHC	major histocompatibility complex
μg	microgram
μL	microliter
μm	micrometer
min	minute
mL	milliliter
mM	millimolar
MS	mass spectrometry
N.D.	not detectable
N.S.	not significant
NECD	Notch extracellular domain
NF-κB	nuclear factor kappa-light-chain-enhancer of activated B cell
ng	nanogram
NICD	Notch intracellular domain
NPF	asparagine-proline-phenylalanine
ºC	degree Celsius

OVA	ovalbumin
PAGE	polyacrylamide gel eletrophoresis
PAMP	pathogen-associated molecular pattern
PBS	phosphate buffer saline
PE	phycoerythrin dye
PECy5	phycoerythrin-indotricarbocyanine dye
PRR	pattern recognition receptor
PTB	phosphotyrosine binding domain
qPCR	quantitative polymerase chain reaction
Rbpjκ	recombination signal binding protein for immunoglobulin kappa J region
RING	Really Interesting New Gene domain
rpm	round per minute
SAP	stress-activated protein kinase
SDS	sodiumdodecylsulfate
SEM	standard error of the mean
shRNA	short-hairpin ribonucleic acid
siRNA	small interference ribonucleic acid
TAB1	TGF-beta activated kinase binding protein 1
TAK1	TGF-beta activated kinase 1
TCR	T cell receptor
TEMED	tetramethylethylenediamine
Thr	Threonine
TLR4	Toll-like receptor 4

TNFα	tumor necrosis factor alpha
U	pharmacological unit
Ub	ubiquitin
V	volt
v/v	volume by volume
w/v	weight by volume
WW	tryptophan repeat domain

จุฬาลงกรณ์มหาวิทยาลัย
CHULALONGKORN UNIVERSITY

CHAPTER I
INTRODUCTION

Macrophages are among the first immune cells to encounter microorganisms, to initiate immune defense mechanism, and to phagocytose invading pathogens and dead cells. They possess ability to recognize and discriminate pathogens from self-molecules through binding of the receptors, collectively known as pattern recognition receptors (PRRs) to components of pathogens, called pathogen-associated molecular patterns (PAMPs). After receptor-ligand engagement, macrophages are activated, through various adaptor proteins transducing signals such as nuclear factor kappa-light-chain-enhancer of activated B cells (NF-κB) and mitogen activated protein kinases (MAPKs), to turn on transcription factors (1, 2), leading to expression of target proteins essential for recruitment of other immune cells to assist pathogen clearance (3). This complex mechanism has to be tightly regulated, otherwise damages to the host cells may occur due to prolonged activation.

An evolutionarily conserved Notch signaling has been reported to regulate development and function of cells in the immune system (4, 5). Notch receptors comprise of transmembrane receptors (Notch1, 2, 3, and 4) and ligands (Jagged1 and 2, Delta-like1, 3, and 4). After ligand-receptor binding, the receptor undergoes enzymatic cleavage, generating a Notch intracellular domain (NICD) that can translocate to the nucleus where it functions as a transcriptional co-activator by association with the transcription factor CSL (CBF1/Rbpjκ, Suppressor of Hairless, LAG-1) and other transcription co-activators, such as p300 and Mastermind-like (MAML), to regulate transcription of specific target genes. Several target genes have been identified, including transcription repressors of the HES family (*Hes1, Hes2*) (6). Previous studies from our group and others demonstrated that, upon stimulation, Notch signaling activates macrophage as the activation can be measured from increase production of pro-inflammatory cytokines, including TNFα, IL-6, IL-12p70. In contrast, when Notch signaling is disrupted by γ-secretase inhibitors and *Notch1* RNAi, the activation of macrophages is subsequently inhibited (7-9).

Furthermore, Notch signaling can be modulated by an inhibition of enzymes that target the cleavage sites located on the transmembrane region of the Notch

receptors. For instance, pharmacological inhibitors targeting enzymes such as furin convertase, disintegrin and metalloproteinase domain-containing protein (ADAM), or γ-secretase, can be used to inhibit enzymatic cleavage at these S1, S2, and S3 cleavage sites, respectively. As a result, Notch signaling is interrupted after treatment (10-12). Moreover, Notch signaling can be modulated by proteasomal and lysosomal degradation of NICD. Negative regulators of Notch signaling, such as F-box and WD40 domain-containing protein 7 (Fbxw7), Itch and Numb, were discovered to promote proteasome-mediated degradation of NICD (13, 14). Furthermore, Notch signaling can be modulated through regulation of its ligands expressing on the surface of their own or of the adjacent cells. For instance, Jagged1 is rapidly expressed in macrophages upon TLR stimulation, resulting in an auto-amplification of Notch signaling (15). Taken together, various methods can be applied to modulate Notch signaling to achieve a desirable outcome.

Numb is a membrane-associated protein composing of a N-terminal phosphotyrosine-binding domain (PTB), Src homology 3-binding sites, Eps 15 homology (EH) regions, and a C-terminal proline-rich repeat region (16). Numb interacts with different intracellular molecules from many signaling pathways, thereby regulating multiple functions of the cells. For example, Numb can function as a cell fate determinant protein that is essential for maintenance of neuronal stem cells during fetal development (17, 18). In cancer cells, Numb can control p53 stability, protecting it from ubiquitin-mediated proteasomal degradation. Moreover, a loss of Numb is reported to correlate with bad prognosis of cancer (19-21). In the immune system, an *in vivo* study in *Numb*$^{-/-}$ mice revealed that *Numb* is dispensable for the development of hemopoiesis of myeloid cells and lymphopoiesis of lymphoid (22). Also, Numb is dispensable for proliferation and function of T cells (23). Although Numb is dispensable for the development of various immune cells, it has recently been shown to play a critical role in regulating asymmetric division of T cells and their differentiation in response to virus infection (24, 25). Taken together, these evidences demonstrate that Numb has multiple functions depending on the environmental contents.

Another negative regulator of Notch signaling is Itch. It is an E3 ubiquitin ligase that belongs to the HECT (homologous to the E6-AP C-terminus) protein

family. It is composed of a C2 domain, four WW domains, and a HECT ligase domain (26). These WW domains are implicated for protein-protein interactions whereas the HECT domain helps in recruitment of E2 ubiquitin loading enzymes and transfers ubiquitin to their substrates (27). *Itch*$^{-/-}$ mice develop a skin-scratching "Itchy" phenotype and severe immune dysregulation, including lymphadenopathy, splenomegaly and inflammation in the lungs and digestive system (28, 29). Recent study reported that Itch was a key player in peripheral T-cell tolerance in which a disruption of Itch-mediated JunB ubiquitination promoted T_h2 (T helper type 2 cells) response (30). Itch also functions as a negative regulator of hemopoietic stem cells homeostasis by regulating the Notch signaling pathway (31).

Because both Numb and Itch can antagonize Notch signaling through degradation of the Notch receptors (32, 33), they may play a role in regulation of inflammation in macrophages wherein Notch signaling is involved. In this study, a novel role of Numb was uncovered and reported that it positively regulated production of pro-inflammatory cytokines TNFα, IL-6 and IL-12p70 partly through interaction with Itch which results in changes in the phosphorylation of p65 of NF-κB and p38 of MAPK signaling pathways. In addition, proteomics analysis revealed that Akt1 was upregulated in *Numb*-silenced macrophages upon LPS stimulation. This evidence further supported the hypothesis that Numb was a positive regulator of inflammation macrophages. Besides, the effect of Itch in LPS-activated macrophages was also studied. Silencing of *Itch* alone caused a reduction in pro-inflammatory cytokine production and the production was co-regulated via Notch signaling pathway. In conclusion, our study showed that Numb, by interacting with Itch, positively regulates pro-inflammatory cytokine production in macrophages.

Objectives

1. To identify the roles of Itch and Numb in LPS-activated macrophages
2. To investigate the molecular mechanism of Itch and Numb in regulating macrophage effector functions via Notch-dependent and -independent manner
3. To identify novel target proteins of Numb in activated macrophages using proteomic approach

Hypothesis

Itch and Numb regulate pro-inflammatory cytokine production in macrophages in response to TLR4 activation via Notch signaling pathway.

CHAPTER II
LITERATURE REVIEW

2.1 Macrophages

Macrophages are cells of the innate immunity, originating from myeloid precursor cells in bone marrow, spleen, and fetal liver (34). They are characterized by the expression of several surface proteins such as F4/80, CD107 and CD68. These markers can be used to distinguish macrophages from other immune cells. Macrophages can be found residing in different tissues, having different appearances and functions: for example, Kuffer cells in liver, alveolar macrophages in lungs, microglia in brain and osteoclasts in bones (35).

Macrophages function as a first line of defense against invading pathogens. They can sense components derived from pathogens through binding of pattern recognition receptors (PRRs) to initiate responses to infection. Once activated, they secrete chemokines and cytokines to attract other immune cells to the infection site to help in clearance of the pathogens. Another important function of macrophages is phagocytosis. The phagocytosed pathogens are later degraded into pieces of peptides and processed for antigen presentation to T cells through interaction between MHC and TCR (Figure 2.1).
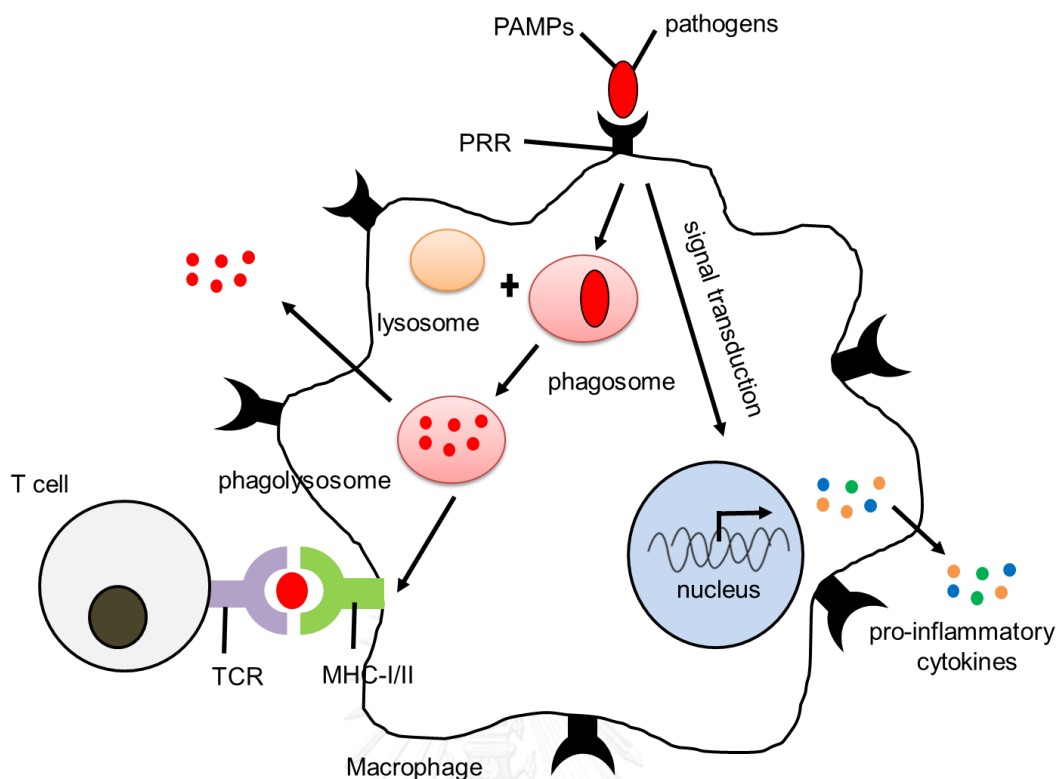
Figure 2.1 Macrophages and their functions in the immune system

A group of the PRRs that has been well-characterized is the Toll-like receptor (TLR) family. TLRs are characterized as type I transmembrane proteins comprising of an ectodomain, the transmembrane region, and the Toll-IL-1 receptor (TIR) domain. The ectodomain containing leucine rich repeats helps in recognition of antigens. The TIR domain located intracellularly functions by activating the downstream signaling pathways of TLR such as NF-κB and MAPK signaling pathways (36). To date, twelve TLRs are identified in mice. Each TLR can specifically detect specific molecular patterns derived from different microorganisms. Examples of these pathogenic antigens include lipopolysaccharide (LPS), lipoprotein, flagellin, double-stranded RNA (dsRNA), single-stranded RNA (ssRNA) and DNA. TLR-ligand binding activity allows macrophages to distinguish non-self from self-antigens and respond immunologically to the particular microorganisms (37).

After binding of TLR and ligand, TLRs activate signaling pathways that orchestrate the immune responses to microbial infection. The signal is transduced

through various adaptor proteins, such as MyD88 (myeloid differentiation primary response 88), TIRAP (Toll-interleukine 1 receptor domain containing adaptor protein), TRIF (Toll-interleukine receptor domain-containing adaptor-inducing interferon beta) or TRAM (translocation-associated membrane protein). They are recruited to the TIR domain of TLRs for transmission of signals to activate cascades of protein kinases, including NF-κB and MAPK (Figure 2.2).
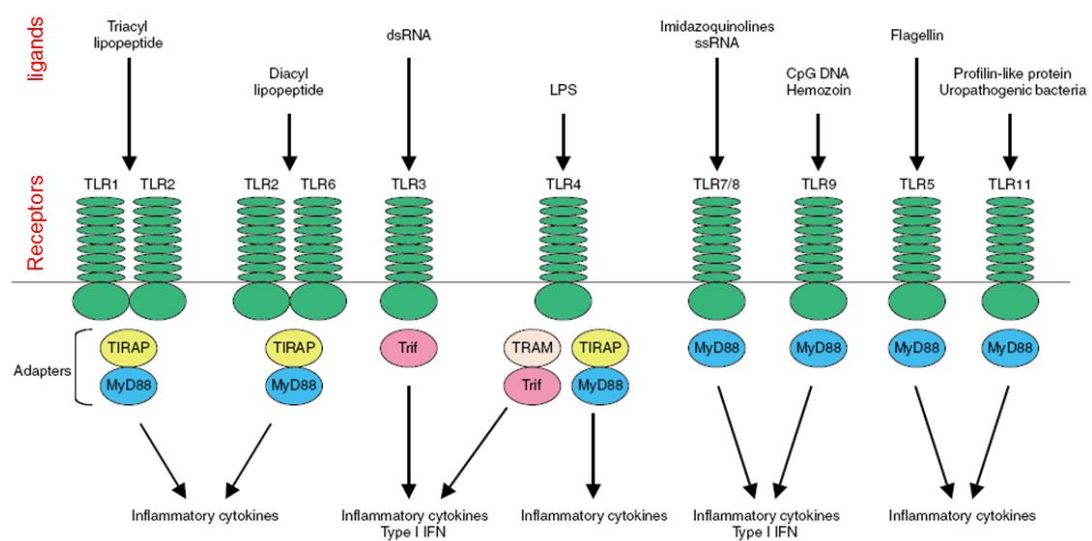
Figure 2.2 Toll-like receptors, ligands, and adaptor proteins for TLR activation

A model showing all TLRs in and their ligands that initiate transduction of signals through different adaptor proteins (adapted from Akira and Takeda, *Nature Review Immunology*, 2004 (38)).

2.2 TLR4 signal transduction in macrophages

Studies of TLR4 in macrophages revealed that a recruitment of multiple adaptor proteins occurs upon ligand binding and this interaction initiates two distinct signaling pathways: the MyD88-dependent and TRIF-dependent pathways (39). TIRAP is an adaptor protein recruited upon TLR4 binding to LPS and served as a bridge between MyD88 and TLR4. The complex, comprising of IRAK4 (IL-1 receptor-associated kinase 4), TRAF6 (tumor necrosis factor receptor-associated factor 6) and TAK1, is formed after MyD88 activation, initiating the activation of NF-

κB and MAPKs. On the other hand, activation through TLR4 allows formation of TRAM-TRIF complex, following by a recruitment of TRAF6 and TAK1 to mediate the activation of NF-κB and MAPKs. Binding between TLR4 and LPS is required for a robust activation of both NF-κB and MAPK signaling pathways, resulting in transcription and translation of pro-inflammatory cytokines (Figure 2.3).

Inflammatory macrophages are under a tight control by various negative regulators and immunosuppressive cytokines to prevent damages caused by excessive inflammation (40, 41). For example, IL-10 transiently activates several key signaling molecules that can dampen the transduction of TLR4 signaling. Resynthesis of IκB prevent nuclear translocalization of NF-κB, thus inhibiting transcriptional activation of downstream target genes (42). Moreover, phosphorylation of MAPKs can be inactivated by dual specificity phosphatase 1 (DUSP1), causing de-phosphorylation of MAPKs to prevent excessive cytokine production (43, 44).
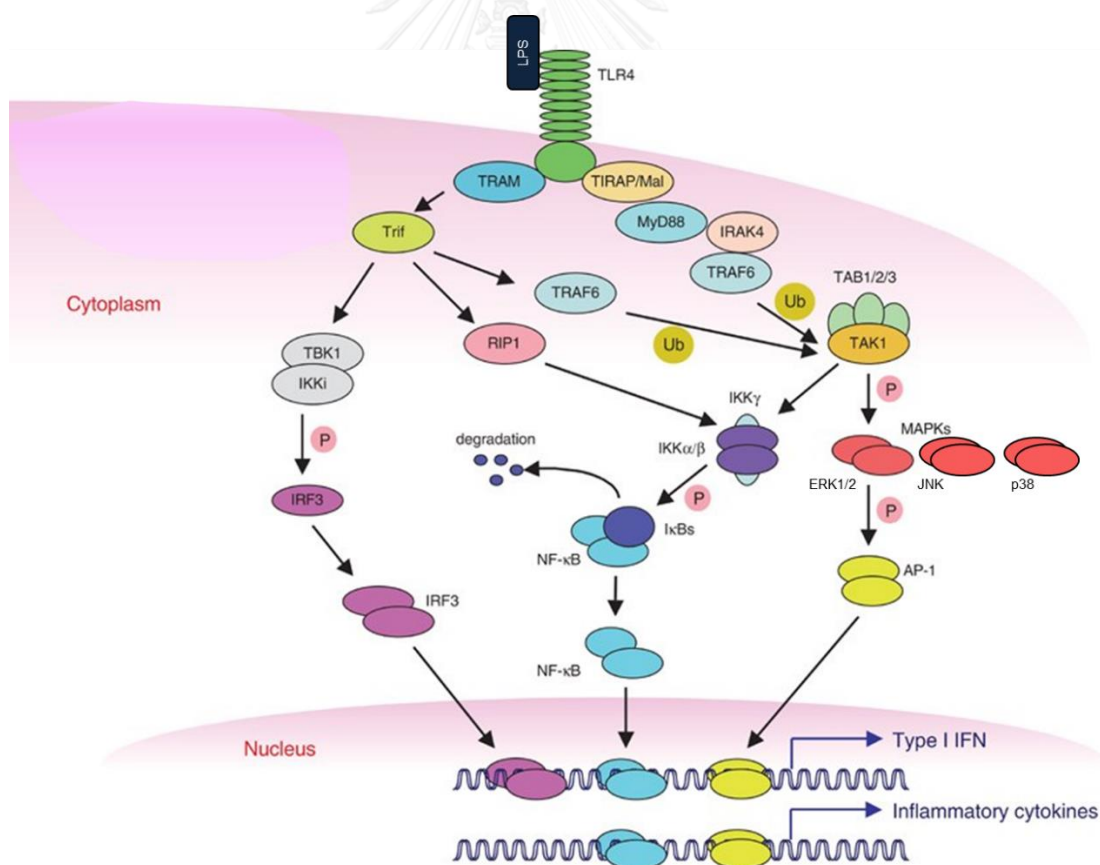
Figure 2.3 TLR4 signaling pathways in macrophages

A schematic diagram showing signal transduction of TLR4 in macrophages (adapted from Kawai & Akira, *Cell Death and Differentiation,* 2006 (45)).

2.3 Notch signaling pathway

2.3.1 Discovery of Notch Signaling

Notch signaling pathway is one of the highly conserved pathways in mammals. It is described as a cell-cell communication system, in which Notch ligand on the signal-sending cell interacts with a Notch receptor on a juxtaposed cell, or the signal-receiving cell. As such, Notch signaling is well-known for the role in determination of cell fate development and differentiation (5, 6). Five ligands of Notch signaling have been reported so far in mammals (46, 47). They are categorized into two closely related subfamilies of Delta-like (Dll1, Dll3 and Dll4) and Jagged (J1 and J2)). Four Notch receptors (N1 to N4) have been reported to be closely related (Figure 2.4). However, the specific effect of ligand and receptor binding and the function of individual receptors and ligands remain to be further explored. An engagement of Notch receptor with Jagged and Delta ligands generates cell context-dependent responses.
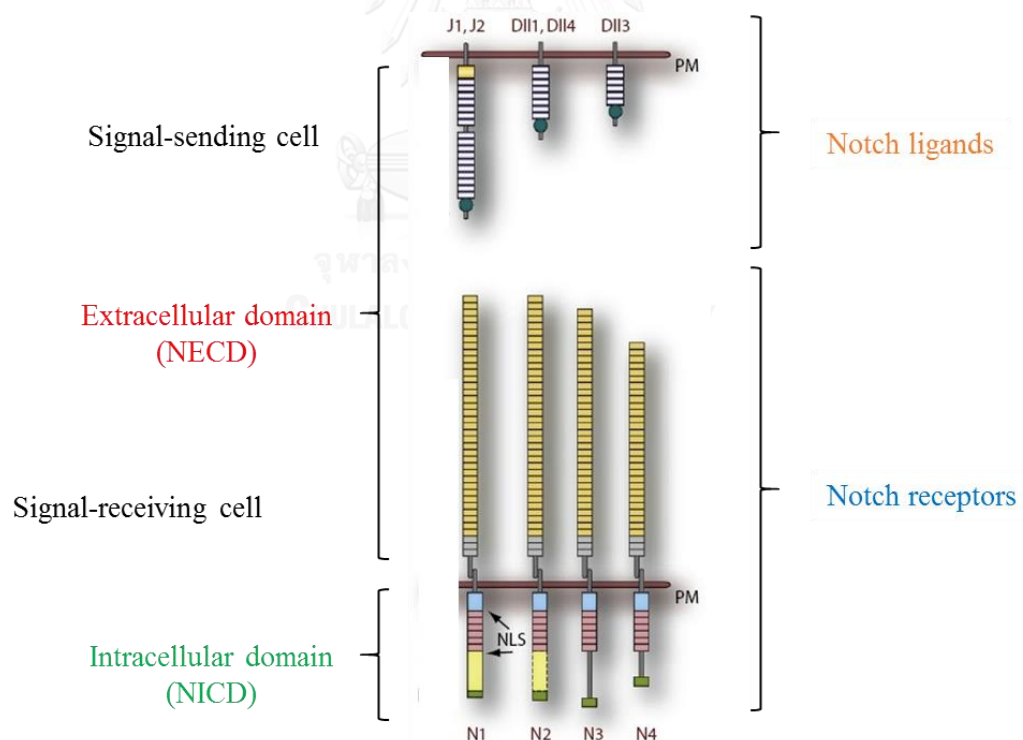
Figure 2.4 Structure of Notch receptors and Notch ligands

A schematic diagram showing Notch receptors (N1-N4) on the signal-receiving cell and ligands (Jagged (J)1, J2, Delta-like (Dll)1, Dll3, Dll4) on the signal-sending cells

are composed of Notch extracellular domain (NECD) and Notch intracellular domain (NICD) (adapted from Radtke, Fasnacht & MacDonald, *Immunity,* 2010 (47)).

2.3.2 Activation of Notch signaling: its mechanism

Upon engagement of Notch receptor and ligand, the receptor is proteolytically processed at two different sites, generating canonical Notch signaling (Figure 2.5). Cleavage at site 1 (S1) by an enzyme furin convertase executes the S1 cleavage on the Notch receptor during protein synthesis. The S1 processing is required for productive ligand-receptor interaction (48). The second cleavage, or S2 cleavage, occurs after receptor-ligand binding. Once the binding occurs, the ligand causes a pulling force on the receptor, generating S2 cleavage site. Then, the ligand removes the extracellular domain of the Notch receptor and internalizes it into lysosomes of the ligand-expressing cell (11, 49). Another enzyme called a disintegrin and metalloproteinase domain-containing protein 10 (ADAM10) or ADAM17 (also known as TACE (tumor necrosis factor alpha-converting enzyme)) immediately engages with the Notch receptor for S2 cleavage (50). At this point ADAM inhibitors can be used to inhibit Notch signaling because S2 cleavages is the rate-limiting step in activation of Notch signaling (12). However, using ADAM inhibitor can generate off-target effects because it do not only control the S2 cleavage but also control the processing of other proteins, including tumor necrosis factor and the interleukin-6 receptor (IL-6R). The S3 cleavage occurs via the γ-secretase complex. The γ-secretase cleaves Notch receptors at the plasma membrane, generating the NICD cleaved at Val1744 (51). Therefore, γ-secretase inhibitors (GSIs) can be used to effectively inhibit Notch activity. Once the cleavage at S3 is complete, NICD translocates to the nucleus and interacts with a transcriptional factor complex called CSL (CBF/Suppressor of hairless/Lag-1)/Rbpjκ (Recombination signal binding protein for immunoglobulin kappa J region) and MAML (Mastermind-like), forming a CSL/Rbpjκ-NICD-MAML complex that directs the expression target genes located downstream of Notch signaling. CSL/Rbpjκ functions as a transcriptional repressor by recruitment of CSL/Rbpjκ along with NICD to DNA-binding sites after activation of Notch signaling (52).

2.3.3 Regulation of Notch signaling by E3 ubiquitin ligases

Because Notch signaling is a conserved signaling pathway that is also involved in regulation of many cellular processes, it has to be tightly regulated to prevent undesirable effects. Ubiquitin-mediated regulation of Notch signaling has been unrevealed previously. Notch intracellular domain can be ubiquitinated by a number of E3 ubiquitin ligases, including atrophin 1-interacting protein 4 (AIP4 or Itch) and F-box and WD40 domain-containing protein 7 (Fbxw7) (14). Particularly, PEST (proline-glutamic acid-serine-threonine) domain-containing Fbxw7 leads to ubiquitin-mediated degradation of NICD (53). Itch also promotes ubiquitination of NICD (33) and together with Numb targets the NICD for ubiquitin-mediated proteasomal degradation (13). In addition, Numb was reported to inhibit Notch signaling via binding with NICD and α-adaptin during formation of endocytic vesicle (54), thereby promoting the endocytosis of NICD and inhibiting Notch signaling. Furthermore, an E3 ubiquitin ligase MDM2 (mouse double min 2) with a dual action that promotes ubiquitination of NICD but degrades Numb, causing an increase of Notch signaling (55) (Figure 2.5).
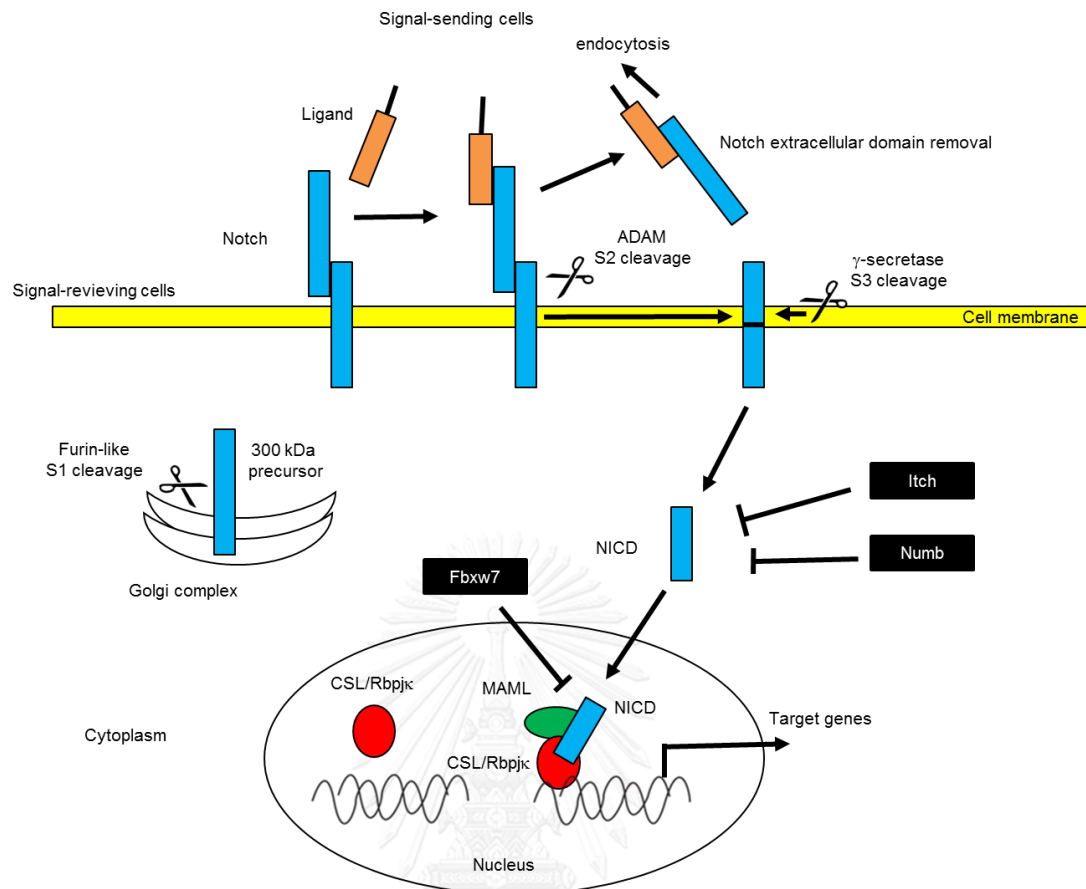
Figure 2.5 Processing of Notch receptor, activation of canonical Notch signaling, and inhibition of Notch signaling

The S1 cleavage of Notch receptor is mediated by furin-like enzyme in the Golgi complex. The S2 cleavage occurs after receptor-ligand binding by ADAM enzyme. The γ-secretase enzyme mediates S3 cleavage at the cell membrane, allowing NICD to translocate to the nucleus and form a CSL/Rbpjκ-MAML-NICD complex that activates transcription of downstream target genes. Itch and Numb promote NICD degradation in cytoplasm whereas Fbxw7 promotes NICD degradation in nucleus.

2.4 Numb

2.4.1 Discovery of Numb protein

Numb is an evolutionarily conserved membrane-associated protein that determine cell fates. It was originally found in *Drosophila* by antagonizing Notch signaling (32). In mice, Numb plays redundant roles in the maintenance of several types of neuronal stem cells during fetal development (17, 18), raising the possibility

that Numb may play a role in other cell lineages. Biochemical studies *in vitro* demonstrated that Numb interacted with several molecules and regulates multiple cell functions as a consequence. These Numb binding partners include Notch1, α-adaptin, E-cadherin, and integrin. *In vivo* studies using *Numb⁻/⁻* mice revealed that *Numb* is dispensable for development of hemopoiesis and lymphopoiesis (22) as well as proliferation and function of T cells (23). However, several studies showed that *Numb* plays critical roles in regulating asymmetric T-cell division occurred during development and differentiation (56) and in response to infection (25).

2.4.2 Multiple functions of Numb

There are four isoforms of mammalian Numb that are generated by alternatively spliced transcripts. Numb is a protein of 72 kDa in molecular weight, containing at N-terminal phosphotyrosine-binding domain (PTB) and at C-terminal proline-rich repeat region. Moreover, Eps15 homology (EH) regions (containing DPF (aspartic acid-proline-phenylalanine) and NPF (asparagine-proline-phenylalanine) have been characterized on Numb protein structure (57). The alternative splicing generates isoforms of Numb with modified PTB and proline-rich repeat domains: p71 Numb isoform has alternative splicing of exon 6 on PTB region, p66 Numb isoform has alternative splicing on proline-rich repeat region, p65 Numb isoform has alternative splicing on both PTB and proline-rich repeat regions (Figure 2.6).
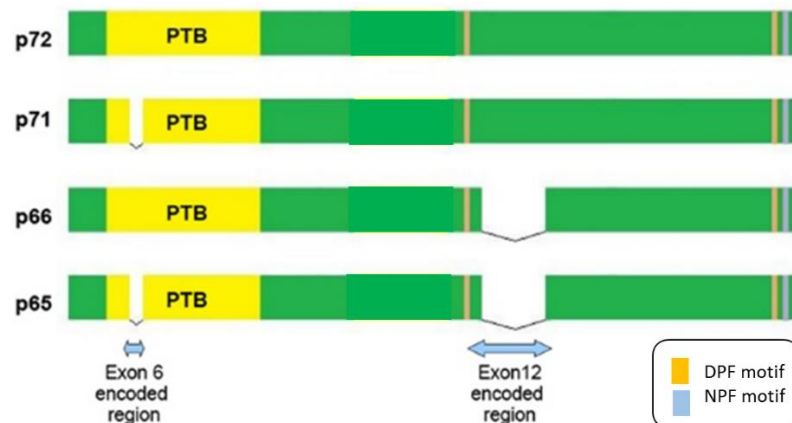
Figure 2.6 Mammalian Numb and its isoforms

A model displaying Numb protein and its isoforms: p72, p71, p66, and p65. PTB indicates phosphotyrosine-binding domain at N-terminus. DPF and NPF motifs indicate Eps15 homology regions at C-terminus (adapted from Ntelios et al., *Frontier in Neuroscience*, 2012. (58)).

A critical region for determining Numb function is the PTB domain that is often involved in cell membrane localization which contributes to the control of cellular endocytosis (59). While the PTB domain is responsible for cell membrane localization, the C-terminus of Numb interacts with several proteins components required for endocytosis. DPF and NPF motifs of all mammalian Numb isoforms are responsible for binding with α-adaptin and various proteins belongs to Eps15 Homology (EH) Domain family involving clathrin-dependent and –independent endocytosis (60, 61). Moreover, Numb was reported to interact with NICD following a recruitment of Itch for ubiquitin-mediated proteasomal degradation of NICD (13). As a result, these binding motifs provide the function of Numb as an adaptor molecule for endocytic activity and as a regulator of number of signaling pathways including Notch signaling (Figure 2.7).
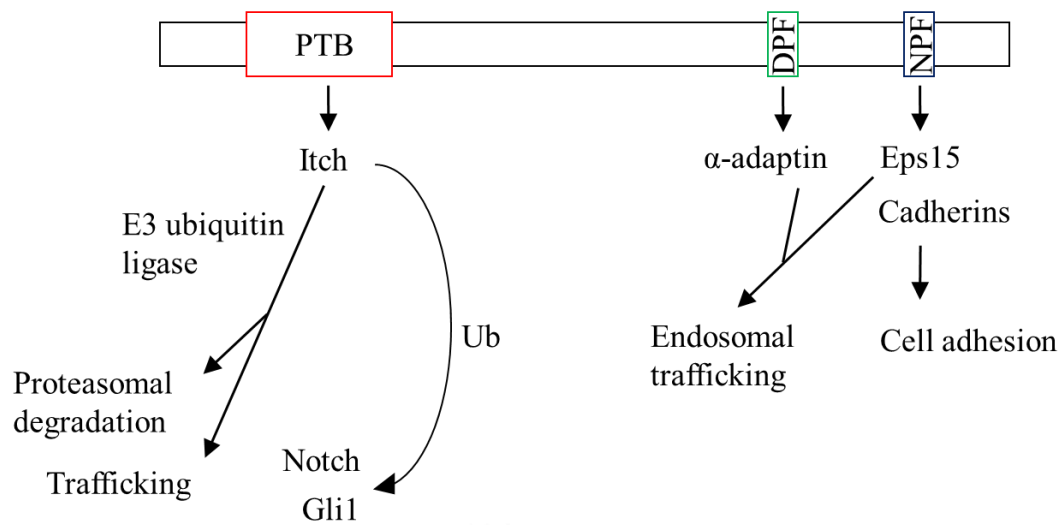
Figure 2.7 Multiple functions of Numb protein

Binding ability of PTB, DPF and NPF domains of Numb contributes to multiple functions of Numb in ubiquitin-mediated trafficking and degradation, endocytosis, cell adhesion and migration. Ub, ubiquitin. (adapted from Gulino, Di Marcotullio and Screpanti, *Experimental Cell Research*, 2010. (57)).

2.4.3 Numb in the immune system

Because T cell development in the thymus is completely abrogated in T progenitors lacking Notch1 or *Rbpjκ* (62, 63) and Notch1 is necessary for the transition of DN3 T cells to the double-positive ones (64), Wilson et al. (22) hypothesized that negative regulators of Notch signaling Numb and its homologue Numb-like might affect hemopoiesis and lymphopoiesis in Notch dependent manner. To their surprise, both Numb and Numb-like were dispensable for the developmental process of hymopoiesis and lymphopoiesis in a combined *Numb$^{-/-}$* and *Numb-like$^{-/-}$* mice, despite the fact that Notch signaling was still activated. Although Numb does not affect development of the immune cells, it is reportedly essential in asymmetric division of T cells at the initiation of infection. The unequal distribution of Numb is during CD8$^+$ T cell division caused the daughter cell with high amount of Numb to acquire markers of effect T cell while the other cell acquired memory T cell phenotypes (25).

2.5 Itch

2.5.1 Discovery of Itch protein

First discovery of *Itch* gene was in 1995 by Perry and his colleagues (29). They found that a specific mutation, a^{18H}, on mouse chromosome 2 led to expression of a darker coat. Mice with this mutation had a skin scratching phenotype and also displayed symptoms of autoimmune disease. Eventually, the mice died at 6-8 months of age because of pulmonary inflammation caused by hypoxia. Hence, they named these a^{18H} mice that displayed this distinct skin scratching phenotype as "Itchy mice". And the gene responsible for it was later named as Itch.

2.5.2 Itch as an E3 ubiquitin ligase

A biological process for targeting a variety of proteins for degradation is known as ubiquitination. Particularly, it is a vital process that controls the turnover of intracellular proteins. Ubiquitination is carried out by three enzymes called E1, E2 and E3 enzymes. The first enzyme, E1 or ubiquitin activating enzyme, catalyzes ubiquitin and the target protein, by transforming a ubiquitin molecule to become adenylated using ATP. Then, the adenylated ubiquitin is transferred to an E2 or ubiquitin-conjugating enzyme and that delivers it to an E3 or ubiquitin ligase. The E3 ubiquitin ligase interacts with its substrate protein to catalyze the formation of the ubiquitin tag (27, 65). The length of this tag controls different fates of the ubiquitinated proteins. For instance, a chain of four or more ubiquitin residues is recognized by 26S proteasome, leading to proteasomal degradation of the polyubiquitinated proteins. In contrast, monoubiquitinated proteins tagging with only one ubiquitin residue are targeted for lysosomal degradation, which contains both proteases and lipases activity (66).

E3 ubiquitin ligases have been extensively studied due to its ability to recognize a repertoire of substrates. Scientists categorized a thousand of recently discovered E3 ubiquitin ligases into two major classes: 1) the RING (Really Interesting New Gene) class E3 ubiquitin ligases, which contain a cysteine-rich RING domain, and 2) the HECT class E3 ubiquitin ligases, containing C-terminal HECT ligase domain. The RING E3 ubiquitin ligases act as a scaffold protein to

catalyze ubiquitination between E2 and its substrate protein. On the other hand, HECT E3 ubiquitin ligases directly use their HECT domain to catalyze ubiquitination of their substrates (67, 68).

Studies of the Itch discovered that it belongs to Nedd4 family of E3 ubiquitin ligase. It has 854 amino acids (aa) in length and has a relative molecular weight of 113 kDa. Like other Nedd4 family members, Itch is a monomeric protein. It has N-terminal C2 domain for membrane targeting, four WW domains at amino acid position 195-246 for recognition of proline rich sequences and C-terminal HECT ubiquitin ligase domain that is responsible for catalytic activity (26). Recently, a number of substrates of Itch have been identified. Examples of the substrates of Itch include transcription factors (e.g. Notch, p63, p73), transmembrane receptors (i.e. C-X-C chemokine receptor 4) and protein kinases (i.e. protein kinase c-θ). They involve in many biological processes including signal transduction, cell differentiation, cell death and the immune response (Figure 2.8).
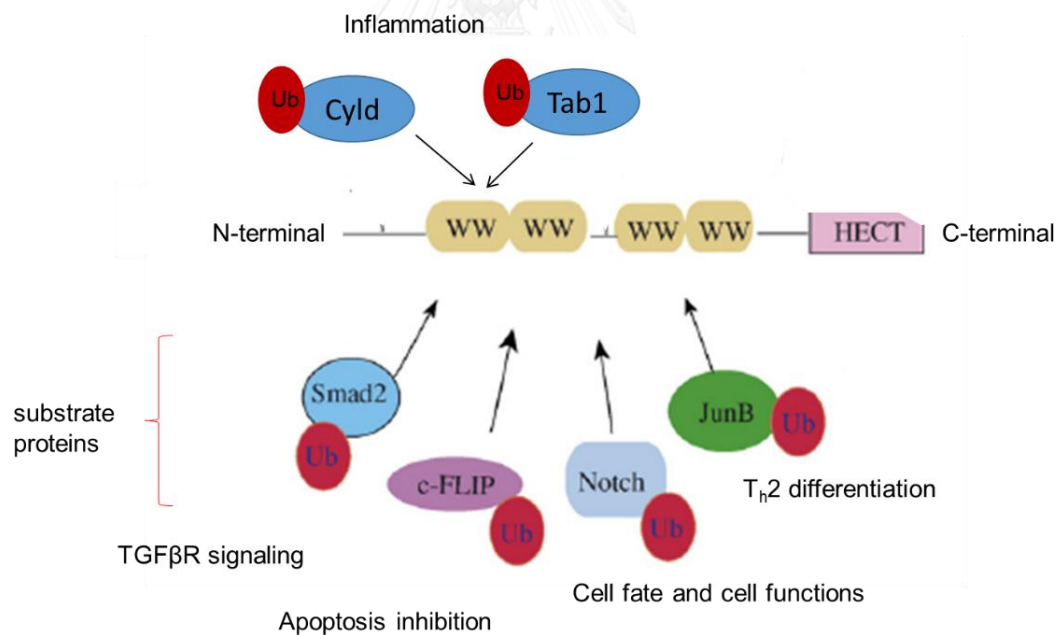
Figure 2.8 Structure of Itch protein and its binding partners that involve in regulation of cellular processes

Itch contains four WW domains and HECT domain at C-terminus. WW domains serve as a binding site for a number of proteins involved in regulation of cellular processes, including inflammation, TGFβR signaling, apoptosis, cell fate

determination and differentiation (adapted from (Y-C. Liu, *Seminars in Immunology*, 2007; Ahmed et al., *Nature Immunology*, 2011.(69-71)).

2.5.3 Itch and cells of the immune system

Functions of Itch in T cell differentiation and immune response have been reported, recently. *In vivo* studies in *Itch*$^{-/-}$ mice showed that the mice develop skin inflammation phenotypes and subsequent immune dysregulation (72, 73). Disruption of Itch results in a break of T cell tolerance causing lymphoid hyperplasia due to accumulation JunB—a transcription factor regulated by Itch ubiquitination. Without Itch, JunB DNA-binding activity accumulated, resulting in an augment of IL-4 production (30). Recently, Itch was identified as a negative regulator of hemopoietic stem cells, homeostasis and function by regulating the Notch signaling pathway (31). In addition, Itch was reported to function as a negative regulator of inflammation in macrophages. Itch can form a protein complex with deubiquitinase Cyld and promotes ubiquitin-mediated proteasomal degradation of TAK1. As a result, macrophages produces excessive amount of pro-inflammatory cytokines (70). Another group reported that Itch inhibited p38α MAPK signaling through ubiquitination of TAB1 in Itchy mice of skin inflammation model (71). Taken together, these findings emphasize the role of Itch in regulation of the cells of the immune system.

Rationale for this study

From biochemical studies, both Itch and Numb function as enzymes to negatively regulate Notch signaling pathway. They target Notch receptors for proteasomal and endocytic degradation (33, 60). *In vivo* studies using *Itch*$^{-/-}$ and *Numb*$^{-/-}$ mice demonstrated that Itch played important role in development of T$_h$2-mediated autoimmune-like disease in mice (30) and Numb regulated asymmetric T cell division during T cell polarization (25), respectively. In addition, results from our groups and others suggested that, upon stimulation of macrophages, Notch signaling was activated and this activation, in turn, up-regulated gene expression patterns characterized by production of both pro- and anti-inflammatory cytokines such as TNFα, IL-6, and IL-10 and costimulatory molecules (9, 74). From these data, we hypothesized that Itch and Numb might negatively regulate phenotypes of LPS-macrophages via Notch signaling pathway.

CHAPTER III
MATERIALS AND METHODS

3.1 Construction of pMKO.1-GFP (control) and pMKO.1-shNumb-GFP (shNumb) plasmids

To construct pMKO.1-shNumb-GFP plasmid, the pMKO.1-GFP retroviral vector was used as a backbone plasmid (Addgene plasmid #10676, USA) and double-stranded oligonucleotides containing *Numb*-specific sequence (5'-AACCACTTTCACAAGAGAAGG -3'), targeting murine *Numb* gene, was inserted into pMKO.1-GFP. The plasmids obtained were called pMKO.1-shNumb-GFP plasmid, respectively. The presence of shNumb insert was confirmed by using restriction enzyme XhoI, which cut at the restriction found on the hairpin loop of the oligonucleotide insert and on the pMKO.1-shNumb-GFP backbone, resulting in a restriction fragment of 415 bps in size. In addition, DNA sequencing of the insert was performed to ensure that the shNumb sequence was not modified.

3.2 Derivation of bone marrow-derived macrophages (BMMs)

3.2.1 Preparation of L929-conditioned medium

L929 cells (ATCC CCL1) were seeded at 5×10^5 cells and maintained in DMEM medium supplemented with 10% FBS at 37°C, 5% CO_2 for three days. After the cell cultures reached 95% confluence, the culture supernatant was harvested, filtered through 0.22 μm filter and stored at -80°C until use.

3.2.2 Derivation of bone marrow-derived macrophages

C57BL/6 mice were purchased from the National Laboratory Animal Center (Mahidol University, Salaya, Thailand). All procedures involving laboratory animals were reviewed and carried out in accordance with the guidelines issued by Chulalongkorn University Institutional Animal Care and Use Committee (CU-IACC #001/2555-20/54). The mice were euthanized and their femurs were extracted. Bone marrows were harvested from the femurs by flooding with DMEM medium

supplemented with 10% FBS. The cell suspension were filtered through 70 μm nylon mesh and incubated in L929-conditioned medium at a density of 5 x 10^6 cells/mL in 10-cm tissue culture dish and maintained in a 5% CO_2 incubator at 37°C. Every three days, a volume of 3 mL of L929-conditioned medium was added. On day 7 the cell cultures were harvested using cold PBS, centrifuged at 1,500 rpm for 5 mins at room temperature, and the supernatant was discarded. Cells were resuspended in DMEM medium supplemented with 10% FBS and subject for subsequent experiments.

3.3 Retroviral transduction of pMKO.1-GFP or pMKO.1-shNumb-GFP into BMMs

3.3.1 Preparation of retroviral particles

Human embryonic kidney 293T cells (ATCC CRL-3216) were cultured in DMEM supplemented with 10% FBS at a concentration of 4 x 10^5 cells/mL for 24 hrs prior to co-transfection with 2 μg of pCL-Eco (Addgene plasmid #12371) and 2 μg of pMKO.1-shNumb-GFP or pMKO.1-GFP using FuGENE HD transfection reagent (Promega, USA). Cells were maintained in DMEM media supplemented with 10% FBS in 5% CO_2 incubator at 37°C. Two days later, cell culture supernatants were harvested and filtered through 0.45 μm filter and used for retroviral transduction.

3.3.2 Retroviral transduction of BMMs

Bone marrows were obtained from C57BL/6 mice as previously described and maintained in L929-conditioned medium. Two days later, the cells were harvested using cold PBS, seeded at 1 x 10^6 cells/well in 12-well plate and maintained in L929-conditioned medium. A volume of 1.2 mL of 293T culture supernatant containing retroviral particles was mixed with 6 μL of FuGENE HD transfection reagent (Promega, USA) prior to addition to the bone marrow cultures. After centrifugation at 2,200 rpm for 1 hr at room temperature, the retroviral particles were allowed to adhere to bone marrows for 1 day at 37°C, 5% CO_2. On the next day, the transduction step was repeated using freshly harvested 293T culture supernatant containing retroviral particles.

Three days later, the culture medium was replaced with L929-conditioned medium and the cells were maintained for another 5 days prior to subject for further experiments. Efficiency of retroviral transduction was 20-25% as indicated by GFP$^+$ F4/80$^+$ population determined by flow cytometry.

3.3.3 Sorting of pMKO.1-GFP or pMKO.1-shNumb-GFP containing BMMs

Ten days after the first retroviral transduction, the cells were harvested using cold PBS and resuspended in cold PBS containing 10% FBS. A population of GFP$^+$ cells was sorted and collected using FACSAria II (BD Biosciences, USA). The sorted BMMs were resuspended and seeded at 1 x 10^5 cells/well in 12-well plate and maintained in L929-conditioned medium for 5 days for surface protein staining or intracellular cytokine staining assay. For Western blotting, cells were seeded at 5 x 10^4 cells/well in 48-well plate. For qPCR assay, cells were seeded at 2 x 10^4 cells/well in 96-well plate.

3.4 Overexpression of Numb in macrophage-like RAW264.7 cells

RAW264.7 cells (ATCC TIB-71) were seeded at 1.5 x 10^5 cells/well in 24-well plate and maintained in DMEM media supplemented with 10% FBS at 37°C, 5% CO$_2$. On the next day, cells were transfected with either control plasmid pCIneoOVA (75) or pCIneoHA mouse Numb (Addgene plasmid #37012) using FuGENE HD transfection reagent (Promega, USA) at a ratio of 3 (μL reagent) : 1 (μg plasmid). After 24 hrs of transfection, RAW264.7 cells were stimulated with 100 ng/mL *E. coli* LPS (Sigma Aldrich, USA). Culture supernatant were collected and protein lysates were harvested using RIPA lysis buffer (150 mM NaCl, 1.0% NP-40, 0.5% sodium deoxycholate, 0.1% SDS, 50 mM Tris-CL pH 7.4) containing protease inhibitors (Roche, Germany) and phosphatase inhibitor cocktail (Sigma-Aldrich, USA) at indicated time points. The protein lysates and culture supernatants were stored at -80°C until use.

3.5 Notch signaling inhibition using γ-secretase inhibitor

A γ-secretase inhibitor, DAPT (Merck, Germany), was used to inhibit Notch signaling in BMMs as previously described (8). To inhibit Notch signaling, 25 μM of DAPT or an equal amount of DMSO was added to the cell cultures 1 hr prior to LPS stimulation.

3.6 Depletion of proteins using siRNA

For depletion of protein of interest in BMMs, the BMMs were seeded at 1.5 x 10^5 cells/well in 12-well plate and maintained in L929-conditioned medium supplemented with 10% FBS at 37°C, 5% CO_2 overnight. On the next day, cells were transfected with non-targeted or targeted siRNA (50 nM) using HiPerFect transfection reagent (Qiagen, Germany). After 24 hrs of incubation, the expression of protein and mRNA of the target gene was monitored by immunoblotting and qPCR, respectively.

The oligonucleotide for depletion of *Rbpjκ* used in the experiments were predesigned and synthesized by the manufacturer (Qiagen, Germany) and included mouse *Rbpjκ* siRNAs (Entrez gene ID:19664; catalog#SI05784121, SI05784114, SI05784107, SI05784100). The oligonucleotide for depletion of Itch used in the experiments were predesigned and synthesized by manufacturer (Qiagen, Germany) and included mouse Itch siRNAs (Entrez gene ID:16396; catalog#SI010788217, SI01078224, SI01078203, SI01078210) and scramble non-targeted siRNA (as a negative control, catalog#SI03650318). Silencing efficiency of the target gene and protein were determined for all samples, comparing with the expression of target protein in negative control transfected with scramble siRNA.

3.7 Sodium dodecyl sulfate-polyacrylamide gel electrophoresis (SDS-PAGE) analysis

3.7.1 Preparation of samples

The cells were harvested for protein lysates by using RIPA lysis buffer (50 μL for 1.5 x 10^5 cells) containing protease inhibitor and phosphatase inhibitor cocktail. The cells were lysed by vigorous vortexing for 1 mins and the crude cell lysates were

centrifuged at 5,000 g at 4ºC for 5 mins. The supernatants were collected and measured for protein concentration by using BCA Assay Protein Assay kit (Pierce, USA). Forty microgram of protein from each sample was prepared by resuspeding in gel loading buffer (50 mM Tri-Cl pH 6.8, 1% β-mercaptoethanol, 10% (v/v) glycerol and 0.1% bromophenol blue) and heating at 100ºC for 10 mins prior to gel loading into the sample well.

3.7.2 Preparation of separating and stacking gel

SDS-PAGE was performed using 8 x 10 x 0.5 cm gel slab. To prepare gel slab, a 8 mL volume of 8% or 10% acrylamide gel were prepared as described in Table 3.1. The mixed solution was gently casted into the gel slab and allowed to polymerized at room temperature for 30 mins. For preparation of stacking gel, a solution of 2 mL volume containing 5% acrylamide was prepared as described in Table 3.1 and layered gently over the separating gel with a comb inserted on the top of the gel. The gel was allowed to polymerize for another 30 mins before use.

3.7.3 Electrophoresis

The electrophoresis chamber (Bio-Rad, USA) was used for electrophoresis. The electrophoresis was carried out using SDS-PAGE running buffer containing Tris, glycine, and SDS at room temperature with a constant current of 100 V and running time of 90 mins for 8% gel or 120 mins for 10% gel.

3.8 Western Blot

When the separation of the proteins in gels was completed, they were equilibrated in transfer buffer containing Tris, glycine, SDS and methanol to remove electrophoresis buffer salts and detergents for 5 mins. Six sheets of blot paper (Whatman, USA) were soaked in transfer buffer. Three sheets of soaked blot paper were placed onto the platinum anode of a semi-dry transfer Trans-Blot SD (Bio-Rad). A sheet of PVDF membrane previously soaked in absolute methanol was placed on top of the wetted blot paper, following by an equilibrated gel placing on top of the PVDF membrane. Another three sheets of pre-wetted blot paper were placed on top of

the gel and air bubbles were removed. The transfer of protein to PVDF membranes (Millipore, Germany) was carried out by using SDS-PAGE semi-dry transfer (Bio-Rad, USA) for 90 mins with a constant current of 80 mA for 1 gel or 150 mA for 2 gels.

Thereafter, the PVDF membrane was blocked with blocking solution (3% (w/v) skim milk in PBS containing 0.5% Tween-20 (PBST)) for 5 mins twice prior to incubation with antibody. Primary antibody specific to the protein of interest was prepared by diluting the antibody in blocking solution according to the ratio provided in Table 3.1. The membrane was incubated with the antibody at 4°C overnight. On the next day, it was washed for 5 mins twice, and for 10 mins three times. Secondary antibody was prepared according to Table 3.1 and incubated with the membranes for 1 hr at room temperature. Following removal of secondary antibody, the washing steps were repeated and kept at 4°C until further use.

3.9 Detecting signal on Western Blot using enhanced chemiluminescence (ECL) method

A volume of 5 mL of the substrate for horse-radish peroxidase (100 mM Tris-HCl pH 8.5, 90 mM coumaric acid, 250 mM luminol, 30% (v/v) H_2O_2) was prepared and applied to the PVDF membrane for 1 mins. The membrane was wrapped by a plastic wrap, placed on a cassette and X-ray film was placed on the top of the membrane. The exposure time required for each protein of interest was listed in the Table 3.1. The X-ray film was developed in developer solution, washed with water, fixed in fixer solution, and washed again with water before allowing to air dry.

3.10 Detection of pro- and anti-inflammatory cytokines by ELISA

Cell culture supernatants were collected at indicated time point after stimulation with LPS and stored at -80°C until further use. The measurement for the amount of TNFα, IL-6, IL-12p70, and IL-10 cytokines was performed using LEGEND MAX^{TM} mouse TNFα, IL-6, and IL-12p70 ELISA kits (BioLegend, USA). The procedure for measuring amount of cytokines was according to manufacturer's instructions. In brief, capture antibody for each cytokine was diluted at the ratio

described in Table 3.2 in coating buffer. For coating, 96-well plate were coated with 100 µL /well of diluted capture antibody, sealed and incubated at 4°C overnight. On the next day, the plate was washed with 150 µL/well of PBST, four times. Then, the plate was blocked with 100 µL/well of assay diluent (10% FBS in PBS) for 1 hr and washed again. Cytokine standards were prepared as described in manufacturer's instruction. Culture supernatants were diluted at a dilution factor of 5 in assay diluent and a volume of 100 µL/well of each diluted samples was added to the plate and incubated at 4°C overnight. On the next day, the washing steps were repeated and 100 µL/well of diluted detection antibody was added to the plate and allowed for 1 hr of incubation at room temperature. Thereafter, the washing steps were repeated and 100 µL/well of diluted avidin-conjugated HRP antibody was added and incubated for another 30 mins at room temperature. After the final washing steps were done, a volume of 100 µL/well of substrate solution was added to each well and allowed for color development for 5-10 mins. A volume of 100 µL/well of stop solution (1M H_2SO_4) was added and the OD_{450} values were read using a microplate reader.

Table 3.1 List of antibodies and their dilutions used for Western blot

Antibody Name	Dilution	Company	Exposure time
anti-Notch1(clone C-20)	1:2,000	Santa Cruz Biotechnology, USA	5 mins
anti-GAPDH	1:4,000	Santa Cruz Biotechnology, USA	5 seconds
anti-cleaved Notch1 (Val1744)	1:1,000	Cell Signaling Technology, USA	30 mins
anti-Numb	1:4,000	Cell Signaling Technology, USA	10 seconds
anti-phospho NF-κB p65	1:2,000	Cell Signaling Technology, USA	5 mins
anti-NF-κB p65	1:2,000	Cell Signaling Technology, USA	2 mins
anti-phospho-p38	1:2,000	Cell Signaling Technology, USA	5 mins
anti-p38	1:2,000	Cell Signaling Technology, USA	2 mins
anti-phospho-ERK1/2 (p42/44)	1:2,000	Cell Signaling Technology, USA	1 min
phospho-ERK1/2 (p42/44)	1:2,000	Cell Signaling Technology, USA	30 seconds

anti-phospho-SAP/JNK	1:2,000	Cell Signaling Technology, USA	1 min
anti-SAP/JNK	1:2,000	Cell Signaling Technology, USA	30 seconds
anti-phospho Akt (Thr308)	1:2,000	Cell Signaling Technology, USA	5 mins
anti-Akt	1:2,000	Cell Signaling Technology, USA	2 mins
anti-Akt1	1:2,000	Cell Signaling Technology, USA	1 min
anti-HA	1:4,000	Cell Signaling Technology, USA	15 mins
anti-Itch	1:2,000	Epitomics, USA	1 min
HRP-conjugated donkey anti-rabbit IgG	1:4,000	Amersham Bioscience, USA	-
HRP-conjugated sheep anti-mouse IgG	1:5,000	Amersham Bioscience, USA	-

Table 3.2 List of antibodies and their dilutions used for ELISA

Name of antibody	Dilution	Company
anti-mouse TNFα capture antibody	1:500	BioLegend, USA
biotin-conjugated TNFα detection antibody	1:500	BioLegend, USA
anti-mouse IL-6 capture antibody	1:500	BioLegend, USA
biotin-conjugated IL-6 detection antibody	1:500	BioLegend, USA
anti-mouse IL-12p70 capture antibody	1:1,000	BioLegend, USA
biotin-conjugated IL-12p70 detection antibody	1:1,000	BioLegend, USA
anti-mouse IL-10 capture antibody	1:200	BioLegend, USA
biotin-conjugated IL-10 detection antibody	1:200	BioLegend, USA
avidin-conjugated antibody-HRP	1:1,000	BioLegend, USA

3.11 Semi-quantitative real-time polymerase chain reaction (qPCR) assay

3.11.1 Total RNA extraction

Total RNA from macrophages was extracted using TRIzol reagent (Invitrogen, UK) according to the manufacturer's instructions. Briefly, the cells were lysed with 500 µL/well of TRIzol reagent and allowed to stand for 5 mins at room temperature. A volume of 100 µL of chloroform (Lab-Scan, Ireland) was added to each sample, mixed vigorously, and allowed to stand for 3 mins at room temperature. Then, the samples were centrifuged at 12,000 g at 4°C for 15 mins. The top aqueous phase was transferred to a new 1.5-mL tube and a volume of 250 µL of isopropanol (Merck, Germany) was added for RNA precipitation. After standing for 10 mins at room temperature, the samples were centrifuged at 12,000 g for 10 mins at 4°C to pellet RNA. The isopropanol was discarded and a volume of 500 µL of 75% Ethanol in 0.01% diethylpyrocarbonate (DEPT)-treated water was added for washing the RNA pellet. The samples were centrifuged again at 7,500 g for 5 mins at 4°C. Once the supernatant was discarded, the RNA pellet was air dried and resuspended in 20 µL of DEPC-treated water, incubated at 55°C for 10 mins and stored at -80°C until further use.

3.11.2 Quantitation of RNA

Amount of RNA of each sample was measured using Quant-iT RNA assay kit (Invitrogen, UK) according to the manufacturer's instruction. Briefly, the working solution was prepared by mixing Quant-iT RNA reagent at 1:200 dilution in Quant-iT RNA buffer. A volume of 190 µL of the working solution was transferred to each 1.0-mL tube serving as RNA standard 1 and RNA standard 2 whereas a volume of 195-199 µL of working solution was transferred to each 1.0-mL tube serving as sample. A volume of 10 µL of each RNA standard was added to the tube labeling as standard and mixed well. Meanwhile, a volume of 1-5 µL of RNA sample was added to the tube labeling as sample and mixed well. The mixtures were allowed to stand for 3 mins at room temperature. Later, they were measured for the fluorescence using Qubit Fluorometer (Invitrogen, UK) and the concentration of RNA was calculated using the equation:

$$Concentration\ of\ sample = QF\ value \times \left(\frac{200}{X}\right)$$

where:

QF value = the value given by the Qubit Fluorometer

X = the number of microliters of sample added to the assay tube

3.11.3 First-strand cDNA synthesis

An amount of 100 ng of total RNA was used to synthesize cDNA of 20 µL total volume, containing a mixture of 0.5 µl of 0.4 mg/mL of random hexamer (Qiagen, Germany), 2 µL of 10 mM dNTP (Fermentas, Germany), 0.5 µL of RiboLock RNase inhibitor (Fermentas, Germany), 1 µL of RevertAid reverse transcriptase (Fermentas, Germany), 4 µL of 5X Reaction Buffer (250 mM Tris-HCl (pH 8.3 at 25°C), 250 mM KCl, 20 mM $MgCl_2$, 50 mM DTT) and remaining volume was filled with DEPC-treated water. The reaction was incubated at 42°C for 1 hr, 70°C for 10 mins, and stored at -20°C until further use.

3.11.4 qPCR assay

The qPCR was performed after making 20 µL of master mixture volume containing 1 µL of cDNA suspension, 0.5 µL of 10 mM specific forward primer, 0.5 µL of 10 mM specific reverse primer, 5 µL of 2X iQ^{TM} SYBR® Green Supermix (Bio-Rad, USA), 3 µL of nuclease-free H_2O. The nucleotide primers sequences used for qPCR were shown in Table 3.3. The amplification condition for a specific gene was shown in Table 3.4. The relative expression levels were calculated as described previously using the $2^{-\Delta\Delta CT}$ equation (76).

Table 3.3 List of nucleotide primer sequences used for qPCR

Primer	Forward primer	Reverse primer	Reference
Numb	act acg gca aag ctt cag ga	tgc att cct ctt gac tca tca	Designed in this study
Numb-like	tac ggt tga atg agc tgc ca	agg cag aag tcc ctg ttg tg	Designed in this study
Itch	cat gtg gtt ttg gca gtt tg	ttg taa ggt ggg agg tcc ag	Designed in this study
Tnfα	cct gta gcc cac gtc gta gc	ttg acc tca gcg ctg agt tg	(77)
Il6	cat gtt ctc tgg gaa atc gtg g	aac gca cta ggt ttg ccg agt a	(9)
Il12p40	aac ctc acc tgt gac acg cc	caa gtc cat gtt tct ttg cac c	(78)
Il10	tca aac aaa gga cca gct gga caa cat act gc	ctg tct agg tcc tgg agt cca gca gac tca a	(9)
Hes1	ccg gtc tac acc agc aac agt	cac atg gag tcc gaa gtg agc	(9)
Rbpjκ	atg ccc tcc ggt ttt cct c	gga caa gcc ctc cga gta gt	Designed in this study
Akt1	gcc tac cga gaa gag act ctg a	gtc ttc atc agc tgg cat tgt	(79)
Akt2	taa aaa gtg gct ctg gtg tgt g	ggc att ctg cta cag aga aat tg	(79)
Ticam	cag agt tgt cta caa agt cg	tgg atg acg tgg tgt ctg c	(80)

| Map3k10 | agt tcc act ttg cag aag gag cga | cat ctg cct ccg caa att ctt cca | (81) |
| GAPDH | acc aca gtc cat gcc atc | tcc acc acc ctg ttg ctg | (82) |

Table 3.4 List of conditions used to amplify specific gene by qPCR

Gene name	Denaturing temperature (ºC)	Annealing temperature (ºC)	Extending temperature (ºC)	Number of cycles
Numb	95	60	72	40
Numb-like	95	60	72	40
Itch	95	58	72	40
Tnfα	95	55	72	40
Il6	95	52	72	40
Il12p40	95	65	72	40
Il10	95	58	72	40
Hes1	95	60	72	50
Rbpjκ	95	62	72	50
Akt1	95	52	72	40
Akt2	95	47	72	50
Ticam	95	50	72	50
Map3k10	95	48.6	72	50
GAPDH	95	60	72	40

3.12 mRNA stability assay

To assess mRNA stability, BMMs were seeded at 1 x 10^4 cells/well in 96-well plate and maintained in DMEM supplemented with 10% FBS in 5% CO_2 incubator at 37°C for 24 hrs. On the next day, the cells were stimulated with 100 ng/mL of *E. coli* LPS for 1 hr prior to the treatment of actinomycin D (Merck, Germany) at the final concentration of 20 μg/mL for indicated time. Total RNA was extracted, converted to cDNA, and subject to be analyzed using qPCR assay as previously described.

The percentage of remaining mRNA was calculated as described in the equation below:

$$Percentage\ of\ remaining\ mRNA = \frac{(ActD\ and\ LPS)}{(LPS)} \times 100$$

where:

ActD and LPS = the relative mRNA expression from BMMs treated with LPS
                 and actinomycin D

LPS   = the relative mRNA expression from BMMs treated with LPS

mRNA half-life was calculated from the linear regression of the mRNA levels at 0, 30 and 60 mins time points following addition of actinomycin D (83).

3.13 Flow cytometry assay

After an overnight incubation, the BMMs were treated with 1 μL of GolgiPlug™ (BD Biosciences, USA) to inhibit protein transportation, according to manufacturer's instructions, just before stimulation with 100 ng/mL of *E. coli* LPS. At each indicated time point, the cells were harvested with cold PBS, washed, and incubated with 2.4G2 antibody (BD Biosciences, USA) to block FcγRII/III receptors. To assess the expression of biological markers on macrophages, the cells were stained with PE-labeled anti-F4/80 and biotin-conjugated anti-CD11b following by avidin-conjugated PECy5 (BioLegend, USA). PE-labeled anti-MHC class II and biotin-conjugated anti-CD86 (BioLegend, USA) following by avidin-conjugated ECD (Beckman Coulter, USA) were used to assess activation markers on macrophages. All

primary and secondary antibodies were diluted in assay diluent (10% FBS in PBS) at 1:1,000 ratio.

To assess the production of intracellular TNFα, IL-6, and IL-12p70 cytokines, BMMs were stained with PE-labeled anti-TNFα, PE-labeled anti-IL-6, and biotin-conjugated IL-12p70, followed by avidin-conjugated PECy5 (BioLegend, USA) at a dilution of 1:1,000 in the assay diluent from BD Cytofix/Cytoperm^{TM} kit (BD Biosciences, USA) according to manufacturer's instructions. The acquired flow cytometry data were analyzed using FlowJo VX software (TreeStar, USA).

3.14 Co-immunoprecipitation

5×10^6 cells of macrophages were maintained in complete DMEM supplemented with 10% FBS. After overnight incubation, cells were stimulated with 100 ng/mL *E. coli* LPS for 30 mins. After stimulation, cells were washed once and detached using 5 mL of cold PBS. Cell pellets were collected by centrifugation at 2,500 rpm at room temperature. Then, they were lysed by vigorous vortex in 200 μl of 0.5% NP-40 lysis buffer containing protease inhibitors and phosphatase inhibitor (Roche, Germany). The lysis step was continued on ice for 30 mins. Later, cells were centrifuged at 14,000 rpm at 4°C and protein lysates were transferred to each of new 1.5-mL tubes. Protein concentration of each sample was determined using BCA Assay Protein Assay kit (Pierce, USA). Starting protein amount for co-immunoprecipitation was 500 μg for each protein sample. Pre-clearing step was performed by adding 10 μL of Protein A agarose beads (Cell Signaling Technology, USA) to each tube and they were incubated on a rotating platform for 2 hrs at 4°C. After centrifugation at 5,000 *g*, the clear lysate of each sample was transferred to a new 1.5-mL tube and 250 ng of anti-rabbit IgG or anti-Numb antibody (Cell Signaling Technology, USA) was added. Then, the samples were incubated on a rotating platform overnight at 4°C. On the next day, 10 μL of Protein A agarose beads was added to each tube and the incubation was continued on a rotating platform for additional 4 hrs. After centrifugation of samples at 5,000 *g*, cell lysate of each sample was transfer to a new tube and mixed with 3X SDS sample loading buffer, heated at

$100^{o}C$ for 10 mins. After centrifugation at 10,000 g, protein samples were subjects for SDS-PAGE and Western blot analysis.

3.15 Protein preparation and fractionation by SDS-PAGE for mass spectrometry analysis

BMMs containing shRNA plasmids were prepared as previously described. The cells were seeded at 2.5 x 10^5 cells/well in 12-well plate in L929-containing media overnight at $37^{o}C$, 5% CO_2. On the next day, the cells were stimulated with 100 ng/mL of *E. coli* LPS for 30 mins and were harvested using RIPA lysis buffer. Cell lysate was stored at $-80^{o}C$ until use. Protein concentration of the samples were measured by Lowry method (84) and measured for absorbance at 750 nm (OD_{750}). The protein concentration was calculated from the standard curve of bovine serum albumin with known concentrations. An SDS-PAGE mini slab gel (8 x 9 x 0.1 cm, AE-6530 mPAGE, ATTO, Japan) was used to separate proteins. Accordingly, the polyacrylamide gel was prepared as described previously in the standard method. The separating gel used for the fractionation of soluble proteins from mammalian cells contained 12.5% acrylamide. Fifteen was 15 μg of protein for each sample was used and mixed with 5 μL of 5X sample buffer (0.125 M Tris-HCl pH 6.8, 20% glycerol, 5% SDS, 0.2 M DTT, 0.02% bromophenol blue), boiled at $95^{o}C$ for 10 mins before loading onto the 12.5% SDS-PAGE. Low molecular weight protein standard marker (Amersham Biosciences, UK) was used to estimate size of polypeptides. The electrophoresis was perform in SDS electrophoresis buffer (25 mM Tris-HCl pH 8.3, 192 mM glycine, 0.1% SDS). Once the tracking dye reached the bottom of the gel, the electrophoresis was stopped. And the gels were silver stained according to Blum et al. (85).

3.16 In-gel digestion

After excision of protein bands, the gel plugs were dehydrated with 100% acetonitrile (ACN), reduced with 10 mM DTT in 10 mM ammonium bicarbonate at room temperature for 1 hr and alkylated at room temperature for 1 hr in the dark in the presence of 100 mM iodoacetamide (IAA) in 10 mM ammonium bicarbonate.

After alkylation, the gel pieces were dehydrated twice with 100% ACN for 5 mins. In-gel digestion of proteins was performed as described here: 10 µL of trypsin solution (10 ng/µL trypsin in 50% ACN/10 mM ammonium bicarbonate) was added to the gels and incubated at room temperature for 20 mins, and then 20 µL of 30% ACN was added to keep the gels immersed throughout digestion. The gels were incubated at 37°C for a few hrs or overnight. A volume of 30 µL of 50% ACN in 0.1% formic acid (FA) was added into the gels to extract peptide products from the digestion process. Later, the gels were incubated for 10 mins in a shaker at room temperature. The extracted peptides were collected and pooled together in the new tube. The pool extracted peptides were dried by vacuum centrifuge and kept at -80°C for further mass spectrometric analysis.

3.17 HCTUltra LC-MS analysis

Peptide solutions were analyzed using an HCTultra PTM Discovery System (Bruker Daltonics Ltd., U.K.) coupled to an UltiMate 3000 LC System (Dionex Ltd., U.K.). Peptides were separated on a nanocolumn (PepSwift monolithic column 100 µm i.d. x 50 mm). Eluent A was 0.1% formic acid and eluent B was 80% acetonitrile in water containing 0.1% formic acid. Peptide separation was achieved with a linear gradient from 10% to 70% B for 13 min at a flow rate of 300 nL/mins, including a regeneration step at 90% B and an equilibration step at 10% B, one run took 20 mins. Peptide fragment mass spectra were acquired in data-dependent AutoMS (2) mode with a scan range of 300−1500 m/z, 3 averages, and up to 5 precursor ions selected from the MS scan 50−3000 m/z.

Peptide peaks were detected and deconvoluted automatically using DataAnalysis version 4.0 (Bruker). Mass lists in the form of Mascot generic files were created automatically and used as the input for Mascot MS/MS Ions searches of the National Center for Biotechnology Information nonredundant (NCBI nr) database (www.matrixscience.com). Default search parameters used were the following: Enzyme = trypsin, max. missed cleavages =1; fixed modifications = carbamidomethyl (C); variable modifications = oxidation (M); peptide tolerance ±1.2 Da; MS/MS tolerance ±0.6 Da; peptide charge = 1+, 2+ and 3+; instrument = ESI-TRAP.

3.18 Proteins quantitation and identification

For proteins quantitation, DeCyder MS Differential Analaysis software (DeCyderMS, GE Healthcare (86, 87) was used. The raw data acquired from LC-MS were converted and the PepDetect module was used for automated peptide detection, charge state assignments, and quantitation based on the peptide ions signal intensities in MS mode. The analyzed MS/MS data from DeCyderMS were submitted to database search using the Mascot software (Matrix Science, London, UK, (88)). To identify the proteins, the data were searched against the NCBI database. Database interrogation was set as the followings; taxonomy (*Mus musculus*); enzyme (trypsin); variable modifications (carbamidomethyl, oxidation of methionine residues); mass values (monoisotopic); protein mass (unrestricted); peptide mass tolerance (1 Da); fragment mass tolerance (±0.4 Da), peptide charge state (1+, 2+ and 3+) and max missed cleavages (1). Proteins considered as identified proteins had at least two peptides with an individual mascot score corresponding to $p<0.05$ and $p<0.1$, respectively.

3.19 Phagocytic assay

BMMs were seeded at 2×10^5 cells/well in 24-well plate containing L929-medium supplemented with 10% FBS. After overnight incubation, the cultures were washed twice with 500 µl of complete DMEM. Alexa Fluor® 488-conjugated *E. coli* (K-12 strain) (Invitrogen, UK) diluted in 500 µl complete DMEM at MOI of 10 was added to each well. The cultures were incubated for 1 hr at 4ºC or 37ºC as indicated. After incubation, the cultures were washed twice with complete DMEM to remove *E. coli* that were not phagocytosed by BMMs. The BMMs were detached from the culture vessel using cold PBS and a rubber policeman. Then, they were stained with 2.4G2 antibody to block FcγRII/III receptors and followed by staining with PE-conjugated anti-F4/80 antibody as previously described. The cells were subjects for analysis of internalized *E. coli* by using flow cytometer (Beckman Coulter, USA).

The percentage of *E. coli* phagocytosis was calculated using the equation provided below:

$$Phagocytosis\ (\%) = \frac{Mx_{t=i}}{Mc_{t=37}} \times 100$$

where:

M_x = mean fluorescence intensity of the sample of interest

M_c = mean fluorescence intensity of the control sample

t   = temperature (^{o}C) at which the culture was incubated with *E. coli*

3.20 Statistical analysis

All experimental data in this study were presented as the means ± SEM of three independent experiments or from a representative experiment of three independent experiments unless indicated otherwise. The statistical significances of the differences in the experimental data were valued by the Student's *t* test. The statistical significance level was set as * *p*<0.05; **p<0.01; ***p<0.001.
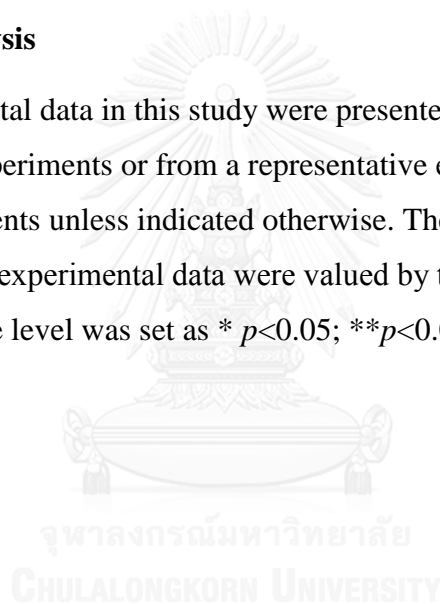
RESULTS

4.1 Expression of Numb is reduced in LPS-stimulated macrophages and silencing of Numb increases activation of downstream components of Notch signaling

We began the investigation by exploring the expression of Numb in LPS-stimulated macrophages. At the transcriptional level, we found that the expression level of *Numb* mRNA significantly decreased to approximately one-half after stimulation with LPS for 3 hrs, comparing with the unstimulated macrophages. This level was maintained up to 24 hrs (Figure 4.1A). However, when examining the level of Numb protein, we found that Numb protein was only slightly decreased after LPS stimulation (Figure 4.1B). These results suggested that the stability of Numb protein was enhanced by LPS treatment.
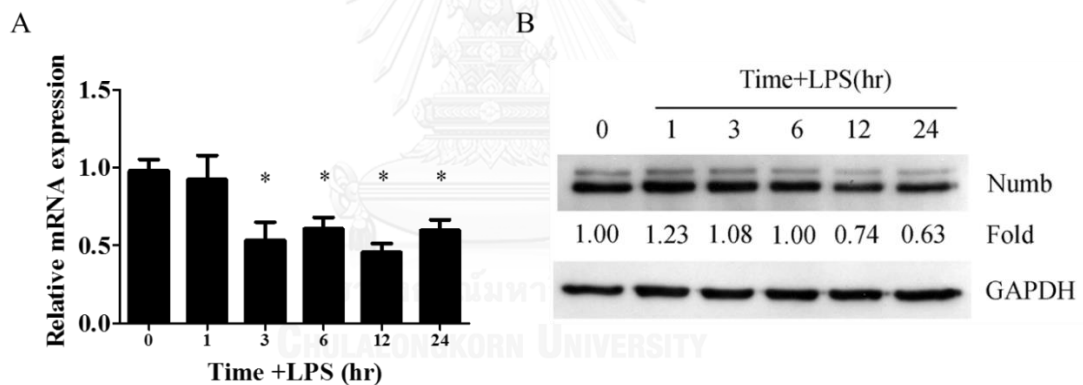
Figure 4.1 Numb expression in macrophages in respose to LPS stimulation

(A) *Numb* mRNA expression in BMMs treated with 100 ng/mL *E. coli* LPS for indicated time was examined by qPCR assay. Data are means ± SEM from representatives of two independent experiments. * $p<0.05$; ** $p<0.01$; *** $p<0.001$. (B) Numb protein expression from BMMs treated with LPS for indicated time was examined using Western blot. Fold number indicates fold-change of the intensity of Numb protein from LPS-treated macrophages, compared with untreated cells.

A loss-of-function approach using shRNA targeting *Numb* gene for silencing was employed to investigate the roles of Numb in macrophages. To test the silencing

function of our plasmids in macrophages, a retroviral transduction method was employed to introduce the pMKO.1-shNumb-GFP plasmid into BMMs and we examined its ability to silence *Numb* gene. We found that approximately 20-25% of total macrophages were successfully transduced containing either pMKO.1-GFP (control) or pMKO.1-shNumb-GFP (shNumb) plasmids as indicated by GFP expression (Figure 4.2A). We found that expression of Numb in the GFP$^+$ population was decreased in macrophages containing pMKO.1-shNumb-GFP plasmids (Figure 4.2B), comparing with that of the control macrophages. In addition, using immunofluorescence staining technique, we found that Numb expression in macrophages containing control plasmids remained unchanged (Figure 4.3A). In contrast, the expression of Numb in macrophages containing shNumb plasmids showed a reduction of Numb (Figure 4.3B).
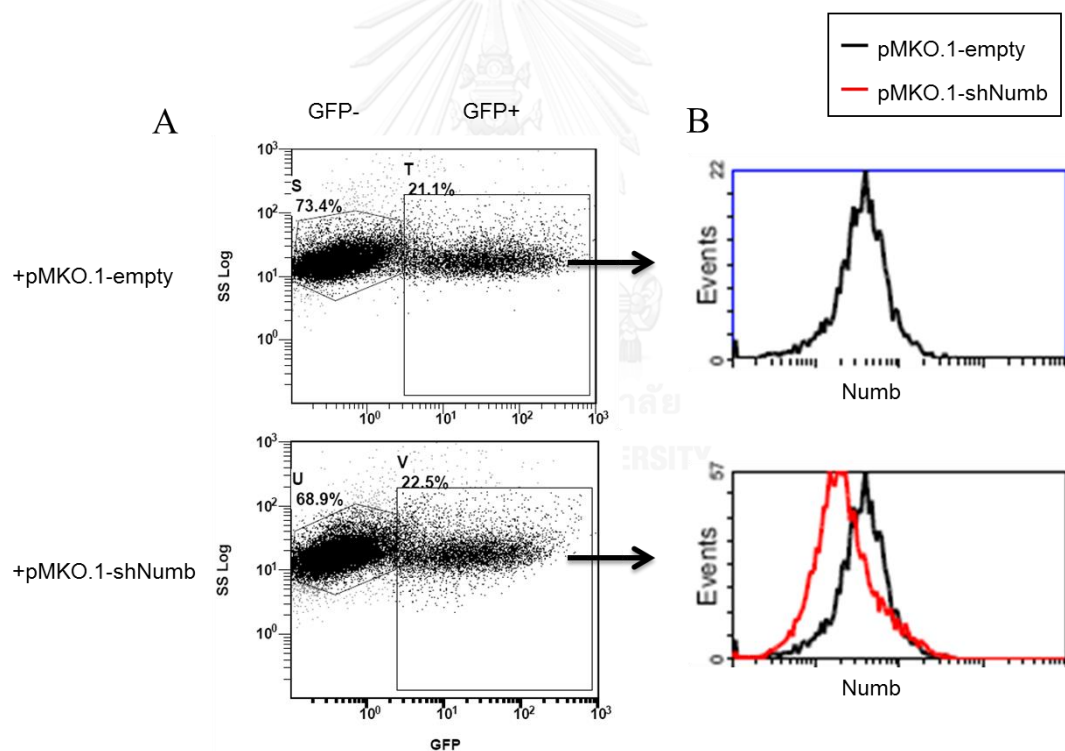
Figure 4.2 Numb expression in BMMs retrovirally transduced with pMKO.1-GFP or pMKO.1-shNumb-GFP plasmids

(A) Flow cytometry analysis of macrophages containing pMKO.1-GFP (or pMKO.1-empty) or pMKO.1-shNumb-GFP (pMKO.1-shNumb) plasmids as indicated by GFP$^+$ population. (B) Overlay histrogram showing a reduction of Numb protein in GFP$^+$

macrophages transduced with pMKO.1-shNumb (red) vs. pMKO.1-empty (black) plasmid. Data are representatives of two independent experiments.
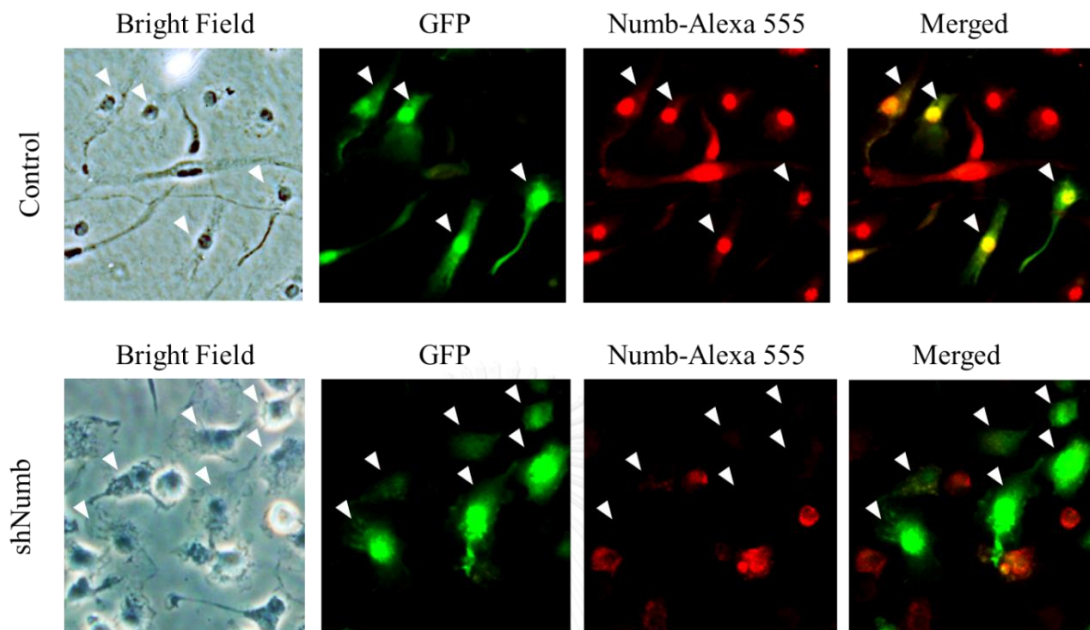
Figure 4.3 Immunofluorescence staining of Numb protein in GFP$^+$ macrophages Macrophages containing pMKO.1-empty (control) or pMKO.1-shNumb (shNumb) plasmids (GFP$^+$ cells) were indicated by white arrows. Expression of Numb was indicated in red as the protein was stained with anti-Numb-Alexa 555 antibody. Data are representatives of two independent experiments.

Next, we confirmed the specificity of our shNumb plasmids by performing a qPCR assay to examine the expression of *Numb* and *Numb-like* genes. Because *Numb-like* gene has approximately up to 80% homology to *Numb* gene and is reported as a Numb homolog. Furthermore, both Numb and Numb-like reportedly have functional redundancy in several cell types, such as neurons (89, 90). Therefore, it was important to ensure that the effect of our silencing strategy on Numb-like was excluded in our study. After GFP$^+$ macrophage sorting using FACS to obtain a homogenous population (>90% as confirmed by flow cytometry) the expression level of *Numb* and *Numb-like* mRNA were examined. We found that the expression level of *Numb* mRNA significantly decreased comparing with the BMMs containing control

vector, whereas the expression level of *Numb-like* mRNA showed no difference between macrophages containing shNumb plasmids or the ones containing control plasmids (Figure 4.4A and 4.4B). These results confirmed that our pMKO.1-shNumb plasmids specifically silenced *Numb* gene in macrophages.
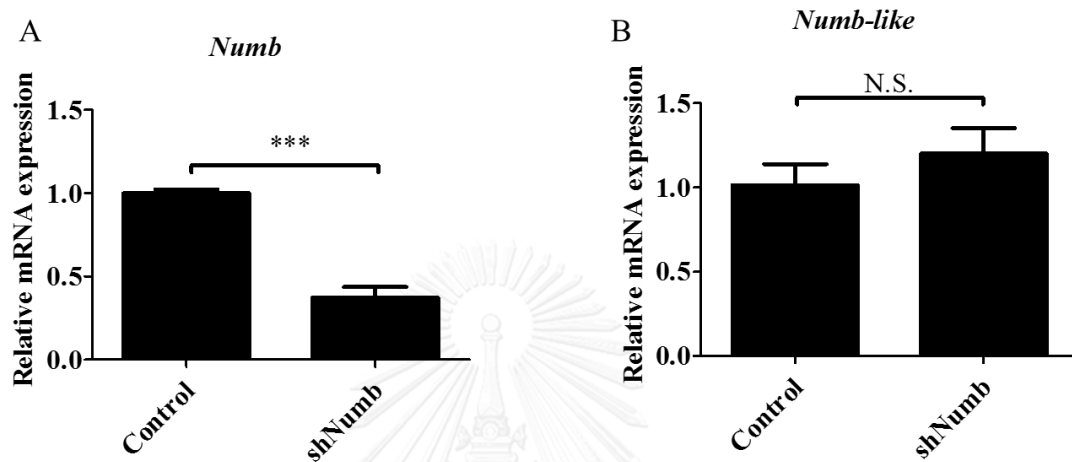
Figure 4.4 Specific silencing of Numb but not Numb-like by pMKO.1-shNumb-GFP plasmid

Numb mRNA (A) and *Numb-like* mRNA (B) expressions in GFP$^+$ BMMs containing control or shNumb plasmids were examined by qPCR. Data are means ± SEM from representatives of two independent experiments. ***$p<0.001$. N.S. indicates no statistical significance.

Because one of the functions of Numb is a negative regulator of Notch signaling, it was important to ensure that Numb still functioned as a regulator of Notch after an introduction of shNumb plasmids into the macrophages. Protein analysis by Western blot showed that there was an increase of cleaved Notch1 (Val1744), an indicator of Notch signaling activation, in LPS-stimulated macrophages lacking Numb protein (Figure 4.5A). We also found the expression levels of *Hes1* mRNA—one of the target genes of Notch signaling—increased in LPS-stimulated macrophages lacking Numb protein (Figure 4.5B). From these results, we confirmed the role of Numb as a negative regulator of Notch signaling by targeting it for degradation in macrophages still operated as usual.
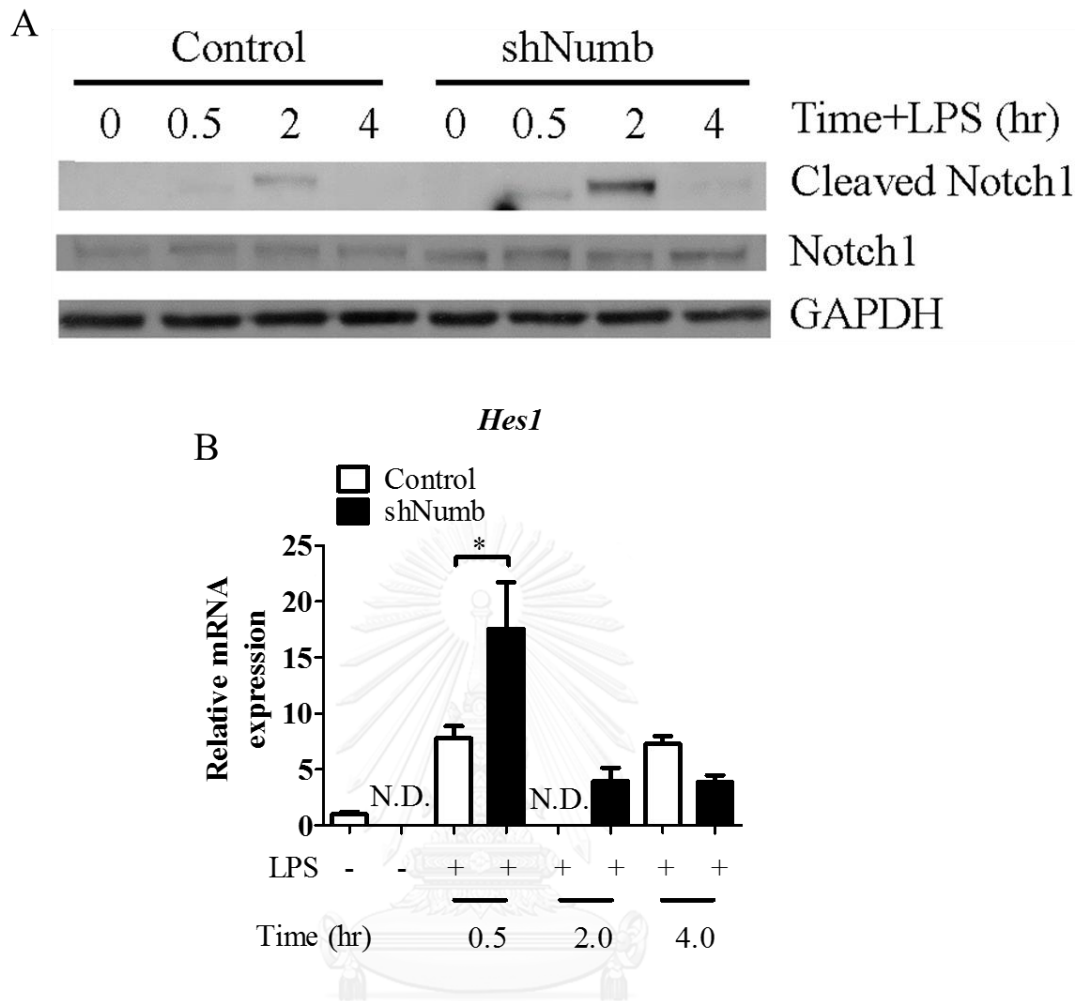
Figure 4.5 Numb functions as a negative regulator of Notch

Activation of Notch signaling was detected by a higher expression of cleaved Notch1 (Val1744) as shown by Western blot (A) and higher expression of *Hes1* mRNA as shown by qPCR (B) in *Numb*-deficient macrophages. Data are means ± SEM from representatives of two independent experiments. * $p<0.05$. N.D. indicates not detectable.

4.2 Numb is dispensable for development of macrophages *in vitro*

The role of Numb in neuronal cell development has been intensively studied in *Drosophila melanogaster* and various murine models (18, 89). Studies of Numb in cells of the immune systems have been driven by the fact that Numb functions antagonistically to Notch signaling. Based on the discovery revealing that Notch signaling altered T cell development and together with the knockdown system we

used to silences *Numb* in bone marrow hematopoietic stem cells, it was essential for us to test whether the bone marrows would develop normally to become macrophages in the absence of Numb. Staining cells with macrophage-specific surface markers, F4/80 and CD11b, we found that percentages of macrophages with *Numb* silencing expressed both the F4/80 and CD11b were comparable to those of the control macrophages as shown by flow cytometry analysis (Figure 4.6A and 4.6B). In addition, the levels of mean fluorescence intensity (MFI) of F4/80 and CD11b in both cell types were no different (Figure 4.6C and 4.6D). These results indicated that Numb was dispensable for macrophage development at least *in vitro* which was consistent with the earlier findings (22). The functional study of Numb in macrophages was further characterized in this study.
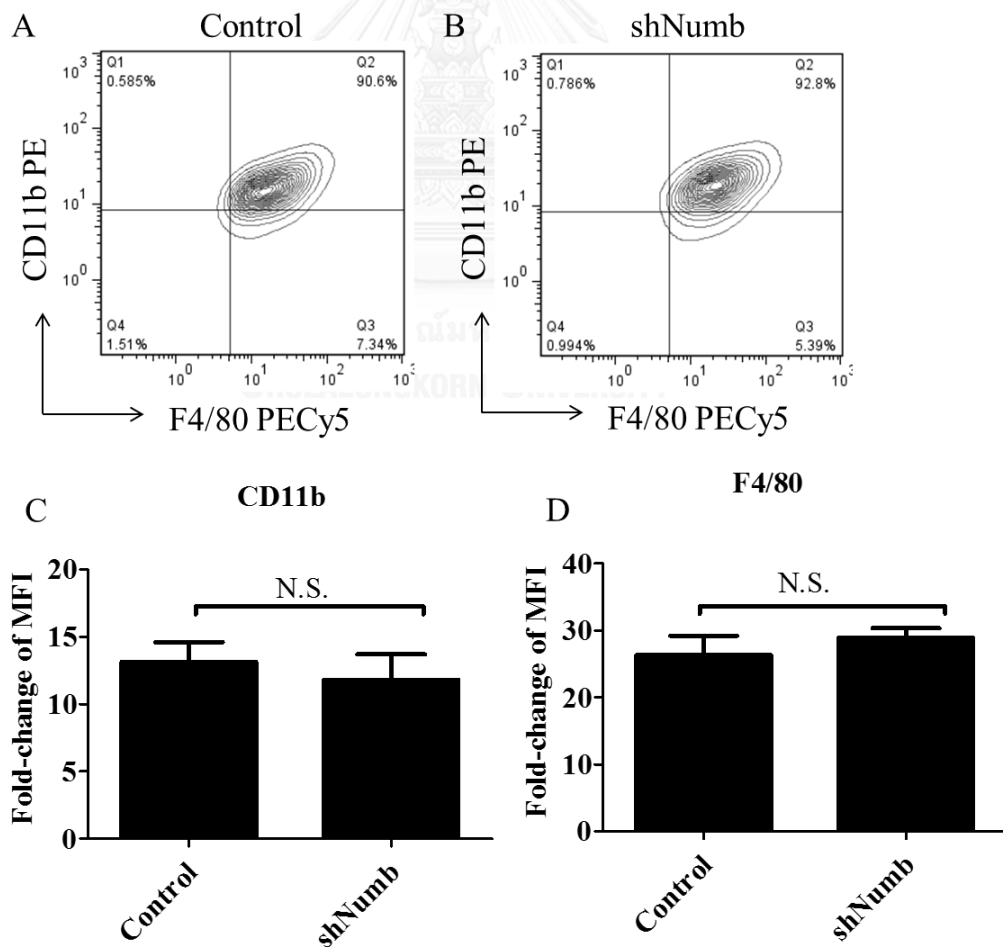
Figure 4.6 Numb does not affect development from bone marrows to macrophages

Macrophage-specific markers CD11b and F4/80 expressing on macrophages containing control (A) or shNumb (B) plasmids were measured by using flow cytometer and the mean fluorescence intensity of F4/80 and CD11b was calculated and represented as in (C) and (D), respectively. Data are means ± SEM from representatives of two independent experiments. N.S. indicates no statistical significance.

4.3 Loss of Numb reduces pro-inflammatory cytokine secretion in macrophages

Recently, the role of Notch signaling in macrophages have been reported, demonstrating that Notch signaling is required for optimal activation of macrophages and subsequent cytokine production upon stimulation by PAMP, such as LPS (7-9). Therefore, we hypothesized that macrophages with reduction of Numb protein might produce higher pro-inflammatory cytokines after LPS stimulation. To our surprises, *Numb*-knockdown macrophages secreted significantly less amount of TNFα, IL-6, and IL-12p70 after LPS stimulation as determined by ELISA (Figure 4.7A-C). In contrast, the amount of IL-10 (Figure 4.7D) in *Numb*-knockdown macrophages was higher significantly after 4 hrs of LPS stimulation.
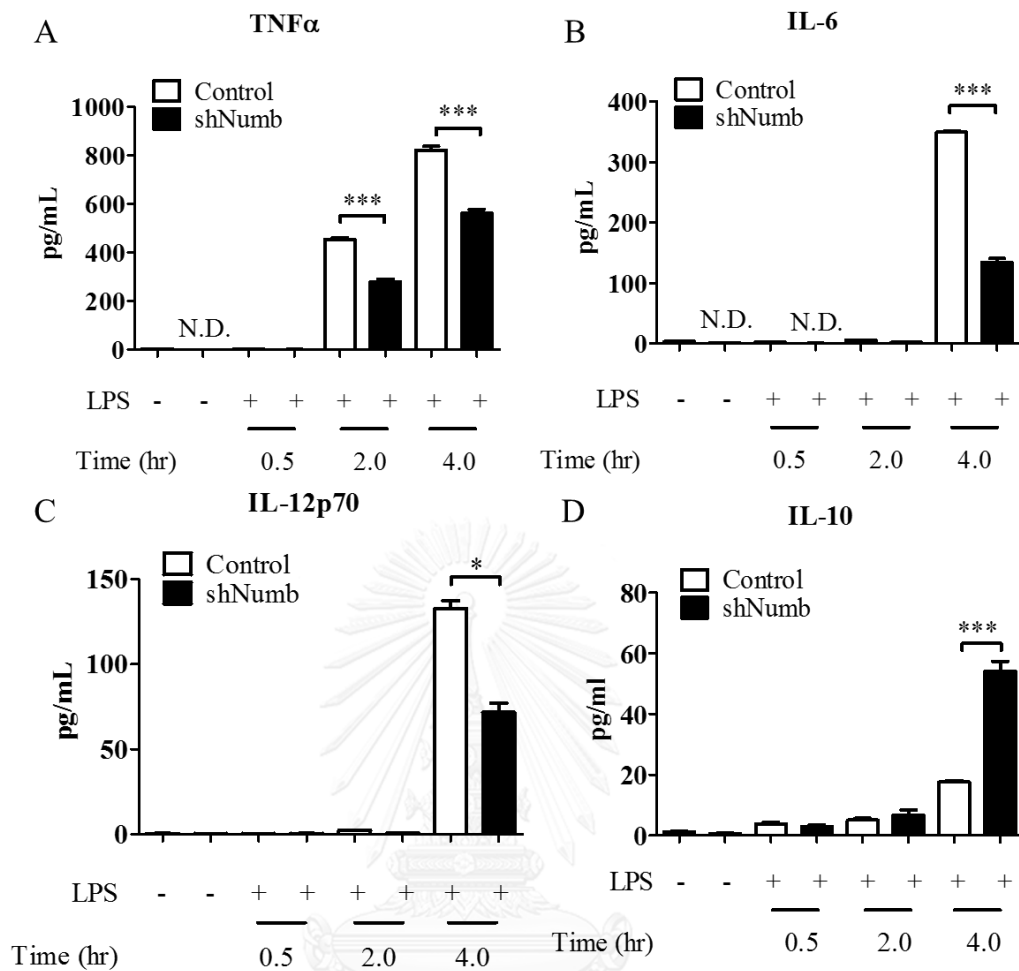
Figure 4.7 Loss of Numb reduces production of pro-inflammatory cytokines in
BMMs

Amount of TNFα (A), IL-6 (B), IL-12p70 (C) and IL-10 (D) from LPS-stimulated
BMMs containing control (white bar) or shNumb (black bar) plasmids were measured
by ELISA. Data are means ± SEM from representatives of two independent
experiments. * $p<0.05$; ***$p<0.001$. N.D. indicates not detectable.

Also, we measured the mRNA level of these cytokines in shNumb and control
macrophages in order to observe the effect of Numb on these cytokines at the
transcriptional level. We found the levels of *Il6* and *Il12p40* mRNA were down-
regulated in *Numb*-silenced macrophages whereas the level of *Tnfα* mRNA remained
comparable in both shNumb and control macrophages (Figure 4.8A-C). Beside the
pro-inflammatory cytokines, anti-inflammatory cytokine *Il10* increased in shNumb

macrophages after LPS stimulation, consistent with our previous cytokines results measured by ELISA (Figure 4.8D). These results suggested that the expressions of IL-6 and IL-12p70, but not TNFα, were regulated by Numb at the transcriptional level. Furthermore, Numb might negatively regulate IL-10 directly or indirectly by the reduction of pro-inflammatory cytokines.
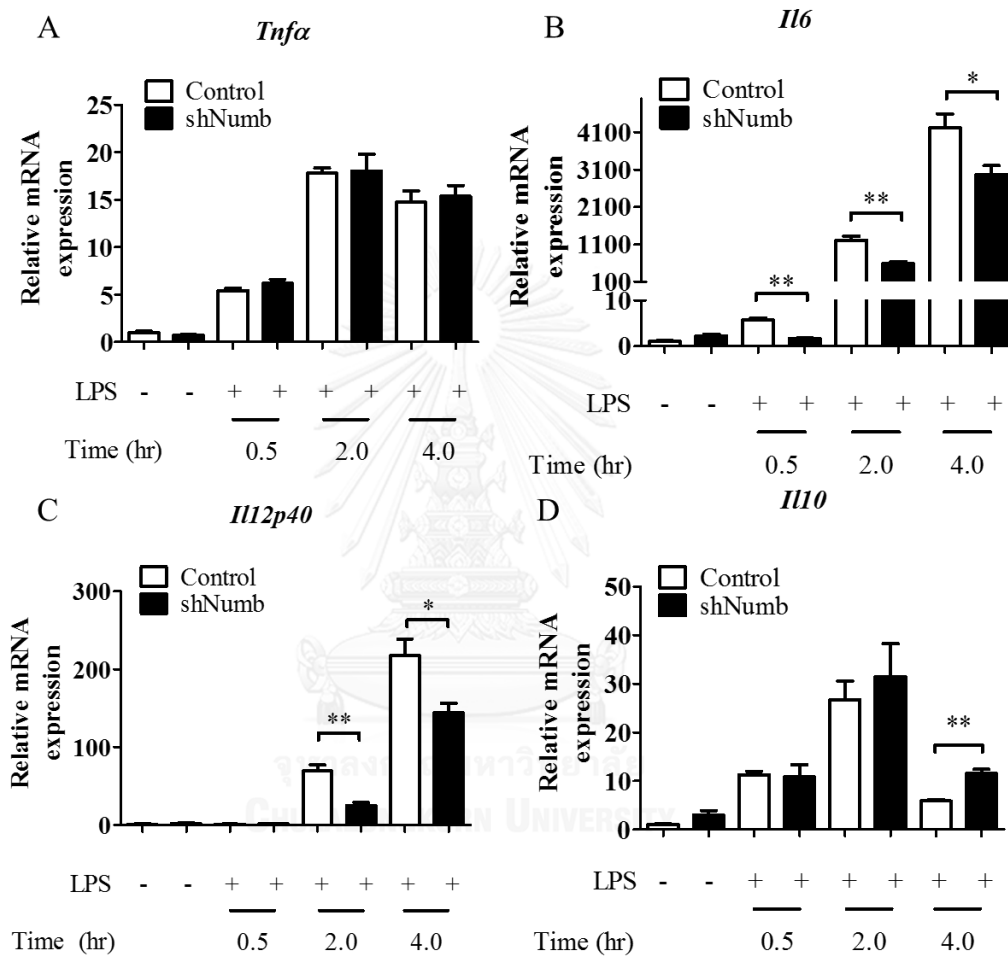
Figure 4.8 The relative mRNA level of pro- and anti-inflammatory cytokines in shNumb macrophages after LPS stimulation

Level of *Tnfα* (A), *Il6* (B), *Il12p40* (C) and *Il10* (D) mRNA expression from LPS-stimulated BMMs containing control (white bar) or shNumb (black bar) plasmid were measured by qPCR. Data are means ± SEM from representatives of two independent experiments. * $p<0.05$; ** $p<0.01$; *** $p<0.001$.

In addition to the changes of the production of pro- and anti-inflammatory cytokines, the levels of costimulatory molecules CD86 in macrophages required for T cell activation (91) were measured. We found that the CD86 expression level decreased significantly on the surface of shNumb macrophages compared with those of the control macrophages (Figure 4.9A). On the other hand, we found that the expression levels of MHC-II molecules, which are important for presenting antigens to CD4$^+$ T cells, remained unchanged on the surface of shNumb and control macrophages after stimulation with LPS (Figure 4.9B). Taken together, these results suggested that Numb played an important role in cytokine production and activation of macrophages through CD86 costimulatory molecules but not MHCII molecules in response to stimulation via TLR4.
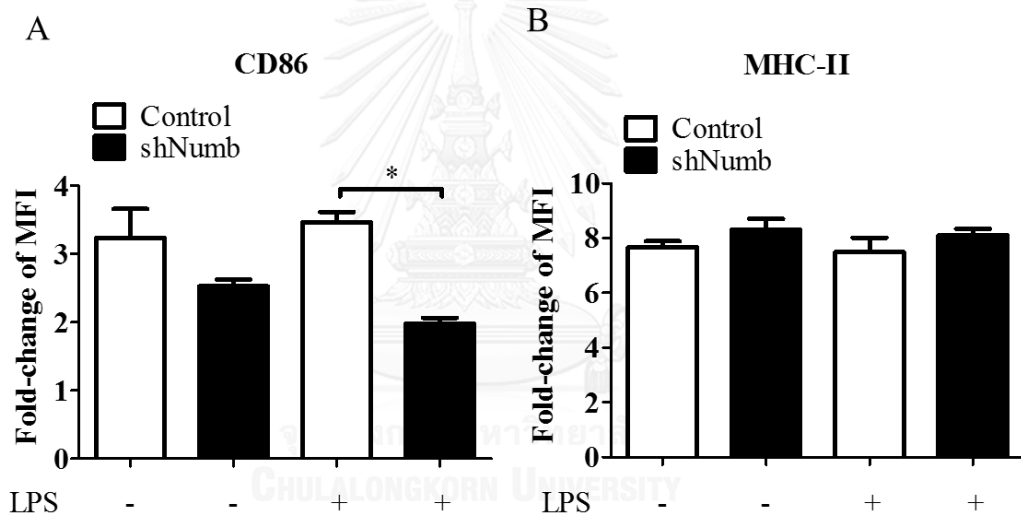
Figure 4.9 CD86 and MHC-II expression on shNumb macrophages

MFI of CD86 (A) and MHC-II (B) on the surface of macrophages containing control (white bar) or shNumb (black bar) plasmid were detected by flow cytometer after LPS stimulation for 6 hrs. Data are means ± SEM from a representative of two independent experiments. * $p < 0.05$.

4.4 Effect of *Numb* silencing on TNFα production is not dependent on the Notch signaling

Previously, we showed that Notch signaling was highly activated in shNumb macrophages after stimulation via TLR4. Evidence from our groups and others showed that Notch signaling was required for optimal activation of macrophages upon

LPS stimulation, resulting in a high production of pro-inflammatory cytokines and expression of other effector molecules (8, 9, 74, 92). Therefore, we hypothesized that Notch signaling might partially take a role in the regulation of pro-inflammatory cytokines by Numb in macrophages. In order to prove this hypothesis, we employed two different methods to inhibit Notch signaling, one method was to use a pharmacological approach by using γ-secretase inhibitor, called DAPT, to inhibit Notch signaling and the other method was to use a genetic approach by using siRNA specifically targeting *Rbpjκ*, a transcription factor target of Notch intracellular domain, to knockdown the transcriptional activity of the canonical Notch signaling pathway. As we expected, the amount of TNFα, IL-6, and IL-12p70 cytokines were decreased in macrophages after inhibition of Notch signaling using both methods, as determined by ELISA. These results indicated that the pro-inflammatory cytokines were partially under Notch signaling regulation. However, once we combined the silencing of *Numb* and inhibition of Notch signaling together, macrophages secreted IL-6 and IL-12p70 cytokines to a further lesser extent whereas the secretion of TNFα remained intact (Figure 4.10). Our results suggested that both IL-6 and IL-12p70 cytokines were regulated by both Numb and Notch signaling. In contrast, TNFα cytokine was regulated by only Numb because the level of secreted TNFα did not reduce further after Notch signaling was inhibited. Taken together, we demonstrated here that, despite the higher activation of the Notch signaling in shNumb macrophages, the expression of TNFα cytokine was largely under the influence of Numb in a Notch-independent manner. Furthermore, the IL-6 and IL-12p70 cytokines were under the influence of both Numb and Notch signaling.
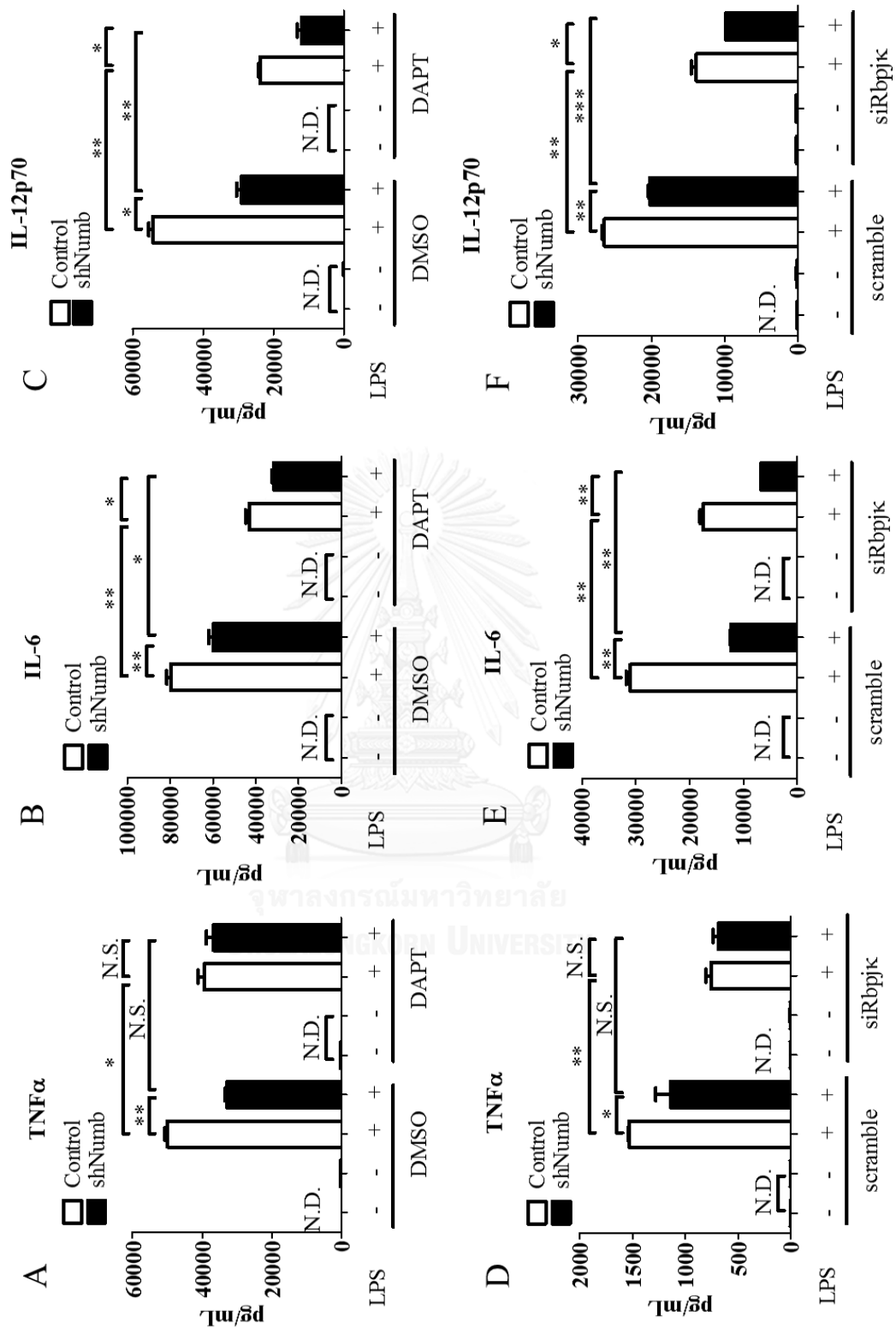
Figure 4.10 Levels of pro-inflammatory cytokines in macrophages in which Numb and Notch signaling are inhibited

TNFα (A), IL-6 (B), and IL-12p70 (C) cytokines production in macrophages containing control (white bar) or shNumb (black bar) plasmids that were inhibited of Notch signaling using 50 µM of DAPT. *Rbpjκ* in macrophages were silenced using scramble siRNA (white bar) or siRbpjκ (black bar) and they were measured for TNFα (D), IL-6 (E), and IL-12p70 (F) cytokines by ELISA. Data are means ± SEM from representative of two independent experiments. * $p<0.05$; ** $p<0.01$; *** $p<0.001$. N.D. indicates not detectable.

4.5 Numb regulates phosphorylation of p65 NF-κB and p38 MAPK upon LPS stimulation

In the past decades, the upstream signaling pathways regulating the production of pro-inflammatory cytokines such as TNFα, IL-6, and IL-12p70 have been extensively studied (1, 2). Our previous results showed that pro-inflammatory cytokines production was reduced in macrophage when *Numb* was silenced. Therefore, we hypothesized that the upstream signaling pathways, including MAPK and NF-κB pathways, would be altered in macrophages when *Numb* was silenced. Western blot analysis revealed that the phosphorylation levels of both p65 of NF-κB and p38 of MAPK were reduced in *Numb*-deficient macrophages after LPS stimulation. Meanwhile, the phosphorylation levels of p44/42 (ERK1/2) and SAP/JNK were similar in both cell types (Figure 4.11A). To confirm that these phenomena was caused specifically by Numb, we overexpressed Numb protein in macrophage-like cell line, called RAW264.7, and found that the phosphorylation levels of p38 MAPK and p65 NF-κB were increased after LPS stimulation (Figure 4.11B). Furthermore, we measured the level of TNFα and found that it significantly increased in Numb overexpressing RAW264.7 cells after LPS stimulation compared to those in the control cells (Figure 4.11C). Collectively, our result demonstrated that Numb regulated pro-inflammatory cytokine production by regulating phosphorylation of p38 of MAPK and p65 of NF-κB upon TLR4 stimulation and production of TNFα.
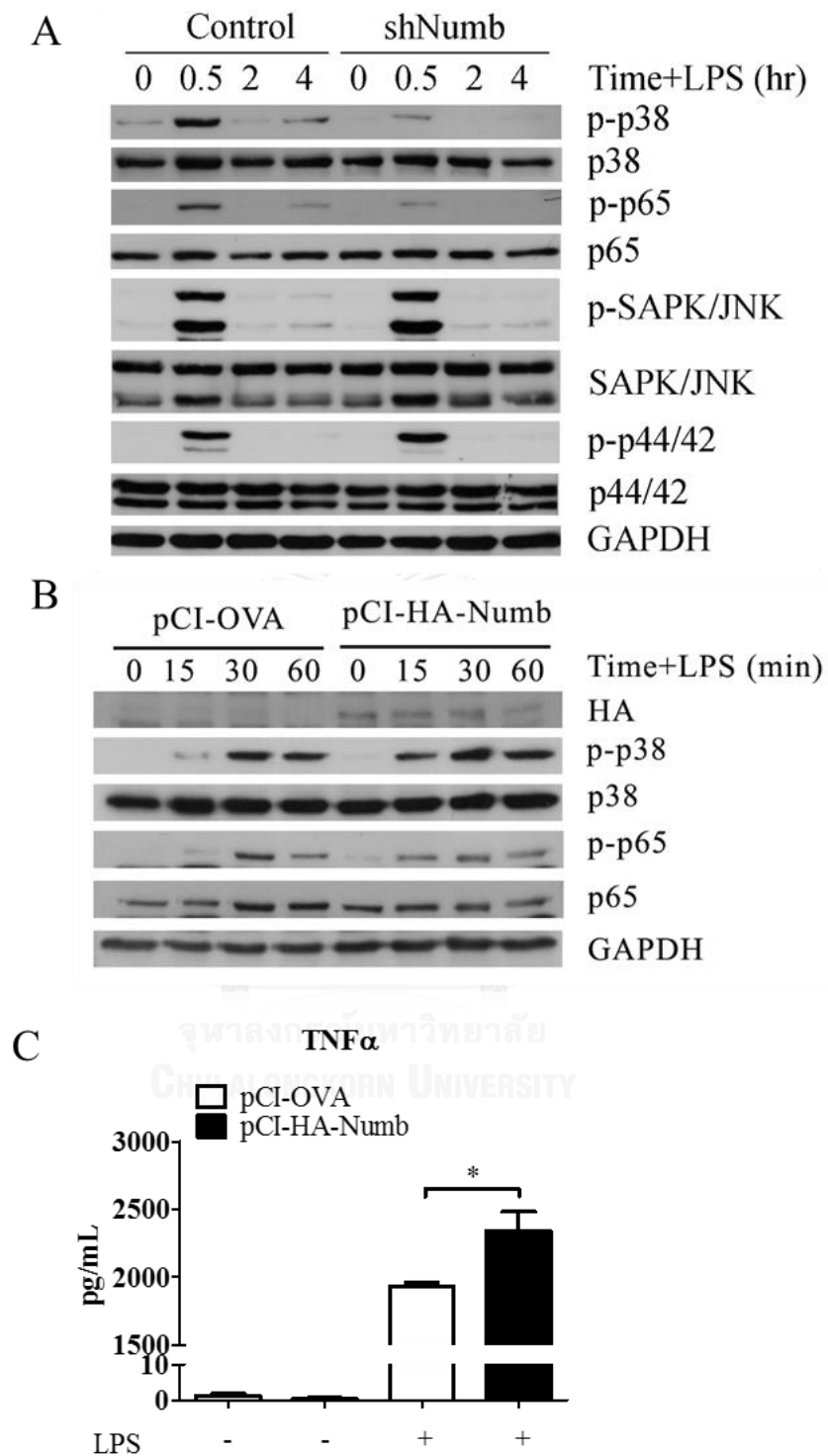
Figure 4.11 Numb regulates p65 NF-κB and p38 MAPK and downstream pro-inflammatory cytokines in macrophages upon LPS stimulation

Western blots of protein lysates from control or shNumb BMMs (A) and from

RAW264.7 overexpressing control plasmid pCI-OVA or pCI-HA-Numb (B) after

LPS stimulation were performed. (C) RAW264.7 cells as in (B) were treated with 100 ng/mL of LPS for 1 hr and TNFα cytokine was measured by ELISA. Data are representatives of two independent experiments. * $p<0.05$.

4.6 *Tnfα* mRNA degrades at a faster rate in macrophages with *Numb* silencing

Previously, our results showed that the mRNA levels of *Tnfα* were not altered in macrophages lacking of Numb protein, suggesting that *Tnfα*, unlike *Il6* and *Il12p40*, was not regulated at the transcriptional level. Recent studies by other groups demonstrated that *Tnfα* mRNA stability was regulated by p38 MAPK at post-transcriptional level (93, 94). Using *Tnfα* mRNA decay assay, we found that *Tnfα* mRNAs degraded at a faster rate (Figure 4.12A) and their half-life was significantly shorter (Figure 4.12B) in LPS-stimulated, *Numb*-silenced macrophages. *Il6* mRNA stability, in contrast, was not altered (Figure 4.12C). These results, together with our previous finding that p38 MAPK phosphorylation level was reduced in *Numb*-silenced macrophages, suggesting that Numb regulated TNFα production at the post-transcriptional level possibly through p38 of MAPK signaling pathway.
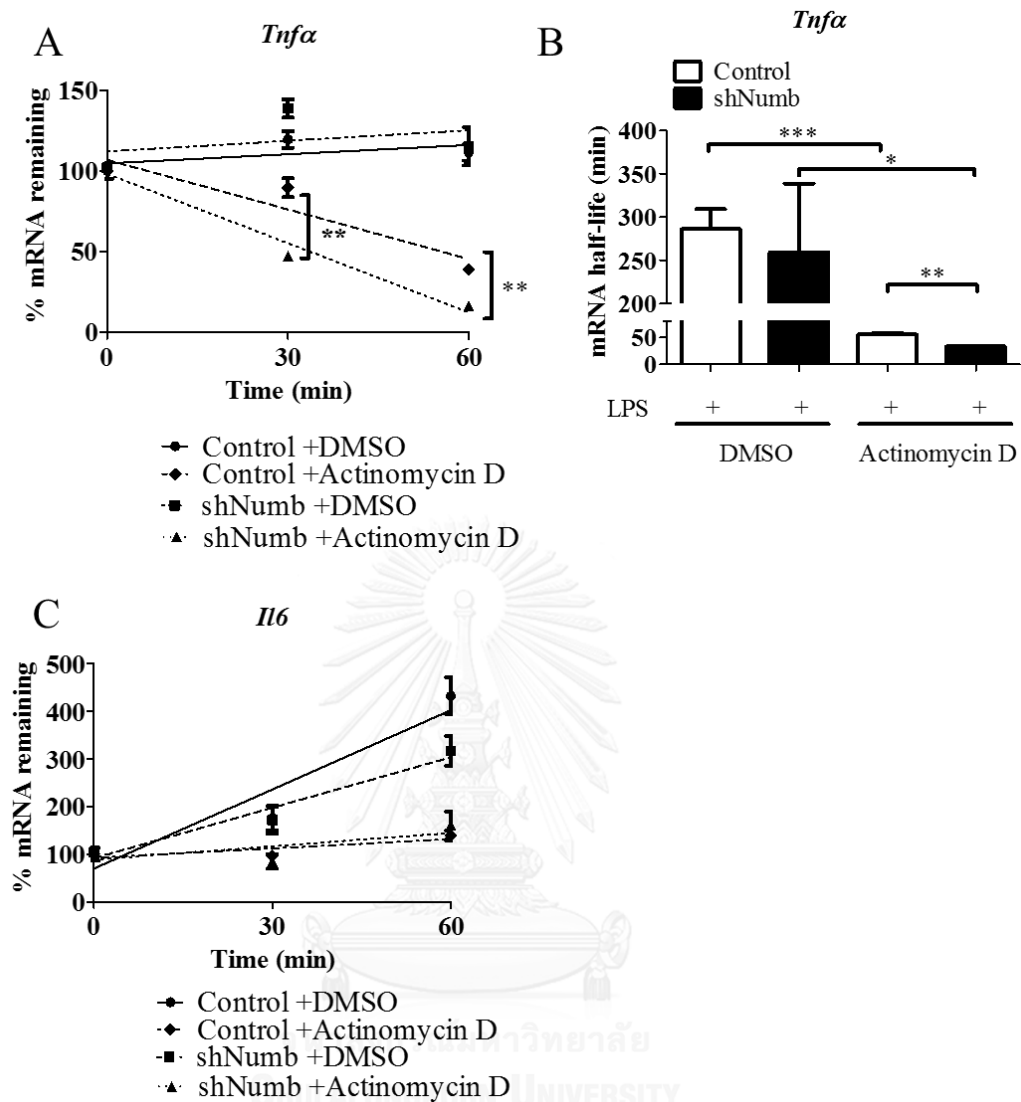
Figure 4.12 Numb regulates *Tnfα* mRNA stability but not other cytokines

(A) *Tnfα* mRNA levels from control or shNumb BMMs pulsed with 100 ng/mL *E. coli* LPS and chased with 20 µg/mL of actinomycin D or vehicle control (DMSO) for indicated time points was quantified by qPCR. (B) Half-life of *Tnfα* mRNAs from each of the macrophage samples was calculated from linear regression equation obtained from (A). (C) *Il6* mRNA stability from control or shNumb BMMs as shown

in (A). Data are means ± SEM from a representative of two independent experiments. * $p<0.05$; **$p<0.01$; ***$p<0.001$.

4.7 Numb interacts with Itch and the expression of Itch increases in macrophages when *Numb* was silenced

Several groups previously demonstrated that Numb and Itch were required for degradation of various proteins, such as Notch receptors (13) and GLI1 protein (95) in various cell types. Itch is a negative regulator of inflammation in macrophages that have been demonstrated both *in vitro* and *in vivo* models (70, 71). Moreover, Itch can inhibit the activation of p38α of MAPK signaling pathway in skin inflammation (71). Therefore, we hypothesized that Numb might regulate p38 of MAPK signaling pathway through interaction with Itch. To elucidate the mechanism underlying regulation of p38 MAPK by Numb, we performed co-immunoprecipitation by using Numb-specific antibody to pull down the endogenous Numb and other protein binding partners from unstimulated or LPS-stimulated macrophages. Using anti-Itch antibody as a probe, we found that Itch bound to Numb in resting macrophages. After LPS stimulation, however, Itch dissociated from Numb (Figure 4.13A). We also observed a higher expression of Itch in shNumb macrophages after LPS activation, comparing with that that of the control cells (Figure 4.13B). To compliment this observation, we transiently overexpressed Numb in RAW264.7 cells and stimulated with LPS. As expected, we found that Itch expression was decreased, comparing with that of the control cells (Figure 4.13C). Taken together, these results suggested that Numb bound to Itch and, in turn, regulated its activity, possibly by preventing Itch from regulatory function that controls phosphorylation of p38 MAPK. Moreover, Numb also negatively regulated expression of Itch in macrophages after LPS stimulation.
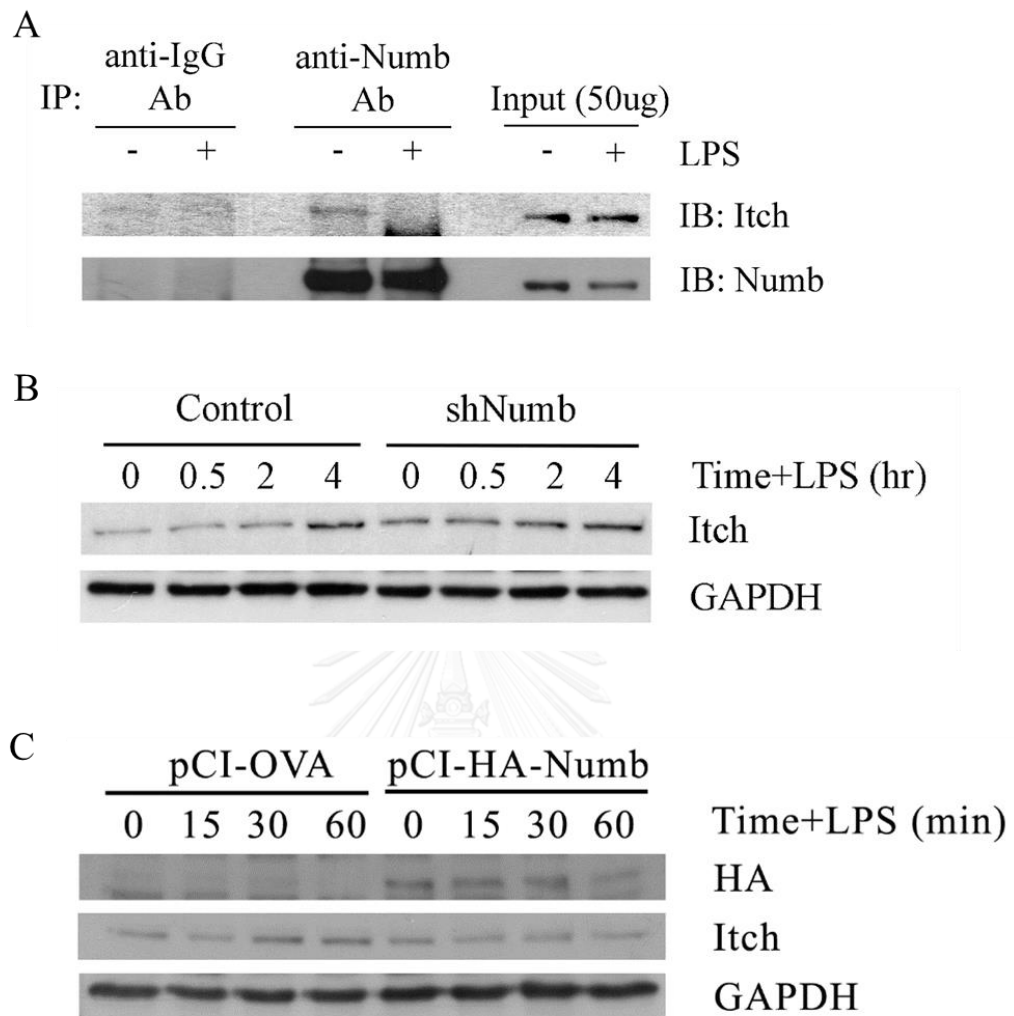
Figure 4.13 Numb interacts with Itch and Itch expression increases in the absent of Numb in macrophages

(A) Co-immunoprecipitation results showing interaction between Numb and Itch in BMMs. (B) Expression of Itch in control or shNumb BMMs after LPS stimulation. (C) Expression of Itch in RAW264.7 cell line transiently transfected with pCI-OVA or pCI-HA-Numb plasmids and stimulated with LPS. Data are representative of two independent experiments.

4.8 Proteomics analysis reveals a global regulatory effect of Numb in macrophages

Our results until now demonstrated that Numb can function as a positive regulator of TNFα, IL-6 and IL-12p70, and all of the cytokines required Notch

signaling for optimal expression in LPS-stimulated macrophages. In addition, we demonstrated that Numb interacted with Itch and possibly regulated p38 MAPK phosphorylation. However, whether Numb also regulates other proteins in macrophages remains to be discovered. To study the effect of Numb on other proteins important for effector functions in macrophages, we employed a proteomic approach by using label-free LC/MS/MS technique to uncover the changes of proteins from the samples collected from control or shNumb macrophages that were unstimulated or stimulated with LPS for 30 mins. The expression of Numb in our samples was examined prior to preparation of the protein samples for SDS-PAGE and trypsin digestion (Figure 4.14A). We found that Numb expression was decreased in shNumb both control and LPS-stimulated macrophages, comparing with those of the control cells. After LC/MS/MS analysis, we identified 758 proteins that were differentially expressed in all of our samples. Among them, 551 proteins were annotated for their names and functions (Figure 4.14B). We categorized the proteins into groups by focusing on the proteins whose function was related to inflammation as determined by Gene Ontology (GO) enrichments for biological processes, a feature provided in the web-based software STRING v9.1 (96). Proteins involved in regulation of MAPK and NF-κB signaling pathways and TNFα production were categorized and depicted as a heatmap (Figure 4.14C). It revealed that a number of the inflammation-related proteins were down-regulated in shNumb macrophages after LPS stimulation, which was consistent to our previous results demonstrating the reduction of pro-inflammatory cytokines and phosphorylation of p38 MAPK and p65 NF-κB. To validate our data, we performed qPCR to examine the mRNA expression levels of some candidate proteins, including Akt1, Map3k10, and Ticam1. As a result, the mRNA levels of each protein correlated with its protein expression as quantitatively determined by proteomic analysis (Figure 4.14D-F). Moreover, we performed Western blot experiment and found that Akt1 expression was higher in LPS-stimulated BMMs containing shNumb plasmid than that in the control cells. (Figure 4.14G). Collectively, our results demonstrated that Numb exerted a global effects in macrophages, turning them to become less inflammatory macrophages, through negative regulation of Akt1 and positive regulation of p38 MAPK and p65 NF-κB signaling pathways.
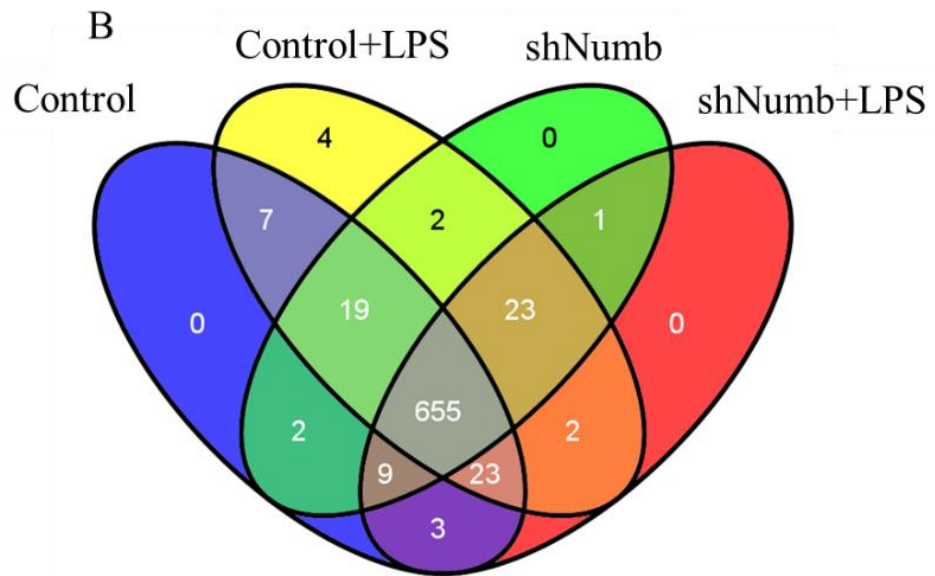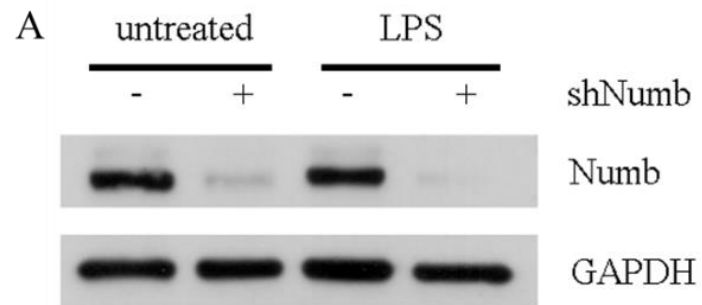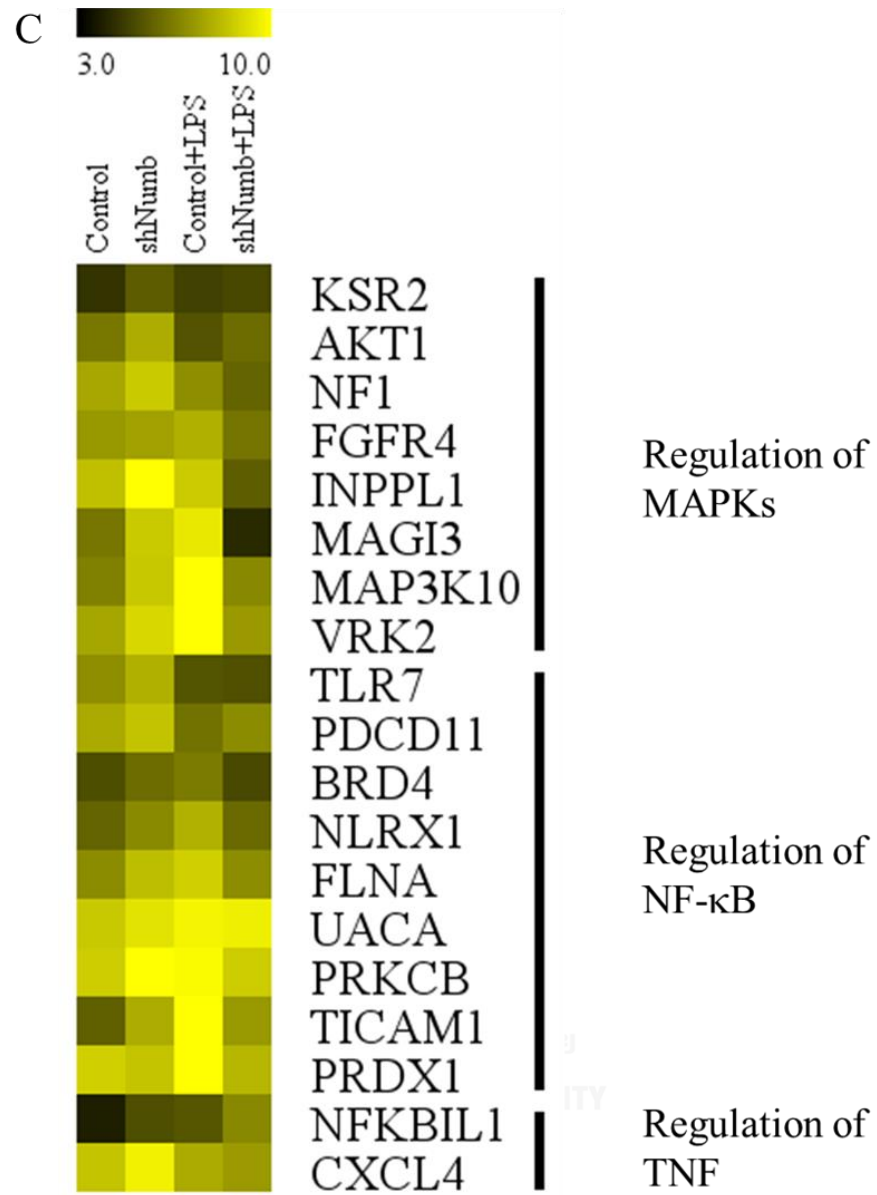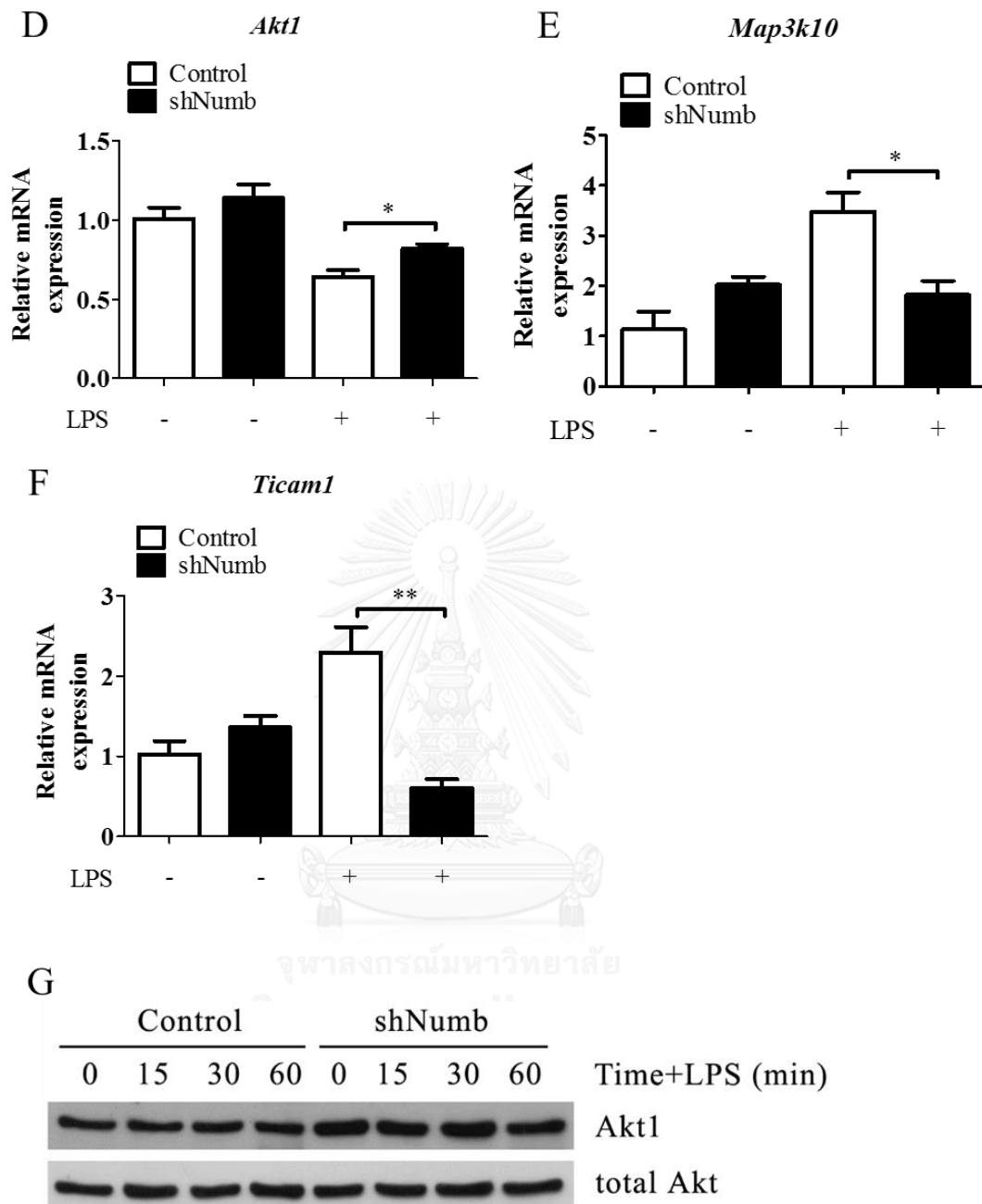
Figure 4.14 Proteomics analysis reveals a regulatory effect of Numb in macrophages upon LPS stimulation

(A) Western blot results showing Numb expression in untreated or LPS-stimulated BMMs containing control or shNumb plasmids prior to LC/MS/MS experiment. (B) A Venn-diagram representing the proteins that were differentially expressed in all BMM samples as described in (A). A heatmap representing amount of proteins identified in (B) whose function was related to regulation of MAPK and NF-κB

signaling pathways and TNF production. (D) mRNA levels of some candidate proteins chosen from the list in (C). (G) Expression of Akt1 in BMMs containing control or shNumb plasmid after LPS stimulation as determined by Western blot. Data are means ± SEM from a representative of two independent experiments. * $p<0.05$; **$p<0.01$.

Because Numb is a multifunctional protein having various binding partners, this allows Numb to play different roles in a cellular context dependent manner (57). To determine which proteins from our proteomics data interacted with Numb, we generated a protein-protein interaction network using STRING v9.1 to find the proteins that potentially interact with Numb and also related to inflammation, based on a set of proteins identified in the Figure 4.14C. Unfortunately, no single protein from the list could potentially bind with Numb. However, the prediction network revealed Akt1 as a protein that potentially interacted with p65 NF-κB (RelA) and p38 MAPK (MAPK14), suggesting that Akt1 may play a key role in regulation of pro-inflammatory cytokines in macrophages (Figure 4.15).
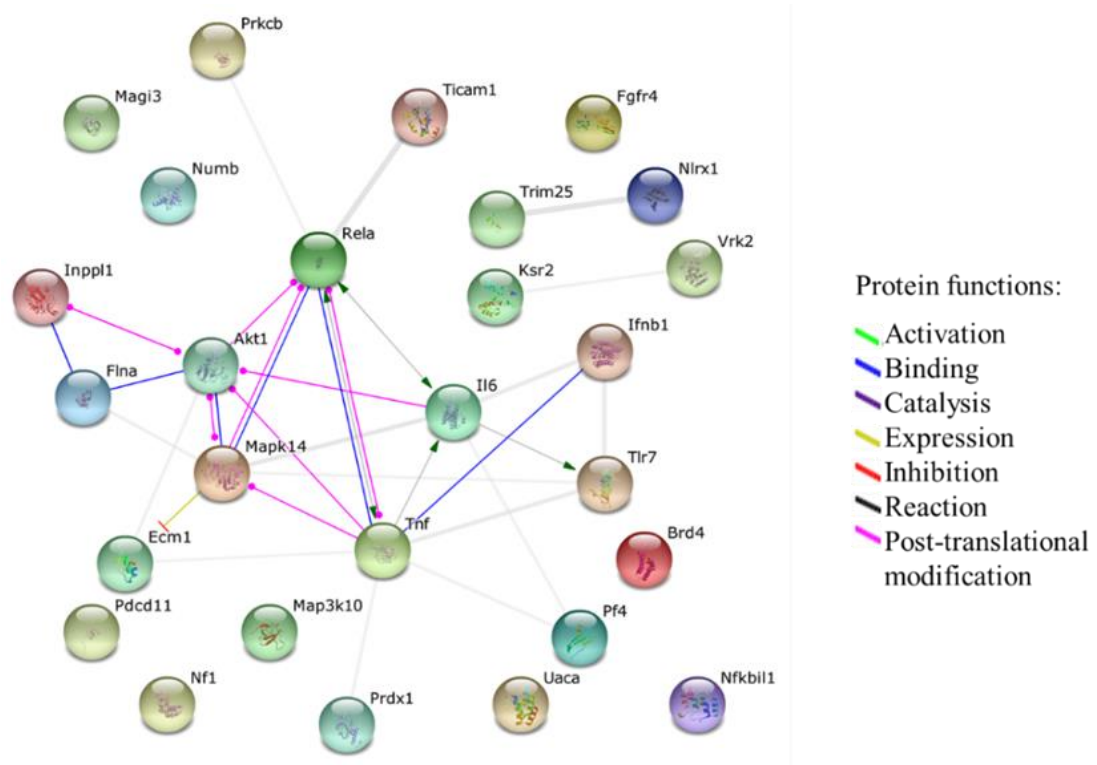
Figure 4.15 A protein-protein interaction network

A network of protein-protein interaction generated by STRING v9.1 showing the interaction of proteins from proteomics data whose function was related to inflammation. Each node represents one protein. Each edge between two nodes represents a relationship of the two proteins and the details were described in protein functions legend as shown in the figure.

To further support our finding, we examined phosphorylation levels of Akt (at Thr308) in shNumb macrophages after LPS stimulation and found that its phosphorylation level of Akt (Thr308) was higher, comparing with that of the control cells. On the other hand, RAW264.7 cells overexpressing Numb exhibited lower Akt (Thr308) phosphorylation level (Figure 4.16), comparing with that of the control cells. Collectively, our results suggest a novel role of Numb as a regulator of pro-inflammatory cytokine production in macrophages by interacting with Itch and regulating p38 MAPK, p65 NF-κB, and Akt signaling pathways.
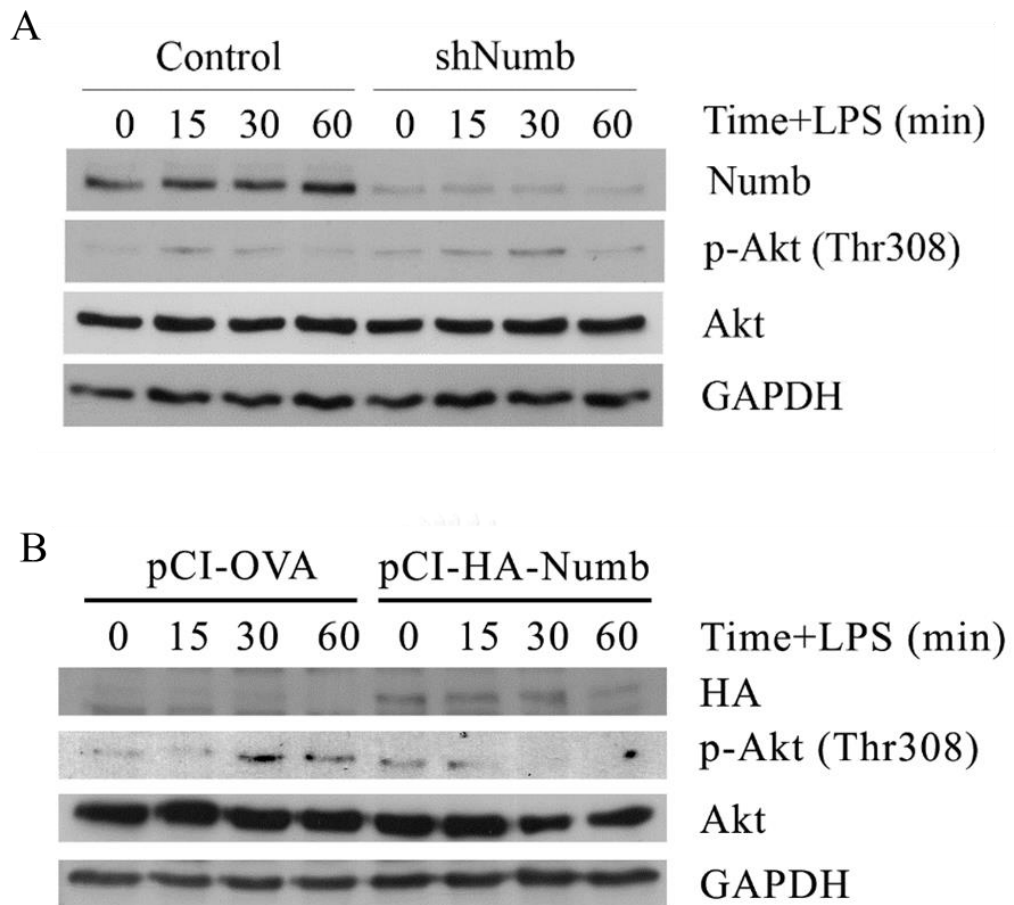
Figure 4.16 Numb regulates Akt in macrophages after LPS stimulation

(A) Western blot results of protein lysates from untreated or LPS-stimulated BMMs containing control or shNumb plasmids showing the different activation of Akt (Thr308) in each sample. (B) Lysates from RAW264.7 cells transiently transfected with the control pCI-OVA or pCI-HA-Numb were also analyzed for Akt activation (Thr308) by Western blot.

4.8 Itch functions as a negative regulator of Notch signaling in macrophages

Previously, Itch has been reported as a negative regulator of inflammation in macrophages and as a mediator of inflammation-related diseases (28, 70, 71). Although the role of Itch as a negative regulator of Notch signal in other cell types has been demonstrated (33, 72), its role in macrophages has not been addressed. Here, we began with an examination of the mRNA and protein expression level of *Itch* in

macrophages in response to LPS. We found that the levels of mRNA were reduced when macrophages were stimulated with LPS. However, its protein levels were barely changed (Figure 4.17A-B). These results suggested that Itch mRNA expression was down regulated in activated macrophages, but its protein might be stabilized or less prone to degradation after LPS stimulation.

Because Itch is a negative regulator of Notch signaling, it was interesting to see whether silencing of Itch would impact Notch signaling in macrophages. We set the experiment using siRNA to transiently silence *Itch*, stimulated with LPS for indicated time points and observed the silencing effect of *Itch* on one of the Notch signaling receptors, Notch1, its target gene, *Hes1* mRNA. The results showed that the level of Notch1 (Figure 4.17C) and *Hes1* mRNA (Figure 4.17D) were increased in LPS-stimulated macrophages comparing to those of the control cells. Taken together, Itch functions as a negative regulator of Notch signaling pathway in macrophages.
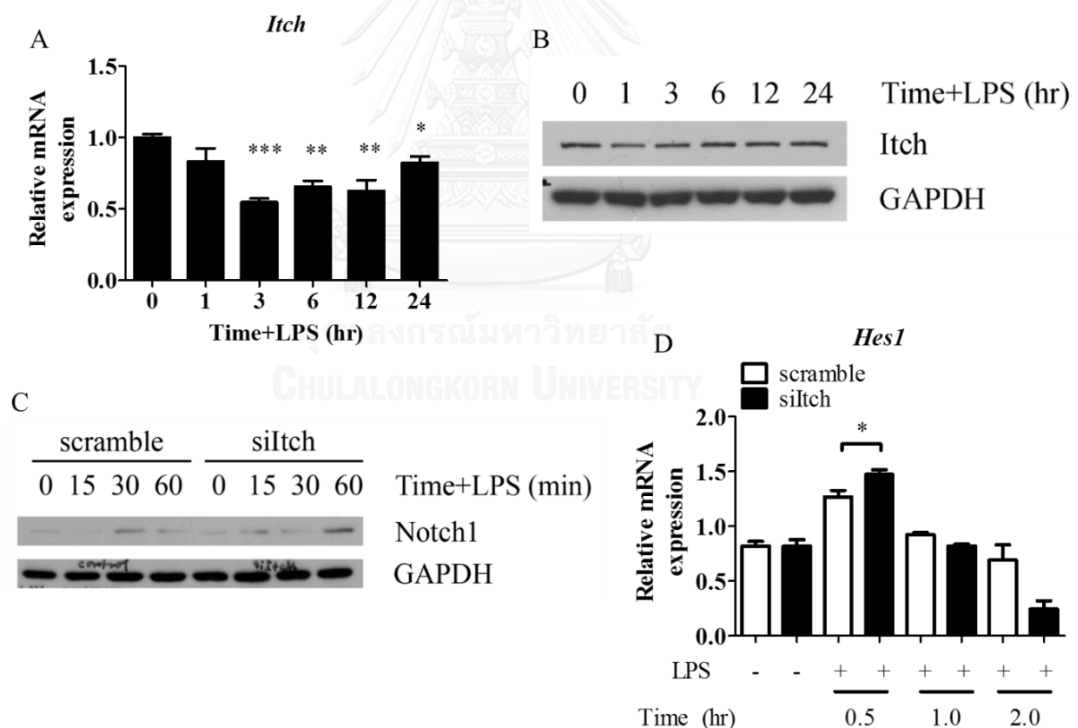
Figure 4.17 Itch expression in macrophages and it functions as a negative regulator of Notch signaling

(A) Expression of *Itch* mRNA was measured by qPCR and (B) expression of Itch protein was measured by Western blot in BMMs after LPS stimulation. (C) Expression of Notch1 and (D) *Hes1* mRNA in BMMs with scramble (white bar) or

siItch (black bar) siRNA and stimulated with LPS. Data are means ± SEM from a representative of two independent experiments. * $p<0.05$.

4.9 Itch regulates pro-inflammatory cytokines through MAPK signaling pathways in macrophages

Itch has been reported as a negative regulator of inflammation in macrophages and skin diseases (70, 71). Thus, we hypothesized that Itch might also negatively regulate the pro-inflammatory cytokines in LPS-stimulated macrophages. Although we could effectively silence *Itch* (approximately 70-80% silencing efficiency, as determined by Western blots (Figure 4.18A)), the results of *Itch*-silenced macrophages after LPS stimulation were quite surprising. We found a significant reduction of TNFα, IL-6 and IL-12p70 cytokines in *Itch*-silenced macrophages when comparing to those of the control cells (Figure 4.18B-D). Furthermore, we examined the regulatory signaling pathways located upstream of the pro-inflammatory cytokines, including MAPKs and NF-κB. There was no change in phosphorylation levels of p65 NF-κB and p44/42 MAPK in siItch macrophages comparing to those of the control cells. In contrast, the phosphorylation levels of p38 and JNK MAPKs were reduced in *Itch*-silenced macrophages after 1 hr of LPS stimulation (Figure 4.18E). Collectively, these results suggested that Itch might regulate the production of pro-inflammatory cytokine through phosphorylation of p38 and JNK of the MAPK signaling pathways.
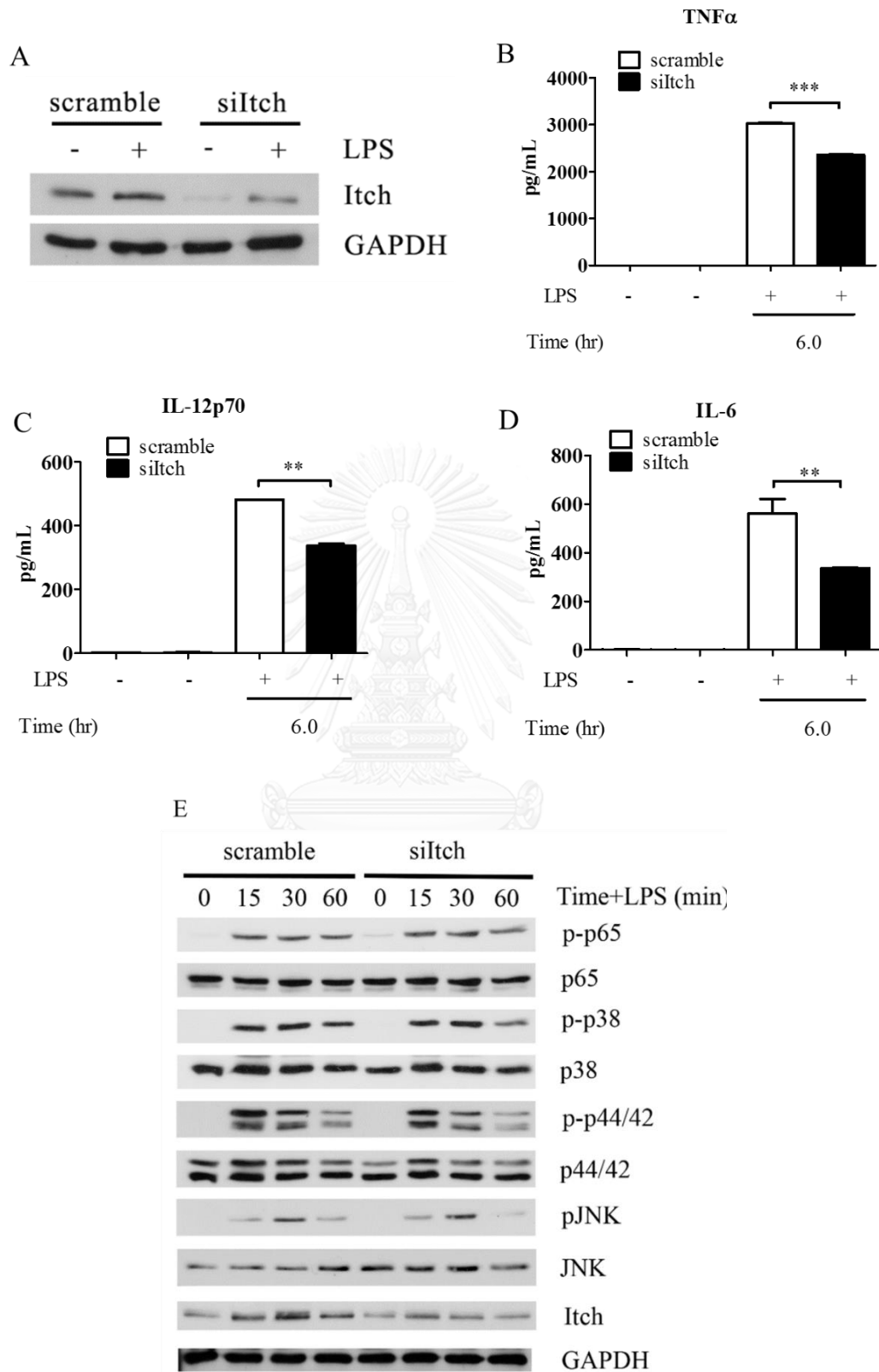
Figure 4.18 Itch regulates production of inflammatory cytokines through p38 and JNK MAPK signaling pathways in macrophages after LPS stimulation

(A) Expression of Itch proteins in BMMs treated with scramble (white bar) or siItch (black bar) siRNA. The culture supernatants from (A) were measured for amount of TNFα (B), IL-6 (C), and IL-12p70 (D) by ELISA. Data are means ± SEM from a representative of two independent experiments. **$p<0.01$; ***$p<0.001$. (E) Phosphorylation levels of NF-κB and MAPKs in BMMs treated with scramble or siItch siRNA were shown as Western blots. Data are representatives of two independent experiments.

4.10 Itch modulates pro-inflammatory cytokines via Notch signaling pathways

Our group and others reported that an inhibition of Notch signaling regulated production of pro-inflammatory cytokines through NF-κB and MAPKs signaling pathways in macrophages after LPS stimulation (9, 97), indicating that Notch signaling operates at upstream of these regulatory signaling pathways. In addition, we previously demonstrated that Itch also regulated the pro-inflammatory cytokines through p38 and JNK of MAPK signaling pathways. Therefore, we hypothesized that the reduction of phosphorylation levels of p38 and JNK MAPKs and the subsequent reduction of the pro-inflammatory cytokines were mainly influenced by Notch signaling. To investigate this hypothesis, we performed double silencing using two different siRNA targeting *Itch* and *Rbpjκ*, simultaneously. Although macrophages were successful in simultaneous silencing of both genes (Figure 4.19A), we found that production of TNFα after LPS stimulation was not further reduced, comparing with that of the macrophages silenced of *Rbpjκ* alone (Figure 4.19B). This result suggested that TNFα was rather dependent on Notch signaling than Itch. Meanwhile, the production of IL-6 and IL-12p70 were further reduced to a lesser extent in double knockdown macrophages after LPS stimulation comparing with those of the macrophages silenced of the *Rbpjκ* alone (Figure 4.19C-D), indicating that their production was under equal influence of Notch signaling and Itch. Taken together, we demonstrated that the Notch signaling was required for TNFα, IL-6 and IL-12p70 production in *Itch*-silenced macrophages.
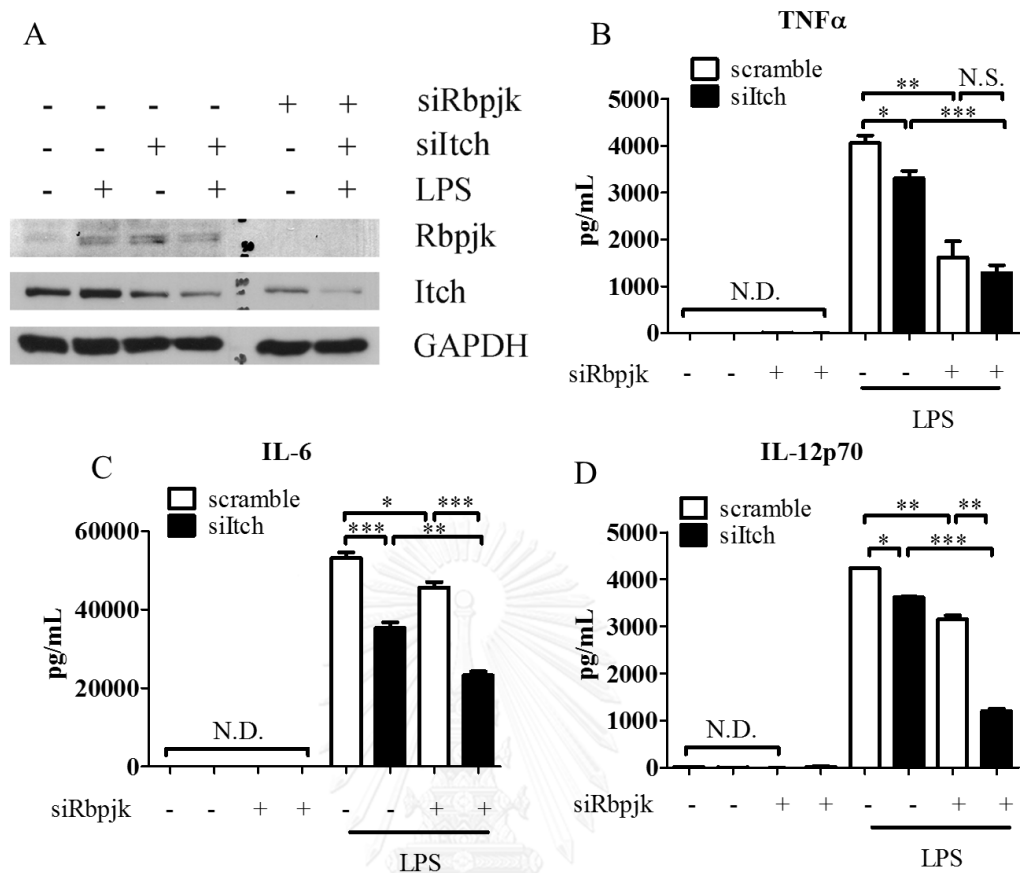
Figure 4.19 Itch and Notch regulated pro-inflammatory cytokines differently

(A) Expression of Rbpjκ and Itch were shown in Western blots using protein lysates from BMMs that were silenced with siRNA targeting *Rbpjκ* or *Itch* or both. The BMMs were stimulated with 100 ng/mL *E. coli* LPS for 1 hr. Amounts of TNFα (B), IL-6 (C), and IL-12p70 (D) cytokines from BMMs simultaneously knocked down of *Itch* and *Rbpjκ* after stimulation with LPS for 6 hrs were measured by ELISA. Data are means ± SEM from a representative of two independent experiments. * $p<0.05$; **$p<0.01$; ***$p<0.001$. N.S. indicates no statistical significance. N.D. indicates data were not detectable.

4.11 Itch does not alter phagocytosis of macrophages after LPS stimulation

We previously demonstrated that Itch modulated pro-inflammatory cytokine production in macrophages. However, other macrophage functions additional to the production of pro-inflammatory cytokines remain to be investigated. Phagocytosis of

macrophages is a hallmark of their effector functions that is dependent on the activation of cells through different TLRs (98, 99). *E. coli* is a gram-negative bacteria whose cell wall is mainly composed of lipopolysaccharide (LPS) recognizable by TLR4. We tested the phagocytic ability of macrophages in the absence of *Itch* by co-incubation with *E. coli*. The percentages of *E. coli* phagocytosis in *Itch*-silenced macrophages was comparable to that of the control macrophages (Figure 4.20), indicating that *Itch* deficiency did not alter macrophage phagocytosis.
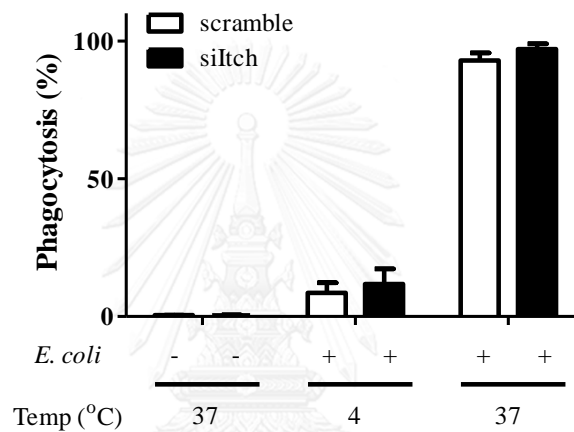
Figure 4.20 Itch does not affect phagocytosis of *E. coli*

F4/80+ BMMs with scramble or siIch siRNA were challenged with Alexa 488-labeled *E. coli* (K-12 strain) at MOI of 10 for 1 hr at indicated temperature. The number of BMMs containing engulfed *E. coli* were determined by using flow cytometer and converted to percentage of phagocytosis. White bars indicate BMMs treated with scramble siRNA and black bars indicate BMMs treated with siItch siRNA.

CHAPTER V
DISCUSSIONS

To our knowledge, the function of Numb in activated macrophage has never been documented. The roles of Numb in activation of macrophages, as demonstrated in this study, were found to be Notch-dependent and Notch-independent. In other cell types, Numb exerts a diverse effect on many proteins regulating signaling pathways. Some of the signaling proteins may dictate the inflammation in macrophages. First of all, our data showed that the amount of cleaved Notch1 (V1744) and the mRNA level of *Hes1* were higher in LPS-stimulated, *Numb*-silenced macrophages comparing to those of the control cells. These results confirm the role of Numb as a negative regulator of Notch signaling. They are also consistent with reports by others demonstrating that Numb is a negative regulator of Notch signaling *in vitro* and *in vivo* in other cell types (13, 100). Thus, we are the first to show that Numb is also a negative regulator of Notch signaling in macrophages.

We found that an activation of Notch signaling after *Numb* silencing in bone marrows did not affect the differentiation from bone marrows to macrophages. This suggests a dispensable role of Numb in hemopoietic cell development. In agreement with our results, study by other groups showed that the combined knockout of *Numb* and *Numb-like* genes *in vivo* had no effect on phenotypes of the cell compartments, such as T cells, B cells, and macrophages which are normally developed from hematopoietic stem cells (22). Moreover, a transgenic overexpression of Numb in T cells results in a reduction of Notch1 target genes but does not alter T cell development, cell cycle, and survival (104). An unequal distribution of Numb in $CD8^+$ T during virus infection causes the cell to divide asymmetrically in which one daughter cell becomes terminally differentiated effector $CD8^+$ T cells and the other becomes memory $CD8^+$ T cells (105). Collectively, our results and reports by others confirm that Numb is dispensable for development of hematopoietic cells including macrophages, and that the function of Numb is cell context-dependent.

We demonstrated that silencing of *Numb* in macrophages resulted in a reduction of pro-inflammatory cytokines, including TNFα, IL-6, and IL-12p70, through p38 of MAPK and p65 of NF-κB signaling pathways, regardless of an

activation of Notch signaling. These results suggest a Notch-independent role of Numb in regulation of pro-inflammatory cytokines at the upstream of p38 MAPK and p65 NF-κB signaling pathways. To support our data, reports by other groups reveal that Itch is a negative regulator inflammation by inducing ubiquitin-mediated degradation of TAK1 and TAB1—adaptor proteins required for activation of NF-κB and MAPK signaling pathways (70, 71, 106). For example, a study in tumor-associated macrophages showed that Itch and a deubiquitinated enzyme, called Cyld, formed a complex that mediated TAK1 proteasomal degradation, attenuating the production of pro-inflammatory cytokines as a result (70). Another study demonstrated that Itch directly interacted with TAB1, targeting it for proteasomal degradation and resulting in reduction of p38α MAPK phosphorylation in macrophages (71). Additionally, we showed here that Itch expression increased in *Numb*-silenced macrophages after LPS stimulation. Our data together with reports by other groups support the role of Itch as negative regulator of inflammation in macrophages.

A number of substrates, including Notch and Numb, bind to the four WW domains of Itch (107). We demonstrated that Numb directly bound to Itch in resting macrophages. Our results are consistent with the study by McGill and McGlade (13) demonstrating that Numb and Itch directly interacted through WW1/2 domains of Itch. These evidences suggest that sequestering by Numb via WW1/2 of Itch may prevent Itch from functioning as a regulator of the pro-inflammatory cytokine production. Also, we found that the interaction between Numb and Itch was abolished after LPS stimulation in macrophages and that Itch expression was increased in *Numb*-silenced macrophages. They imply that after LPS stimulation, Numb is separated from Itch and it allows Itch to negatively regulate pro-inflammatory cytokine production in macrophages. However, a specific WW1 or WW2 domain of Itch serves as a docking site for Numb binding is unclear. Moreover, Cyld and TAB1 also bind to WW domains of Itch, forming a protein complex that negatively regulated pro-inflammatory cytokines (70, 71). Whether Numb may competitively binds to Itch at the same binding site required for binding of Cyld and TAB1 requires further investigation.

From our proteomics data, we constructed a protein-protein interaction network based on the proteins that regulated pro-inflammatory cytokines and predicted that Akt1 might play a central role in regulation of p65 NF-κB and p38 MAPK signaling pathways. The protein and mRNA results were validated showing that Akt1 and its phosphorylation levels were increased in *Numb*-deficient macrophages after LPS stimulation. This evidence suggests an important role of Akt1 in regulation of pro-inflammatory cytokine production. Studies in *Akt1^{-/-}* mice supports our data because they demonstrated that production of TNFα and IL-6 increased in *Akt1^{-/-}* macrophages after stimulation with LPS (108, 109). Akt has three isoforms and each of the Akt isoforms displays a distinct tissue distribution and function. Akt1 is required for induction of nitric oxide synthase and endothelial cell function whereas Akt2 is required for insulin-responsive signaling (110-112). On the other hand, Akt3 involves in brain development despite of its largely undefined functions (113, 114). In our study, we observed a high mRNA expression of *Akt1* in *Numb*-deficient macrophages after LPS stimulation comparing with that of the control cells. However, the expression level of *Akt2* remained unchanged in those cell types. Our observation is in agreement with the study by Arranz et al. (115) reporting that changes in Akt isoforms did not affect the phosphorylation of Akt in LPS-stimulated macrophages. Taken together, we demonstrate that Akt1 negatively regulates inflammation in macrophages possibly through MAPK and NF-κB signaling pathways.

In B-cell lymphoma, loss of GLI1 reduces *Akt1* expression, indicating that *Akt1* is a direct target gene of a transcriptional factor GLI1 (116). Moreover, GLI1 is accumulated in medulloblastoma cell line overexpressing NumbΔPTB compared with the cells overexpression Numb, suggesting a negative effect of Numb in regulation of GLI1 (95). Collectively, our result showing that Akt1 increased in *Numb*-silenced macrophages and reports by others implicitly suggest that a high expression of Akt1 may be a result of the accumulation of GLI1 *Numb*-silenced macrophages.

In our study for the role of Itch in macrophages, we demonstrate that Itch is a negative regulator of Notch signaling because we detected higher expression of Notch1 and *Hes1* mRNA in LPS-stimulated, *Itch*-silenced macrophages, comparing with those of the control cells. The results are consistent with the reports by other

groups showing that Notch signaling was activated in hematopoietic progenitor cells when *Itch* was absence (117). Surprisingly, the amounts of TNFα, IL-6, and IL-12p70 cytokines were significantly reduced in macrophages treated with siItch siRNA and stimulated with LPS. These results are controversial to the fact that Itch is a negative regulator of pro-inflammatory cytokines by forming a complex with Cyld and TAK1 (26, 70, 71). However, TAp73 is another Itch binding protein that is also degraded by ubiquitin-mediated proteasomal degradation (118). A study in TAp73$^{-/-}$ macrophages reported that TNFα and IL-6 cytokines were increased after LPS stimulation (119), demonstrating that TAp73 is required to maintain an anti-inflammatory stage in macrophages. The expression level of TAp73 in *Itch*-deficient macrophages needs to be further investigated.

A reduction of p38 and JNK MAPK activation we observed in *Itch*-silenced macrophages after LPS stimulation is consistent with the finding by Tao et al. (120) who demonstrated that silencing of *Itch* caused differential effects on NOD2/RIP2-mediated activation of NF-κB and MAPK signaling pathways. They also showed that the activations of p38 and JNK MAPKs but not NF-κB were reduced when *Itch* was silenced *in vitro* and *in vivo* in macrophages after challenging with *Listeria monocytogenes*. Taken together, these findings demonstrate that regulation of pro-inflammatory cytokines by Itch depends on various protein binding partners and types of cells and stimuli.

Silencing of *Rbpjκ* demonstrates that Notch signaling is required for pro-inflammatory cytokines production in macrophages, especially the productions of IL-6 and IL-12p70 that are mainly dependent on Notch signaling. Meanwhile, TNFα is dependent on Itch rather than on Notch signaling. Our observation is in agreement with reports by other groups confirming the role of Notch signaling that is optimally required for the production of pro-inflammatory cytokines in macrophages (8, 9, 92).

In summary, we report a novel role of Numb and its molecular mechanism in regulation of pro-inflammatory cytokine production in macrophages in response to activation through TLR4. Numb directly binds to Itch, forming a protein complex which controls production of TNFα, IL-6 and IL-12p70 cytokines possibly through the phosphorylation of p65 NF-κB and p38 MAPK signaling pathways (Figure 5.1). Furthermore, both Numb and Itch regulate the production of pro-inflammatory

cytokines IL-6 and IL-12p70 in Notch-dependent manner but not TNFα. This present study provides a deep insight to the complex and tight regulation of pro-inflammatory cytokine production in macrophages in response to LPS.

Figure 5.1 The proposed model of Numb and Itch in regulation of pro-inflammatory cytokine production in macrophages in response to TLR4 activation

CHAPTER VI
CONCLUSIONS

The expression of pro-inflammatory cytokines in macrophages are tightly regulated through different molecular mechanisms. We present here a novel regulatory mechanism that involves Numb and Itch that are very well-known inhibitors of Notch signaling. A novel role of Numb is characterized in this study. In macrophages, Numb positively regulates pro-inflammatory cytokine production, regardless of its ability to inhibit Notch signaling. In addition, the production of pro-inflammatory cytokines occurs through p65 NF-κB and p38 MAPK signal pathways. Numb directly binds to Itch, forming a complex that inhibits Itch from function as a negative regulator of inflammation. Changes of Numb expression also alter Itch expression. Moreover, the proteomics data reveals that deletion of Numb causes a change of overall proteins in LPS-stimulated macrophages to become less pro-inflammatory.

Finally, we demonstrate that Itch is a positive regulator of pro-inflammatory cytokine production which is controversial. Silencing of Itch leads to lower phosphorylation of p38 and JNK MAPK signaling pathways. Moreover, Notch signaling is still important for an optimal production of the pro-inflammatory cytokines, but it is less important for TNFα. In conclusion, this present study provides a deep insight to the complex and tight regulation of pro-inflam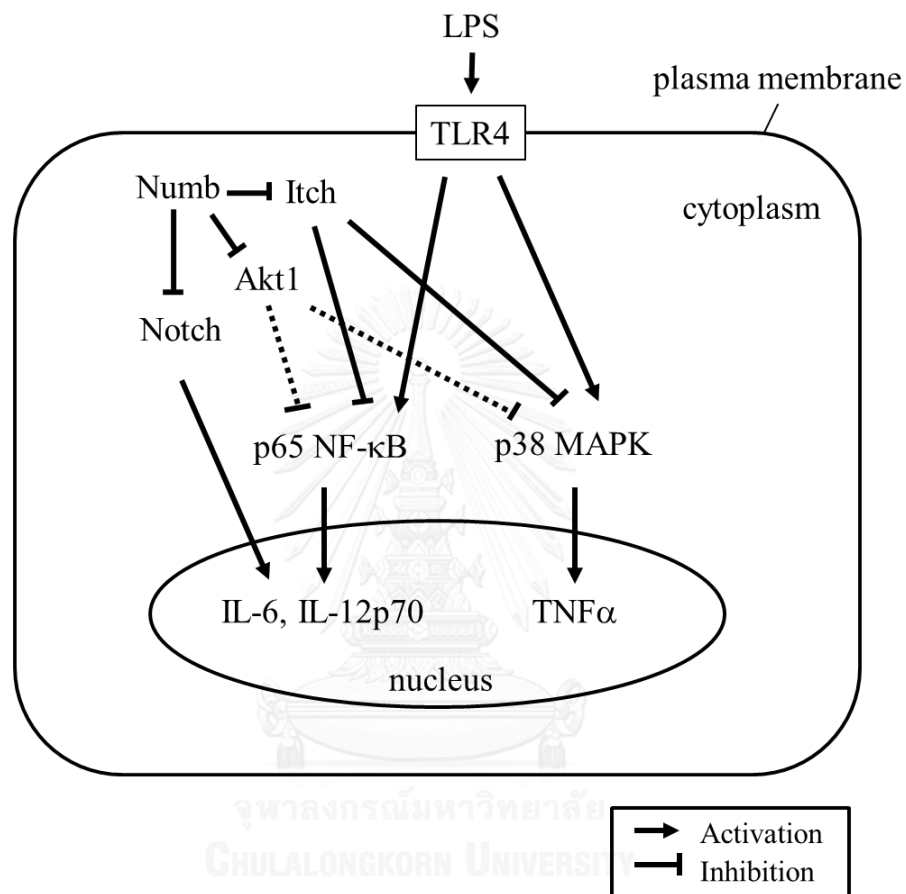matory cytokine production in macrophages in response to LPS, yet it was an *in vitro* study. It is essential to further investigate whether similar results occur in *in vivo* models or humans with inflammatory-related diseases.

REFERENCES

1.   Ghosh S, May MJ, Kopp EB. NF-kappa B and Rel proteins: evolutionarily conserved mediators of immune responses. Annual review of immunology. 1998;16:225-60.

2.   Lee JC, Laydon JT, McDonnell PC, Gallagher TF, Kumar S, Green D, et al. A protein kinase involved in the regulation of inflammatory cytokine biosynthesis. Nature. 1994;372(6508):739-46.

3.   Kawai T, Akira S. The role of pattern-recognition receptors in innate immunity: update on Toll-like receptors. Nature immunology.11(5):373-84.

4.   Amiel E, Alonso A, Uematsu S, Akira S, Poynter ME, Berwin B. Pivotal Advance: Toll-like receptor regulation of scavenger receptor-A-mediated phagocytosis. Journal of leukocyte biology. 2009;85(4):595-605.

5.   Artavanis-Tsakonas S, Rand MD, Lake RJ. Notch signaling: cell fate control and signal integration in development. Science. 1999;284(5415):770-6.

6.   Lai EC. Notch signaling: control of cell communication and cell fate. Development. 2004;131(5):965-73.

7.   Monsalve E, Ruiz-Garcia A, Baladron V, Ruiz-Hidalgo MJ, Sanchez-Solana B, Rivero S, et al. Notch1 upregulates LPS-induced macrophage activation by increasing NF-kappaB activity. European journal of immunology. 2009;39(9):2556-70.

8.   Wongchana W, Palaga T. Direct regulation of interleukin-6 expression by Notch signaling in macrophages. Cellular & molecular immunology. 2012;9(2):155-62.

9.   Palaga T, Buranaruk C, Rengpipat S, Fauq AH, Golde TE, Kaufmann SH, et al. Notch signaling is activated by TLR stimulation and regulates macrophage functions. European journal of immunology. 2008;38(1):174-83.

10.   Watanabe K, Nagaoka T, Lee JM, Bianco C, Gonzales M, Castro NP, et al. Enhancement of Notch receptor maturation and signaling sensitivity by Cripto-1. The Journal of cell biology. 2009;187(3):343-53.

11.   Nichols JT, Miyamoto A, Olsen SL, D'Souza B, Yao C, Weinmaster G. DSL ligand endocytosis physically dissociates Notch1 heterodimers before activating proteolysis can occur. The Journal of cell biology. 2007;176(4):445-58.

12.   Tousseyn T, Thathiah A, Jorissen E, Raemaekers T, Konietzko U, Reiss K, et al. ADAM10, the rate-limiting protease of regulated intramembrane proteolysis of Notch and other proteins, is processed by ADAMS-9, ADAMS-15, and the gamma-secretase. The Journal of biological chemistry. 2009;284(17):11738-47.

13.   McGill MA, McGlade CJ. Mammalian numb proteins promote Notch1 receptor ubiquitination and degradation of the Notch1 intracellular domain. The Journal of biological chemistry. 2003;278(25):23196-203.

14.   Le Bras S, Loyer N, Le Borgne R. The multiple facets of ubiquitination in the regulation of notch signaling pathway. Traffic. 2011;12(2):149-61.

15.   Foldi J, Chung AY, Xu H, Zhu J, Outtz HH, Kitajewski J, et al. Autoamplification of Notch signaling in macrophages by TLR-induced and

RBP-J-dependent induction of Jagged1. Journal of immunology. 2010;185(9):5023-31.

16. Dho SE, French MB, Woods SA, McGlade CJ. Characterization of four mammalian numb protein isoforms. Identification of cytoplasmic and membrane-associated variants of the phosphotyrosine binding domain. The Journal of biological chemistry. 1999;274(46):33097-104.

17. Zhong W, Feder JN, Jiang MM, Jan LY, Jan YN. Asymmetric localization of a mammalian numb homolog during mouse cortical neurogenesis. Neuron. 1996;17(1):43-53.

18. Zhong W, Jiang MM, Weinmaster G, Jan LY, Jan YN. Differential expression of mammalian Numb, Numblike and Notch1 suggests distinct roles during mouse cortical neurogenesis. Development. 1997;124(10):1887-97.

19. Rennstam K, McMichael N, Berglund P, Honeth G, Hegardt C, Ryden L, et al. Numb protein expression correlates with a basal-like phenotype and cancer stem cell markers in primary breast cancer. Breast cancer research and treatment. 2010;122(2):315-24.

20. Sheng W, Dong M, Zhou J, Li X, Liu Q, Dong Q, et al. Cooperation among Numb, MDM2 and p53 in the development and progression of pancreatic cancer. Cell and tissue research. 2013;354(2):521-32.

21. Flores AN, McDermott N, Meunier A, Marignol L. NUMB inhibition of NOTCH signalling as a therapeutic target in prostate cancer. Nature reviews Urology. 2014.

22. Wilson A, Ardiet DL, Saner C, Vilain N, Beermann F, Aguet M, et al. Normal hemopoiesis and lymphopoiesis in the combined absence of numb and numblike. Journal of immunology. 2007;178(11):6746-51.

23. Anderson AC, Kitchens EA, Chan SW, St Hill C, Jan YN, Zhong W, et al. The Notch regulator Numb links the Notch and TCR signaling pathways. J Immunol. 2005;174(2):890-7.

24. Aguado R, Martin-Blanco N, Caraballo M, Canelles M. The endocytic adaptor Numb regulates thymus size by modulating pre-TCR signaling during asymmetric division. Blood. 2010;116(10):1705-14.

25. Chang JT, Palanivel VR, Kinjyo I, Schambach F, Intlekofer AM, Banerjee A, et al. Asymmetric T lymphocyte division in the initiation of adaptive immune responses. Science. 2007;315(5819):1687-91.

26. Melino G, Gallagher E, Aqeilan RI, Knight R, Peschiaroli A, Rossi M, et al. Itch: a HECT-type E3 ligase regulating immunity, skin and cancer. Cell death and differentiation. 2008;15(7):1103-12.

27. Hershko A, Ciechanover A. The ubiquitin system. Annual review of biochemistry. 1998;67:425-79.

28. Matesic LE, Copeland NG, Jenkins NA. Itchy mice: the identification of a new pathway for the development of autoimmunity. Current topics in microbiology and immunology. 2008;321:185-200.

29. Perry WL, Hustad CM, Swing DA, O'Sullivan TN, Jenkins NA, Copeland NG. The itchy locus encodes a novel ubiquitin protein ligase that is disrupted in a18H mice. Nature genetics. 1998;18(2):143-6.

30. Fang D, Elly C, Gao B, Fang N, Altman Y, Joazeiro C, et al. Dysregulation of T lymphocyte function in itchy mice: a role for Itch in TH2 differentiation. Nature immunology. 2002;3(3):281-7.

31. Rathinam C, Matesic LE, Flavell RA. The E3 ligase Itch is a negative regulator of the homeostasis and function of hematopoietic stem cells. Nature immunology.12(5):399-407.

32. Guo M, Jan LY, Jan YN. Control of daughter cell fates during asymmetric division: interaction of Numb and Notch. Neuron. 1996;17(1):27-41.

33. Qiu L, Joazeiro C, Fang N, Wang HY, Elly C, Altman Y, et al. Recognition and ubiquitination of Notch by Itch, a hect-type E3 ubiquitin ligase. The Journal of biological chemistry. 2000;275(46):35734-7.

34. Mosser DM, Edwards JP. Exploring the full spectrum of macrophage activation. Nature reviews Immunology. 2008;8(12):958-69.

35. Gordon S, Taylor PR. Monocyte and macrophage heterogeneity. Nature reviews Immunology. 2005;5(12):953-64.

36. Akira S, Takeda K. Functions of toll-like receptors: lessons from KO mice. Comptes rendus biologies. 2004;327(6):581-9.

37. Takeda K, Akira S. Microbial recognition by Toll-like receptors. Journal of dermatological science. 2004;34(2):73-82.

38. Akira S, Takeda K. Toll-like receptor signalling. Nature reviews Immunology. 2004;4(7):499-511.

39. Kawai T, Akira S. The role of pattern-recognition receptors in innate immunity: update on Toll-like receptors. Nature immunology. 2010;11(5):373-84.

40. Lang R. Tuning of macrophage responses by Stat3-inducing cytokines: molecular mechanisms and consequences in infection. Immunobiology. 2005;210(2-4):63-76.

41. Liew FY, Xu D, Brint EK, O'Neill LA. Negative regulation of toll-like receptor-mediated immune responses. Nature reviews Immunology. 2005;5(6):446-58.

42. Vallabhapurapu S, Karin M. Regulation and function of NF-kappaB transcription factors in the immune system. Annual review of immunology. 2009;27:693-733.

43. Salojin KV, Owusu IB, Millerchip KA, Potter M, Platt KA, Oravecz T. Essential role of MAPK phosphatase-1 in the negative control of innate immune responses. Journal of immunology. 2006;176(3):1899-907.

44. Hammer M, Mages J, Dietrich H, Servatius A, Howells N, Cato AC, et al. Dual specificity phosphatase 1 (DUSP1) regulates a subset of LPS-induced genes and protects mice from lethal endotoxin shock. J Exp Med. 2006;203(1):15-20.

45. Kawai T, Akira S. TLR signaling. Cell death and differentiation. 2006;13(5):816-25.

46. Radtke F, Wilson A, MacDonald HR. Notch signaling in hematopoiesis and lymphopoiesis: lessons from Drosophila. BioEssays : news and reviews in molecular, cellular and developmental biology. 2005;27(11):1117-28.

47. Radtke F, Fasnacht N, Macdonald HR. Notch signaling in the immune system. Immunity. 2010;32(1):14-27.

48.   Gordon WR, Vardar-Ulu D, L'Heureux S, Ashworth T, Malecki MJ, Sanchez-Irizarry C, et al. Effects of S1 cleavage on the structure, surface export, and signaling activity of human Notch1 and Notch2. PLoS One. 2009;4(8):e6613.

49.   Hansson EM, Lanner F, Das D, Mutvei A, Marklund U, Ericson J, et al. Control of Notch-ligand endocytosis by ligand-receptor interaction. Journal of cell science. 2010;123(Pt 17):2931-42.

50.   Brou C, Logeat F, Gupta N, Bessia C, LeBail O, Doedens JR, et al. A novel proteolytic cleavage involved in Notch signaling: the role of the disintegrin-metalloprotease TACE. Molecular cell. 2000;5(2):207-16.

51.   Schroeter EH, Kisslinger JA, Kopan R. Notch-1 signalling requires ligand-induced proteolytic release of intracellular domain. Nature. 1998;393(6683):382-6.

52.   Castel D, Mourikis P, Bartels SJ, Brinkman AB, Tajbakhsh S, Stunnenberg HG. Dynamic binding of RBPJ is determined by Notch signaling status. Genes & development. 2013;27(9):1059-71.

53.   Tsunematsu R, Nakayama K, Oike Y, Nishiyama M, Ishida N, Hatakeyama S, et al. Mouse Fbw7/Sel-10/Cdc4 is required for notch degradation during vascular development. The Journal of biological chemistry. 2004;279(10):9417-23.

54.   Berdnik D, Torok T, Gonzalez-Gaitan M, Knoblich JA. The endocytic protein alpha-Adaptin is required for numb-mediated asymmetric cell division in Drosophila. Developmental cell. 2002;3(2):221-31.

55.   Pettersson S, Sczaniecka M, McLaren L, Russell F, Gladstone K, Hupp T, et al. Non-degradative ubiquitination of the Notch1 receptor by the E3 ligase MDM2 activates the Notch signalling pathway. The Biochemical journal. 2013;450(3):523-36.

56.   Aguado R, Martin-Blanco N, Caraballo M, Canelles M. The endocytic adaptor Numb regulates thymus size by modulating pre-TCR signaling during asymmetric division. Blood.116(10):1705-14.

57.   Gulino A, Di Marcotullio L, Screpanti I. The multiple functions of Numb. Experimental cell research. 2010;316(6):900-6.

58.   Ntelios D, Berninger B, Tzimagiorgis G. Numb and Alzheimer's disease: the current picture. Frontiers in neuroscience. 2012;6:145.

59.   Dho SE, Trejo J, Siderovski DP, McGlade CJ. Dynamic regulation of mammalian numb by G protein-coupled receptors and protein kinase C activation: Structural determinants of numb association with the cortical membrane. Molecular biology of the cell. 2006;17(9):4142-55.

60.   McGill MA, Dho SE, Weinmaster G, McGlade CJ. Numb regulates post-endocytic trafficking and degradation of Notch1. The Journal of biological chemistry. 2009;284(39):26427-38.

61.   Santolini E, Puri C, Salcini AE, Gagliani MC, Pelicci PG, Tacchetti C, et al. Numb is an endocytic protein. The Journal of cell biology. 2000;151(6):1345-52.

62.   Radtke F, Wilson A, Stark G, Bauer M, van Meerwijk J, MacDonald HR, et al. Deficient T cell fate specification in mice with an induced inactivation of Notch1. Immunity. 1999;10(5):547-58.

63. Han H, Tanigaki K, Yamamoto N, Kuroda K, Yoshimoto M, Nakahata T, et al. Inducible gene knockout of transcription factor recombination signal binding protein-J reveals its essential role in T versus B lineage decision. International immunology. 2002;14(6):637-45.

64. Wolfer A, Wilson A, Nemir M, MacDonald HR, Radtke F. Inactivation of Notch1 impairs VDJbeta rearrangement and allows pre-TCR-independent survival of early alpha beta Lineage Thymocytes. Immunity. 2002;16(6):869-79.

65. Hochstrasser M. Ubiquitin-dependent protein degradation. Annual review of genetics. 1996;30:405-39.

66. Thrower JS, Hoffman L, Rechsteiner M, Pickart CM. Recognition of the polyubiquitin proteolytic signal. The EMBO journal. 2000;19(1):94-102.

67. Deshaies RJ, Joazeiro CA. RING domain E3 ubiquitin ligases. Annual review of biochemistry. 2009;78:399-434.

68. Rotin D, Kumar S. Physiological functions of the HECT family of ubiquitin ligases. Nature reviews Molecular cell biology. 2009;10(6):398-409.

69. Liu YC. The E3 ubiquitin ligase Itch in T cell activation, differentiation, and tolerance. Seminars in immunology. 2007;19(3):197-205.

70. Ahmed N, Zeng M, Sinha I, Polin L, Wei WZ, Rathinam C, et al. The E3 ligase Itch and deubiquitinase Cyld act together to regulate Tak1 and inflammation. Nat Immunol. 2011;12(12):1176-83.

71. Theivanthiran B, Kathania M, Zeng M, Anguiano E, Basrur V, Vandergriff T, et al. The E3 ubiquitin ligase Itch inhibits p38alpha signaling and skin inflammation through the ubiquitylation of Tab1. Science signaling. 2015;8(365):ra22.

72. Matesic LE, Haines DC, Copeland NG, Jenkins NA. Itch genetically interacts with Notch1 in a mouse autoimmune disease model. Human molecular genetics. 2006;15(24):3485-97.

73. Hustad CM, Perry WL, Siracusa LD, Rasberry C, Cobb L, Cattanach BM, et al. Molecular genetic characterization of six recessive viable alleles of the mouse agouti locus. Genetics. 1995;140(1):255-65.

74. Monsalve E, Perez MA, Rubio A, Ruiz-Hidalgo MJ, Baladron V, Garcia-Ramirez JJ, et al. Notch-1 up-regulation and signaling following macrophage activation modulates gene expression patterns known to affect antigen-presenting capacity and cytotoxic activity. Journal of immunology. 2006;176(9):5362-73.

75. Yoshida A, Nagata T, Uchijima M, Higashi T, Koide Y. Advantage of gene gun-mediated over intramuscular inoculation of plasmid DNA vaccine in reproducible induction of specific immune responses. Vaccine. 2000;18(17):1725-9.

76. Radonic A, Thulke S, Mackay IM, Landt O, Siegert W, Nitsche A. Guideline to reference gene selection for quantitative real-time PCR. Biochemical and biophysical research communications. 2004;313(4):856-62.

77. Lee YG, Kim JY, Lee JY, Byeon SE, Hong EK, Lee J, et al. Regulatory effects of Codonopsis lanceolata on macrophage-mediated immune responses. Journal of ethnopharmacology. 2007;112(1):180-8.

78. Tada R, Yoshikawa M, Kuge T, Tanioka A, Ishibashi K, Adachi Y, et al. Granulocyte macrophage colony-stimulating factor is required for cytokine induction by a highly 6-branched 1,3-beta-D-glucan from Aureobasidium pullulans in mouse-derived splenocytes. Immunopharmacology and immunotoxicology. 2011;33(2):302-8.

79. Norrby M, Evertsson K, Fjallstrom AK, Svensson A, Tagerud S. Akt (protein kinase B) isoform phosphorylation and signaling downstream of mTOR (mammalian target of rapamycin) in denervated atrophic and hypertrophic mouse skeletal muscle. Journal of molecular signaling. 2012;7(1):7.

80. Oshiumi H, Matsumoto M, Funami K, Akazawa T, Seya T. TICAM-1, an adaptor molecule that participates in Toll-like receptor 3-mediated interferon-beta induction. Nat Immunol. 2003;4(2):161-7.

81. Fijneman RJ, Bade LK, Peham JR, van de Wiel MA, van Hinsbergh VW, Meijer GA, et al. Pla2g2a attenuates colon tumorigenesis in azoxymethane-treated C57BL/6 mice; expression studies reveal Pla2g2a target genes and pathways. Cellular oncology : the official journal of the International Society for Cellular Oncology. 2009;31(5):345-56.

82. Ichiyama K, Yoshida H, Wakabayashi Y, Chinen T, Saeki K, Nakaya M, et al. Foxp3 inhibits RORgammat-mediated IL-17A mRNA transcription through direct interaction with RORgammat. The Journal of biological chemistry. 2008;283(25):17003-8.

83. Deleault KM, Skinner SJ, Brooks SA. Tristetraprolin regulates TNF TNF-alpha mRNA stability via a proteasome dependent mechanism involving the combined action of the ERK and p38 pathways. Molecular immunology. 2008;45(1):13-24.

84. Lowry OH, Rosebrough NJ, Farr AL, Randall RJ. Protein measurement with the Folin phenol reagent. The Journal of biological chemistry. 1951;193(1):265-75.

85. Blum H, Beier H, Gross HJ. Improved silver staining of plant proteins, RNA and DNA in polyacrylamide gels. Electrophoresis. 1987;8(2):93-9.

86. Johansson C, Samskog J, Sundstrom L, Wadensten H, Bjorkesten L, Flensburg J. Differential expression analysis of Escherichia coli proteins using a novel software for relative quantitation of LC-MS/MS data. Proteomics. 2006;6(16):4475-85.

87. Thorsell A, Portelius E, Blennow K, Westman-Brinkmalm A. Evaluation of sample fractionation using micro-scale liquid-phase isoelectric focusing on mass spectrometric identification and quantitation of proteins in a SILAC experiment. Rapid communications in mass spectrometry : RCM. 2007;21(5):771-8.

88. Perkins DN, Pappin DJ, Creasy DM, Cottrell JS. Probability-based protein identification by searching sequence databases using mass spectrometry data. Electrophoresis. 1999;20(18):3551-67.

89. Petersen PH, Zou K, Hwang JK, Jan YN, Zhong W. Progenitor cell maintenance requires numb and numblike during mouse neurogenesis. Nature. 2002;419(6910):929-34.

90. Rasin MR, Gazula VR, Breunig JJ, Kwan KY, Johnson MB, Liu-Chen S, et al. Numb and Numbl are required for maintenance of cadherin-based adhesion and polarity of neural progenitors. Nat Neurosci. 2007;10(7):819-27.

91. Van Parijs L, Sethna MP, Schweitzer AN, Borriello F, Sharpe AH, Abbas AK. Functional consequences of dysregulated B7-1 (CD80) and B7-2 (CD86) expression in B or T lymphocytes of transgenic mice. Journal of immunology. 1997;159(11):5336-44.

92. Boonyatecha N, Sangphech N, Wongchana W, Kueanjinda P, Palaga T. Involvement of Notch signaling pathway in regulating IL-12 expression via c-Rel in activated macrophages. Molecular immunology. 2012;51(3-4):255-62.

93. Liu L, Zhao Y, Xie K, Sun X, Gao Y, Wang Z. Estrogen-induced nongenomic calcium signaling inhibits lipopolysaccharide-stimulated tumor necrosis factor alpha production in macrophages. PLoS One. 2013;8(12):e83072.

94. Guma M, Hammaker D, Topolewski K, Corr M, Boyle DL, Karin M, et al. Antiinflammatory functions of p38 in mouse models of rheumatoid arthritis: advantages of targeting upstream kinases MKK-3 or MKK-6. Arthritis Rheum. 2012;64(9):2887-95.

95. Di Marcotullio L, Greco A, Mazza D, Canettieri G, Pietrosanti L, Infante P, et al. Numb activates the E3 ligase Itch to control Gli1 function through a novel degradation signal. Oncogene. 2011;30(1):65-76.

96. Franceschini A, Szklarczyk D, Frankild S, Kuhn M, Simonovic M, Roth A, et al. STRING v9.1: protein-protein interaction networks, with increased coverage and integration. Nucleic acids research. 2013;41(Database issue):D808-15.

97. Hassed SJ, Wiley GB, Wang S, Lee JY, Li S, Xu W, et al. RBPJ mutations identified in two families affected by Adams-Oliver syndrome. American journal of human genetics. 2012;91(2):391-5.

98. Doyle SE, O'Connell RM, Miranda GA, Vaidya SA, Chow EK, Liu PT, et al. Toll-like receptors induce a phagocytic gene program through p38. J Exp Med. 2004;199(1):81-90.

99. Suzuki E, Umezawa K. Inhibition of macrophage activation and phagocytosis by a novel NF-kappaB inhibitor, dehydroxymethylepoxyquinomicin. Biomedicine & pharmacotherapy = Biomedecine & pharmacotherapie. 2006;60(9):578-86.

100. Frise E, Knoblich JA, Younger-Shepherd S, Jan LY, Jan YN. The Drosophila Numb protein inhibits signaling of the Notch receptor during cell-cell interaction in sensory organ lineage. Proceedings of the National Academy of Sciences of the United States of America. 1996;93(21):11925-32.

101. Tang H, Rompani SB, Atkins JB, Zhou Y, Osterwalder T, Zhong W. Numb proteins specify asymmetric cell fates via an endocytosis- and proteasome-independent pathway. Molecular and cellular biology. 2005;25(8):2899-909.

102. Cayouette M, Raff M. The orientation of cell division influences cell-fate choice in the developing mammalian retina. Development. 2003;130(11):2329-39.

103. Ohishi K, Varnum-Finney B, Flowers D, Anasetti C, Myerson D, Bernstein ID. Monocytes express high amounts of Notch and undergo cytokine specific

apoptosis following interaction with the Notch ligand, Delta-1. Blood. 2000;95(9):2847-54.

104. French MB, Koch U, Shaye RE, McGill MA, Dho SE, Guidos CJ, et al. Transgenic expression of numb inhibits notch signaling in immature thymocytes but does not alter T cell fate specification. Journal of immunology. 2002;168(7):3173-80.

105. Kuo CW, Chang CF, Chen MH, Chen SY, Wu YD. A new approach of planar multi-channel wavelength division multiplexing system using asymmetric super-cell photonic crystal structures. Optics express. 2007;15(1):198-206.

106. Ajibade AA, Wang Q, Cui J, Zou J, Xia X, Wang M, et al. TAK1 negatively regulates NF-kappaB and p38 MAP kinase activation in Gr-1+CD11b+ neutrophils. Immunity. 2012;36(1):43-54.

107. Venuprasad K, Zeng M, Baughan SL, Massoumi R. Multifaceted role of the ubiquitin ligase Itch in immune regulation. Immunology and cell biology. 2015.

108. Xu F, Kang Y, Zhang H, Piao Z, Yin H, Diao R, et al. Akt1-mediated regulation of macrophage polarization in a murine model of Staphylococcus aureus pulmonary infection. The Journal of infectious diseases. 2013;208(3):528-38.

109. Androulidaki A, Iliopoulos D, Arranz A, Doxaki C, Schworer S, Zacharioudaki V, et al. The kinase Akt1 controls macrophage response to lipopolysaccharide by regulating microRNAs. Immunity. 2009;31(2):220-31.

110. Yang ZZ, Tschopp O, Hemmings-Mieszczak M, Feng J, Brodbeck D, Perentes E, et al. Protein kinase B alpha/Akt1 regulates placental development and fetal growth. The Journal of biological chemistry. 2003;278(34):32124-31.

111. Cho H, Thorvaldsen JL, Chu Q, Feng F, Birnbaum MJ. Akt1/PKBalpha is required for normal growth but dispensable for maintenance of glucose homeostasis in mice. The Journal of biological chemistry. 2001;276(42):38349-52.

112. Cho H, Mu J, Kim JK, Thorvaldsen JL, Chu Q, Crenshaw EB, 3rd, et al. Insulin resistance and a diabetes mellitus-like syndrome in mice lacking the protein kinase Akt2 (PKB beta). Science. 2001;292(5522):1728-31.

113. Easton RM, Cho H, Roovers K, Shineman DW, Mizrahi M, Forman MS, et al. Role for Akt3/protein kinase Bgamma in attainment of normal brain size. Molecular and cellular biology. 2005;25(5):1869-78.

114. Tschopp O, Yang ZZ, Brodbeck D, Dummler BA, Hemmings-Mieszczak M, Watanabe T, et al. Essential role of protein kinase B gamma (PKB gamma/Akt3) in postnatal brain development but not in glucose homeostasis. Development. 2005;132(13):2943-54.

115. Arranz A, Doxaki C, Vergadi E, Martinez de la Torre Y, Vaporidi K, Lagoudaki ED, et al. Akt1 and Akt2 protein kinases differentially contribute to macrophage polarization. Proceedings of the National Academy of Sciences of the United States of America. 2012;109(24):9517-22.

116. Agarwal NK, Qu C, Kunkalla K, Liu Y, Vega F. Transcriptional regulation of serine/threonine protein kinase (AKT) genes by glioma-associated oncogene homolog 1. The Journal of biological chemistry. 2013;288(21):15390-401.

117. Rathinam C, Matesic LE, Flavell RA. The E3 ligase Itch is a negative regulator of the homeostasis and function of hematopoietic stem cells. Nat Immunol. 2011;12(5):399-407.
118. Rossi M, Inoue S, Walewska R, Knight RA, Dyer MJ, Cohen GM, et al. Caspase cleavage of Itch in chronic lymphocytic leukemia cells. Biochemical and biophysical research communications. 2009;379(3):659-64.
119. Tomasini R, Secq V, Pouyet L, Thakur AK, Wilhelm M, Nigri J, et al. TAp73 is required for macrophage-mediated innate immunity and the resolution of inflammatory responses. Cell death and differentiation. 2013;20(2):293-301.
120. Tao M, Scacheri PC, Marinis JM, Harhaj EW, Matesic LE, Abbott DW. ITCH K63-ubiquitinates the NOD2 binding protein, RIP2, to influence inflammatory signaling pathways. Current biology : CB. 2009;19(15):1255-63.

APPENDIX

Reagents for tissue culture

Complete DMEM medium (100 mL)

1X DMEM medium supplemented with L-glutamine	100 mL
Heat-inactivated FBS	10%
Penicillin	10,000 U
Streptomycin	400 mg
Sodium pyruvate	1%
HEPES	1%

BMM medium (100 mL)

L929 culture supernatant	20 mL
Complete DMEM medium	70 mL
Horse serum	10 mL

FBS inactivation

Commercial FBS kept at -20ºC was thawed at 4ºC overnight and heat inactivated at 56ºC for 30 mins.

Freezing medium A and B for BMM cryopreservation

Freezine medium A (10 mL)

DMEM	8 mL
FBS	2 mL

Freezine medium B (10 mL)

DMEM	6 mL
DMSO	2 mL
FBS	2 mL

Preparation is to mix A:B at 1:1 ratio.

Freezing medium for RAW264.7 cell line (10 mL)

Complete DMEM	9.5 mL
DMSO	0.5 mL

Reagents for SDS-PAGE

12.5% SDS-polyacrylamide gel (10 mL)

Sterile water	4.197 mL
40% acrylamide and Bis-acrylamide solution	3.125 mL
1.5 M Tris-HCl pH 8.8	2.5 mL
10% SDS	0.125 mL
10% APS	0.05 mL
TEMED	0.003 mL

10% SDS-polyacrylamide gel (8 mL)

Sterile water	3.8 mL
40% acrylamide and Bis-acrylamide solution	2 mL
1.5 M Tris-HCl pH 8.8	2 mL
10% SDS	0.08 mL
10% APS	0.08 mL
TEMED	0.004 mL

8% SDS-polyacrylamide gel (8 mL)

Sterile water	4.2 mL
40% acrylamide and Bis-acrylamide solution	4.2 mL
1.5 M Tris-HCl pH 8.8	2 mL
10% SDS	0.08 mL
10% APS	0.08 mL
TEMED	0.004 mL

5% stacking gel (2 mL)

Sterile water	1.204 mL
40% acrylamide and Bis-acrylamide solution	0.25 mL
1.0 M Tris-HCl pH 6.8	0.504 mL
10% SDS	0.02 mL
10% APS	0.02 mL
TEMED	0.002 mL

5X LaemmLi buffer (20 mL)

1.5 M Tris-Cl pH 6.8	4 mL
Glycerol	10 mL
β-mercaptoethanol	5 mL
SDS	2 g
1% bromphenol blue	1 mL

5X running buffer for SDS-PAGE (1 L)

Trisma base	15.1 g
Glycine	94 g
SDS	5 g
Sterile water	1,000 mL

Transfer buffer for Western blot

Trisma base	5.08 g
Glycine	2.9 g
SDS	0.37 g
Sterile water	800 mL
Absolute methanol	200 mL

1X PBS pH 7.4 (1 L)

NaCl	8 g
KCl	0.2 g
Na_2HPO_4	1.44 g

KH$_2$PO$_4$	0.24 g
Sterile water	1,000 mL

Autoclaved at 121°C, 15 psi for 15 mins.

1X PBS-Tween Washing buffer (500 mL)

1X PBS	500 mL
Tween-20	0.05%

Blocking solution for Western blot (200 mL)

1X PBST	200 mL
Non-fat dry milk	6 g

Substrates for ECL

Substrate A

100 mM Tris-HCl pH 8.5	2.5 mL
90 mM coumaric acid	11 μL
250 mM luminol	23 μL

Substrate B

100 mM Tris-HCl pH 8.5	2.5 mL
H$_2$O$_2$	1.5 mL

Developer and fixer solution of X-ray film development

Working developer solution is prepared by mixing developer solution : water at 1:1 ratio.

Working fixer solution is prepared by mixing fixer solution : water at 1:1 ratio.

RIPA lysis buffer (150 mM NaCl, 1.0% NP-40, 0.5% sodium deoxycholate, 0.1% SDS, 50 mM Tris-CL pH 7.4) (10 ml)

1 M Tris-HCl pH 7.4	0.5 mL
0.5 M NaCl	3 mL

NP-40	0.5 mL
10% (w/v) sodium deoxycholate	0.5 mL
20% (w/v) SDS	0.05 mL
Sterile water	fill up to 10 mL

Reagents for RNA extraction

DEPC water (100 mL)

A volume of 10 mL of DEPC (0.01% (v/v)) is added to 100 mL of HPLC-grade water. The DEPC water is autoclaved at 121°C, 15 psi for 16 mins.

75% Ethanol in DEPC water (50 mL)

DEPC water	12.5 mL
Absolute ethanol	37.5 mL

Reagents for Lowry Protein Assay

CTC reagent (100 mL)

0.2% (w/v) $CuSO_4$	0.2 g
0.4% (w/v) Tatalic acid	0.4 g

0.8 N NaOH (50 mL)

NaOH	1.6 g
HPLC-grade water	fill up to 50 mL

5% SDS (50 mL)

SDS	2.5 g
HPLC-grade water	fill up to 50 mL

20% Na_2CO_3 (50 mL)

Na_2CO_3	10 g
HPLC-grade water	fill up to 50 mL

Solution A (10 mL)

CTC reagent	1.25 mL
20% Na_2CO_3	1.25 mL
0.8 N NaOH	2.5 mL
5% SDS	5 mL

Solution B (3 mL)

Folin-ciocalteu's phenol reagent	0.5 mL
HPLC-grade water	2.5 mL

Procedure for Lowry Protein Assay is perform as described below:

1. Add 5 ml of sample in 96-well plate in triplicates.
2. Add 200 ml of Solution A and incubate for 30 mins at room temperature.
3. Add 50 ml of Solution B and incubate for 30 mins at room temperature.
4. Measure light absorbance value at 750 nm.

Reagents for silver staining

Fixing solution (50% Methanol, 12% acetic acid, 0.05% Formatin (37% formaldehyde) (1 L)

Methanol	500 mL
Acetic acid	120 mL
37% formaldehyde	500 μL
HPLC-grade water	fill up to 1,000 mL

Washing solution (55% Ethanol) (1 L)

Absolute ethanol	350 mL
HPLC-grade water	fill up to 1,000 mL

Sensitizing solution (0.02% sodium thiosulfate) (1 L)

Sodium thiosulfate	0.2 g
HPLC-grade water	1,000 mL

Silver staining solution (1 L)

Silver nitrate	2 g
HPLC-grade water	1,000 mL

Developing solution (1 L)

Sodium carbonate	60 g
0.02% sodium thiosulfate	20 mL
HPLC-grade water	fill up to 1,000 mL

Stopping solution (1 L)

Sodium EDTA	14.6 g
HPLC-grade water	1,000 mL

Reagents for trypsin digestion

10 mM NH₄HCO₃ (40 mL)

NH_4HCO_3	31.624 mg
HPLC-grade water	40 mL

10 mM dithiothreitol (DTT) (40 mL)

DTT	61.7 mg
10 mM NH_4HCO_3	40 mL

100 mM iodoacetamide (IAA) (20 mL)

IAA	370 mg
10 mM NH_4HCO_3	20 mL

30% acetonitrile (30 mL)

100% Acetonitrile	12 mL
HPLC-grade water	28 mL

Extract solution (50% acetonitrile, 0.1% formic acid) (20 mL)

100% acetonitrile	20 mL
Formic acid	40 μL

Trypsin solution (20 ng/mL in 10 mM sodium bicarbonate)

Trypsin (10 ng/μL)	2 μL
10 mM sodium bicarbonate	1 mL

VITA

Name: Patipark Kueanjinda

Date and place of birth: June 16, 1981, Bangkok, Thailand

Education:

Chulalongkorn University, Bangkok, Thailand

 Medical Microbiology (Ph.D.), 2015

University of Washington, Seattle, USA

 Microbiology (B.S.), 2007

Work Experience:

2006-2007 Laboratory Assistant, Male Fertility Laboratory

    University of Washington Medical Center,

    Seattle, WA, USA

Academic Publications:

1. P. Kueanjinda, S. Roytrakul, T. Palaga. (2015). A Novel Role of Numb as A Regulator of Pro-inflammatory Cytokine Production in Macrophages in Response to Toll-like Receptor 4. Scientific Reports. (In press)

2. T. Palaga, S. Ratanabunyong, T. Pattarakankul, N. Sangphech, W. Wongchana, Y. Hadae, P. Kueanjinda. (2013) Notch Signaling regulates expression of Mcl-1 and apoptosis in PPD-treated macrophages. Cellular & Molecular Immunology.